Additive Manufacturing of Concrete Structures

A Major Qualifying Project submitted to the faculty of
WORCESTER POLYTECHNIC INSTITUTE
in partial fulfillment of the requirements for the Degree of Bachelor of Science

Submitted By:
Ariana Cruz-Rivera
Jacob Grady
Joseph Tzanetos

April 6th, 2021

Submitted To:
Mingjiang Tao
Steven Van Dessel

Acknowledgements

We would like to thank our advisors Professor Steven Van Dessel and Professor Mingjiang Tao for their assistance and feedback throughout the entire project. We would also like to thank Kaven Hall laboratory manager Russ Lang for his advice and assistance in the laboratory. Lastly, we would like to acknowledge Professor Leonard Albano for taking time to assist us with the structural design. The time and effort that everyone contributed is much appreciated.

Abstract

The main objective of this major qualifying project was to develop a pavilion structure for the WPI campus that provided an outdoor, sheltered space, using the techniques of additive manufacturing and concrete 3D printing. This was achieved through researching precedent studies, drawing inspiration from geometric origami, and making use of techniques other studies used in order to create the structure utilizing the gantry style printer specific to WPI. A printable concrete mix design was developed specific to this project, instructions on 3D printing were developed, structural analysis for the pavilion was conducted, and hypothetical heating, ventilation, and air conditioning calculations were conducted for the space.

Capstone Design Statement

This Major Qualifying Project exemplifies the use of design processes for the development of a pavilion that incorporated both structural and mechanical components into its design that would be used as a study and presentation space on WPIs campus. Solidworks, AutoCAD inventor, Abaqus, RISA 2D Educational, and Cura were employed to apply the requirements imposed upon the architectural and structural designs.

The architectural design was developed through the concept of geometry and was sketched by hand. It was then drawn into Solidworks to work towards the analysis of the structural components. Daylighting and artificial light were considered in the establishment of the concept to allow for the maximization of daylight for the users. The structure was developed with the intent of using a building permit as well as a zoning permit as required for Massachusetts and the creation of a foundation.

The MEP design considered heating, ventilation, and air conditioning system analysis throughout the structure. The design is intended to be open, but hypothetical heating and cooling loads were calculated in order to establish heating requirements if the structure were to be enclosed. The calculations were based on equations and tabulated values provided in the 1980 ASHRAE Cooling and Heating Load Calculation Manual.

The structural design consisted of the analysis of the possible final structures. Following the completion of Solidworks models, the structures were transferred to Abaqus for a more comprehensive analysis. Varying thickness catenary arches were analyzed using the software to determine the structural stability of each version of the arches and comparing those to compression and tension values for thin wall structures. As the structure was entirely concrete, the maximum allowable compression values were significantly greater than the maximum allowable tension values.

Moreover, a variety of structure thickness, composition, size, and mix design were analyzed in order to provide a structure that recognized the need for effective structure performance. Collaboration between team members was critical in the development of the design as well as the analysis of the structure so as to make sure that all team members were equally inputting thoughts and processes for the creation of the pavilion. Team meetings were held several times a week to hold each member accountable for tasks that needed to be completed in a given time frame.

Professional Licensure Statement

As a Professional Engineer (PE), an individual is expected to uphold the health, safety, and wellbeing of those affected by their work. It is required that a PE sign, seal, and approve all engineering plans before their implementation. It is becoming common for individuals in high ranking engineering positions to be a practicing PE.

The first step in acquiring a PE is to graduate from a four year ABET-accredited engineering program or by having four years of engineering experience that is satisfactory to the board of engineering. The second step is to complete the Fundamentals of Engineering (FE) exam. Once an individual passes the FE, they become an Engineer in Training (EIT). Once an EIT the individual must work under the direct supervision of a PE for at least four years, which is the minimum amount of years required by the National Society of Professional Engineers. During those four years the individual must develop a portfolio of their work that they must submit to the board for approval. Once their portfolio is approved, the individual must then take the Principles and Practice of Engineering Exam, which is also known as the PE exam. Upon passing the PE exam the individual will receive their PE license. In order to retain their license the individual must consistently demonstrate and professionally develop their skills.

Executive Summary

3D printing provides an alternative approach to designing and constructing a number of structural objects. While many 3D printers use materials like plastic or metal, there are also printers that use concrete or cement paste mixes. By 3D printing concrete, it is possible to print specialized pieces, especially those with complex and intriguing geometries, and assemble them into a structure. Although this is a relatively new field, it is rapidly developing. In order to fully print a structure from concrete, it is necessary to understand the simpler elements involved with the 3D printing, as well as the analyzing and understanding the structure. This project focuses on the basics of developing a mix design for the concrete 3D printer and designing a theoretical structure that could be printed using only concrete through structural analysis.

Architectural and Structural Design

The goal with the design was to develop a pavilion structure that would take advantage of the fact that it would be 3D printed. The inspiration for the design concept of the structure was taken from modular origami. Modular origami takes several pieces, called units, to make one unified structure. In this project, the structure consisted of a hemispherical arch composed of hexagon modules, as well as an alternative design composed of diamonds. The final iteration of the structural design consisted of diamond modules, as they provided a more direct load path than hexagon modules, however, they followed the form of a catenary arch. The catenary shape was determined by fixing two ends and following the path provided by gravity. This was then reflected along the x-axis and used throughout the remainder of the project. The structural analysis of each arch iteration was carried out using Solidworks and Abaqus to ensure structural stability and safety. These softwares determined the areas of the arches that had the greatest amounts of stress and strain in both tension and compression. This was able to provide an understanding and explanation of where the greatest weaknesses in the arch would be found.

Mix Design

A literature review on the capabilities of 3D printers was conducted as there are a variety of details that are specific to each system. While many concrete printers have a hose, the one used in this project had a screw that was used to extract the concrete. This provided specific requirements that were necessary for the mix design. It needed a favorable level of extrudability, to be extracted with ease from the printhead, as well as adequate buildability, to allow multiple layers of the mix to be printed on top of each other. After both criteria were met, the strength of the mix after curing was also a key parameter. Much of the project was spent determining a mix design that could best be used in the future with this printer. A

perfect mix design was not achieved in the span of this project, however, the end result was a mix that satisfied a majority of the criteria for the printer.

In unison with developing the mix design was understanding how the printer operated. Setting up the printer itself and understanding and implementing the g-code were key goals for this sector of the project. In order to print, a g-code needed to be provided for the printer to follow. The manufacturer's instructions provided for the g-code were vague, and thus proved difficult to develop. The manufacturer specified that Cura software was required and within Cura, a custom printer needed to be set up for this specific printer, which from there the new code was developed.

Mechanical Design

The heating and cooling capabilities for the pavilion were calculated in order to determine user comfortability while using the structure. Using average and worst case-scenario temperatures in both the summer and winter, and a variety of module compositions, the best composition in terms of structure heating and cooling was determined from the results of this analysis.

Conclusions

The final design of the pavilion aimed to offer a structurally sound and comfortable space for users through the architectural design, the analysis of the structure, mechanical heating analysis and innovative manufacturing practices. As a result of time constraints and particular focuses throughout the length of this project, there are aspects that can be further progressed. A few recommendations to improve the design and continuation of the project include:

- Determining accurate properties of concrete used in the printer
- Finding methods of reinforcing the structure and its connections
- Fine-tuning the mix design to work well with the specific printer used in this project
- Developing additional mechanical systems such as lighting

Authorship

The concept, analysis, and writing of this report and project were done by Ariana Cruz-Rivera, Jacob Grady, and Joseph Tzanetos. Together, the team developed the architectural concept of the pavilion. Ariana Cruz-Rivera focused on the further development of the architectural concept, the precedent studies, and the mechanical systems. Jacob Grady focused on the creation of the computer model and the use of the printer. Joseph Tzanetos focused on the structural analysis of the pavilion and the mix design of the concrete that would be used. Each component of this project was reviewed and edited by each of the other team members, and as a whole, the team created recommendations and presented results to assist in completion of the project in the future.

Table of Contents

List of Figures, Tables, and Equations

1.0 Introduction

Pavilions can range from a simple open structure to very complex enclosed structures created from ornate components. Their use varies widely from purely appearance based, to a functional structure that provides protection from the elements. These structures are also made from a diverse range of materials; some created using common items, such as plastic buckets (Donnelly, 2017), or cardboard cylinders (Chino, 2011). The recycling of ordinary materials to create pavilions have led to the development of completely unfamiliar forms from anything seen prior. While an abundance of those pavilions have been made from the unexpected, most often they consist of more practical materials, such as wood or concrete.

Concrete has been a predominant building component for centuries. From structures such as the Pantheon, completed in 125 AD, to the Sagrada Familia, scheduled to be completed in 2026. It has proven to have many advantages that make it an attractive building material. It can consist simply of cement, water and aggregate - all three of which are easily obtainable, and at very low costs. Apart from the simplicity of concrete, it is also an exceptionally strong material that is able to withstand great amounts of compressive force. However, it falters once a tensile force is applied. The tensile strength of concrete can be increased in a variety of ways, through reinforcement with steel (rebar), or the addition of different types of fibers into the mix design. The addition of the rebar withstands the tension forces in the concrete, and the concrete on its own tolerates the compressive forces acting on the structure. Utilization of fibers is another method of increasing tensile strength. The addition of reinforcements within the concrete enable it to endure greater amounts of tension than pure concrete.

To construct with concrete, it is poured into a mold and then removed from that mold once it sets. This process limits the shape of the concrete to the abilities of the molds to create said formations. In recent years, research has begun to look into the feasibility of concrete 3D printing. Using a 3D printer eliminates the need for concrete casts, as the printer can form the concrete into the desired shape given by a code. The concrete 3D printing process is still new technology and it has its limitations, such as the requirement of a specialized mix design so that the aggregate does not clog the feed system to the print nozzle. Due to this restriction, concrete 3D printing is generally done on a small scale, and it is mostly used for artistic pavilions or other forms of art.

This project focuses on the design of a pavilion made predominantly of concrete, with the intent of the components being 3D printed with a gantry style concrete printer. The goal of the project was to create a space where students at WPI would be able to connect through studying or presenting, in a partially enclosed structure on campus. This was going to be carried out by using the techniques provided by the concept of additive manufacturing. Preliminarily, the idea was to design the pavilion based on a concept from modular origami.

As the project evolved, the goal was to design a structure that works entirely in compression to avoid the need for reinforcing steel. In addition to the creation of the architectural design, mix designs were developed and tested while making use of the concrete 3D printer.

2.0 Background

2.1 Additive Manufacturing

Additive manufacturing is the process by which one constructs an object by adding layers upon layers of material. The process first emerged in 1987 when 3D Systems used ultraviolet (UV) light-sensitive monomers that were polymerized using a laser. This specific process, using the polymer and laser, was known as stereolithography. Over the next four years many companies would work to improve the stereolithography system using different materials, like epoxy resin and synthetic rubber (Gornet, 2014).

In 1991 three more additive manufacturing processes were commercialized, fused deposition modeling (FDM), solid ground curing (SGC), and laminated object manufacturing (LOM). In FDM thermoplastic material is used in the form of filament to produce objects layer by layer. In SGC UV-sensitive liquid polymer is placed in a layer and then solidified by using electrostatic toner on a glass plate to produce UV light. LOM used materials in sheet form which was bonded and cut using a guided laser. In the years that followed other processes were introduced. In 1992 selective laser sintering (SLS) was developed, by using a laser to heat and solidify powder material. In 1993 direct shell production casting (DSPC) was commercialized and used powder form shells filled with a liquid binder. Companies around the world competed by creating printers that use these processes, endlessly improving them and working to sell affordable 3D printers (Gornet, 2014).

Early 3D printing was often used to create scale models or prototypes of complex 3D designs. Companies chose to use 3D printing for prototyping because it was cheaper to use and more efficient than hand making models. In recent years different types of additive manufacturing are being used to manufacture end use products at a high rate.

2.2 Concrete 3D Printing

2.2.1 Printing in Practice

The 3D printing of concrete structures is an emerging field in engineering that has gained momentum. By 3D printing instead of pouring concrete, it makes it possible to construct more intricate shapes and geometries. It allows for the customization of structural pieces based on their respective stress levels and required strength at a relatively low price. Each module can be unique and the change required would be in the design controlling the printing.

The process of 3D printing with concrete is comparatively straightforward. It is a related process to other types of 3D printers, except with concrete as the filament. Depending on the type of printer, it can have a hose and pump, while others have a small hopper where the concrete can be loaded prior to printing. There is also a computer which allows the printer to be programmed to print objects that are designed in other programs. The computer converts data into a file that it is able to understand and execute. Examples of concrete 3D printers can be seen below in Figures 1 and 2. Concrete printers can typically print approximately five layers before letting the concrete set (Malaeb et.al., 2015). If more layers are printed, the print may deform, and even collapse. It is also important that the concrete is sufficiently stiff to hold its shape. This will be discussed further when looking at the workability of concrete.

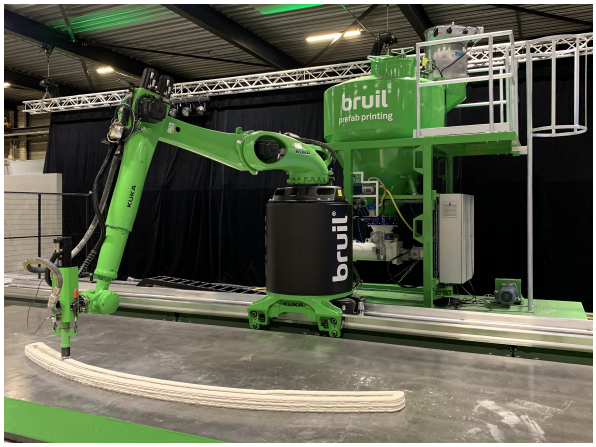

Figure 1: Bruil Concrete 3D Printer

Figure 2: Gantry 3D Printer used in Project

2.2.2 Workability of Concrete

Properties such as extrudability, buildability, and workability must be evaluated when working with concrete as a medium for 3D printing. The extrudability of concrete in 3D printing is defined as “the ability of the material to be extruded continuously and to be transported through pipes” (Krimi, 2017). Buildability of the mixed design must also be evaluated when printing with concrete. The buildability of concrete in the context of 3D printing refers to “the capacity of the material to support its own weight and the one of the deposited layers” (Krimi, 2017). In the development of various mix designs, the ratios of ingredients must bind together for the concrete to hold its shape once extruded. Inherently, concrete does not support its own weight, and thus, further chemical additives such as superplasticizer and accelerator must be added to not only increase buildability, but to assist in the drying time and binding of the layers. Workability of concrete is then defined by the prior characteristics, in addition to time, that combine to make it usable for the 3D printing process (Li, et.al., 2020).

To quantitatively analyze the workability of fresh concrete, a variety of tests must be conducted to determine the final mix design that will be used in printing. The extrudability of the material is measured through various slump tests to define its fluidity and segregation resistance. A slump-flow test is used to "measure the flowability of fresh concrete mixes with high flowability in unconfined conditions" (Ma, 2018), whereas a T50 slump test is the regulated slump test. A T50 test gives a flow time of the concrete for how long it will take to reach 50 cm in diameter. Along with providing settling time, it provides information on the uniformity of the concrete mix through the observation process. The viscosity of fresh concrete is determined using a V-funnel test. In this examination, a V-shaped funnel is filled with concrete and the time between when the concrete first goes through the outlet and when the funnel is empty determines the materials viscosity. In order to successfully pass this test, the concrete must pass through the outlet with no significant blockages throughout the pouring process.

2.2.3 Mix Designs

Determining proper mix design for a 3D printer is vital as 3D printers require a mix different from typical. Due to small nozzle sizes, the maximum size of the aggregate must be small as well. As the largest printer nozzle that will be used is 30 mm, the maximum size of coarse aggregate should be roughly one tenth of that size, or 3mm (Ma, 2018). By using smaller aggregate, strength will be sacrificed, but the incorporation of chemical additives will assist in strengthening the properties of the mix. An additional method to increase strength is to add cellulose fibers to the mixture, which improve the low tensile strength of concrete. However, the mixture might not be fluid enough to extract from the nozzle as fibers may clump together, and fail to make it through.

Analyzing the strength of the concrete is a key parameter, however it is also necessary to consider how much water and other liquids will be included in the mixture. The water to cement ratio needs to be a minimum of 0.48 (Malaeb, 2015), however, by adding superplasticizer it is possible to include less water. Superplasticizer aids in increasing the flowability of concrete and thus, the more superplasticizer used, the less water will be required. These are some key specifications that will need to be considered when developing the best mix design for this design. Table 1 below shows the mix design that was suggested by the printer manufacturer. These values are in terms of mass percentage of the suggested mixture.

Table 1. Manufacturer Suggested Mix Design

Material	Quantity (%)
Cellulose	0.01
Cement	33.46
Expansive Agent	3.18
Fast Setting/Hardening Cement	3.70
Micro-Silica	4.18
Sand	41.83
Water	13.23
Water Reducer	0.41

2.3 Modular Origami

Origami is the Japanese art of paper folding, and it has existed since the 15th century. This technique creates three dimensional figures through folds and creases to make intricate, movable, and simple designs. Typically, this process begins with a square sheet, and the development of the figure proceeds without the need to cut the paper. Today, new developments in folding techniques have allowed all practitioners to delve even further into the capabilities of paper.

It is said that the process of folding paper in this manner began soon after the creation of paper; however, it is disputed on which country engineered this process first. Traditionally, origami is created with paper or foil sheets that are lightweight in order for several layers to be folded together. In recent years, modern origami has delved out of traditional norms and has utilized new techniques for folding and new materials to fold with. From these new techniques, a variation known as “modular origami”, or “unit origami”, was created which comprised several individual units that would be assembled to make a decorative structure(Origami).

Modular origami stays true to the original origami in the sense that no cutting or adhesion is involved in the process. It is said to have evolved from the techniques of Kusudama, which are a series of paper flowers created from the assembly of pyramidal units. The modules of the modular piece are folded in a manner in which they create pockets, or tabs, that can be interlocked with the other modules, which reduce the need for any type of adhesion. The origin, and main baseline, for modular origami units comes from the Sonobe Module. The sonobe design is a parallelogram that contains two pockets and two tabs (Modular Origami). From there, the units can be arranged in a variety of series to create highly complex 200 piece structures, or simple 30 piece sonobe balls.

Unit origami draws its inspiration from nature and free forms that humans find in everyday life. Artists create forms that are representative of DNA helix structures, torus rings, cell capsules, animals, and much more. This technique encompasses a new model for the development of structures. There has especially been a focus on the use of origami to help cities bounce back from natural disasters through the "zippered tube" technique. This technique uses the strip folding of paper to create zigzagging shapes that will be joined together. When the shape is in tube form, it is incredibly strong, but it is still able to be made completely flat, making this a versatile technique for fast building applications (Peters, 2015).

2.4 Literature Studies

Literature studies were the inspiration of which ideas were drawn for what needed to be incorporated into the pavilion design. Reviewing what had already been developed with a similar concept or functionality, provided foundational knowledge of where to begin. As this project is the exploration of additive manufacturing and its applications with the creations of pavilions, literature study research was based on those parameters.

The first literature study was the Vulcan, which was created in 2015 and designed by LCD (laboratory for creative design). This structure can be seen in Figure 3. It was awarded the Guinness World Record for the largest 3D printed architectural pavilion. Created from 1086 individually printed modules over the course of 30 days using 20 large scale printers, it stood at 2.88 m tall and 8.08 m long. "As the name suggests, this pavilion conveys the essence of an erupting volcano...Volcano here symbolically depicts the transcendence of Nature, over and above the frail existence of humans" (Vyas, 2016). The designers sought to connect the users with nature while simultaneously providing something man made and to increase visibility for digital architecture. Additionally, the structure was constructed from three main components so that the structure was able to maintain ease in assembly and mobility.

Figure 3: Various Photographs of Vulcan Pavilion (Vyas, 2016)

The Deciduous Pavilion was another literature study which aimed to connect its visitors with nature through a botanical structure. Designed by MEAN (Middle East Architecture Network) with lead architect Riyad Joucka for the DIFC (Dubai International Financial Center) in 2019, it wanted to explore the potential of 3D printing as a sustainable means of production. This can be seen in Figure 4. The entire structure was made from three materials: birch plywood flooring, a 3D printed concrete base, and 3D printed recycled plastic polymer "branches" from 30,000 water bottles. The structure was made in such a way that the "parts can be mechanically joined on a clean site with no need for heavy machinery" (Sher, 2019).

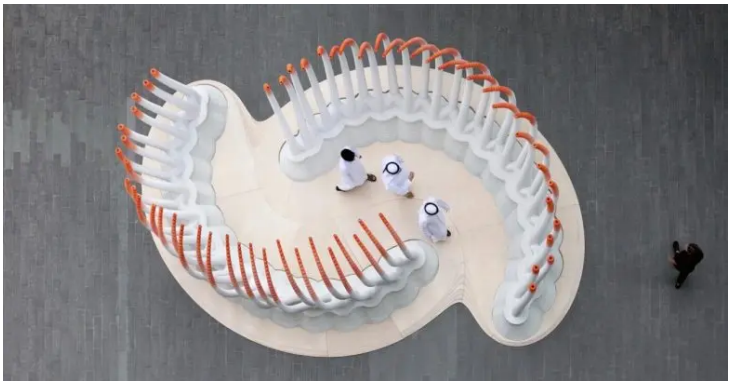

Figure 4: Deciduous Pavilion (Sher, 2019)

Sandy was a pavilion with the purpose of community and rest for its villagers in Darak, Iran and was designed by Amir Armani Asl and Kiana Ghader in 2020 to be constructed in 2021. The concept model for the pavilion can be seen in Figure 5. The structure was modeled after the topography of the surrounding land, as the sand dunes meet the sea. This structure used a layer by layer technique for construction which utilized 3D printers that printed with natural materials such as clay and sand to "create the form without any harm or disruption to the environment and the natural surrounding" (Kharvari, 2020).

The pavilion stood at 18 meters by 18 meters on a circular platform and followed a dome shape with vaulted openings so that it was more stable.

Figure 5: Sandy Pavilion Concept (Kharvari, 2020)

The final literature study was the Bloom Pavilion, which followed different print and construction forms than the others. The guiding floor plans can be seen in Figure 6. Designed by Emerging Objects in 2015, it was constructed from a series of 830 building blocks printed from portland cement by 11 powder 3D printers. By printing this way, it allowed for outer designs to be mapped onto each block in a way that followed traditional Thai flower patterns which can be seen in Figure 7. Unlike most 3D printed projects, this pavilion had chemical additives which allowed for the printing process to reduce greenhouse gas emissions by 50%. Additionally, the pieces were printed with structural ribs that made it so that the structure needs no additional support other than the bolts holding the pieces together (Slott, 2015).

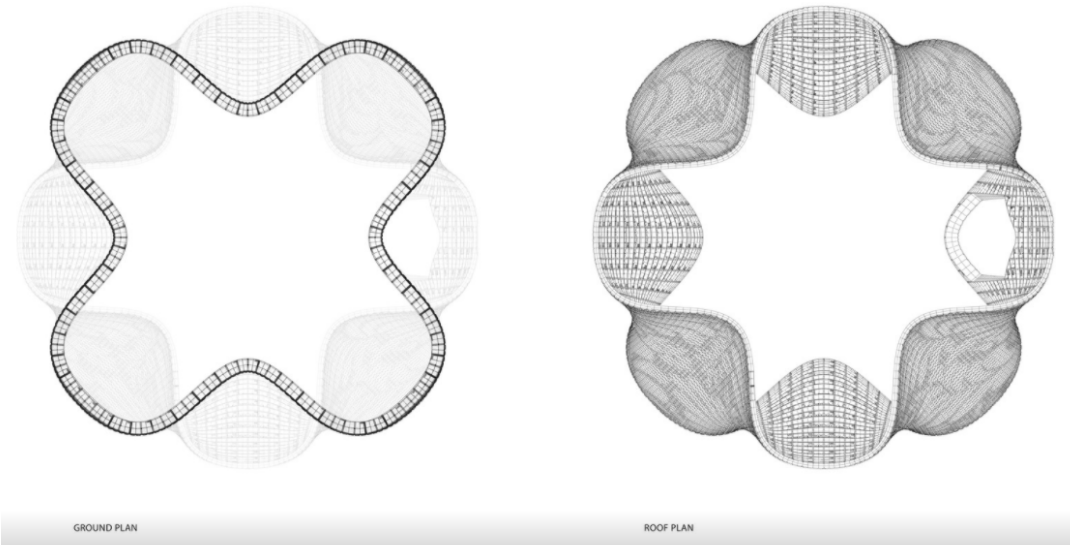

Figure 6: Bloom Pavilion Floor Plans

Figure 7: Bloom Pavilion Constructed

3.0 Methodology

3.1 Structural Design

The structural design and analysis of the pavilion were tested to determine the stability of the design through stress, strain, and deformation values. The primary method for such an analysis was done through finite element analysis in Abaqus. Each iteration of the design was drawn in Solidworks and then transferred to Abaqus, as the latter program is designed specifically for finite element analysis of larger structures. In this analysis, a linear elastic model was used to determine stability, and a concrete damaged plastic analysis was used to evaluate critical failure points. The design objective was to minimize the amount of tension as it was made of concrete. Generic properties for concrete were assumed and can be seen in Table 2 below:

Table 2: Assumed Properties of Concrete in Abaqus Analysis

Property	Value
Compressive Strength	4000 psi
Density	140 lb/ft^3
Elastic Modulus	4.0 x 10^6 psi
Poisson's Ratio	0.2
Shear Modulus	3.0 x 10^6 psi
Tensile Strength	500 psi
Yield Strength	3.41 x 10^6 psi
Maximum Permissible Tensile Strain	0.00015-0.00025
Maximum Permissible Compressive Strain	0.003-0.0035

3.2 Mix Design

The proper mix design required for use with the 3D printer was developed to account for buildability, extrudability and compressive strength. Base level mixes were generated by the combination of water, sand, and portland cement. To increase the design's extrudability, varying ratios of water to binder and binder to sand were analyzed. The buildability and strength of the concrete were increased through the addition of chemical additives such as superplasticizer and accelerator.

To qualitatively test buildability and extrudability, samples of each mix were poured to determine how fluid the mix was. A slump test is typically conducted to measure this for concrete, however, due to a lack of research in this area for 3D printed concrete, a simple pour was done to visually analyze these properties. If the mixture sufficiently held its shape in the first pour, additional pours were done to test the mix design's buildability. Extrudability was tested by placing the mix in the printer and running the code for a basic print. If the mix was too dry the extrudability was low, as the mix would remain in the

printhead and when it extruded, would break along the print. If the mix was too wet, the extrudability was high, but buildability was low as it would not retain its shape.

After providing a seven day curing period, the mixes were tested for compressive strength. Cylinders were tested in a Tinius Olsen Machine that would provide tabulated values for average compressive strength. From this, the maximum value was given and the Young's Modulus was derived from the slope of the linear portion of the stress-strain curve provided from tested samples.

3.3 Mechanical Design

The design of the pavilion will leave the two ends of the arch system open for access and air flow. However, to determine user comfortability while seated on the interior, an HVAC analysis to determine the amounts of heating and cooling that were coming into and out of the pavilion was calculated. Hand calculations were performed that determined the respective R and U-Values for the original iteration of the final concept, as well as the final iteration of the final concept. These values were then used to calculate heating loads for the winter in Worcester, MA at an average temperature of 41.75^{o}F (5.42^{o}C) and at a worst case-scenario temperature of -6.9^{o}F (-21.61^{o}C) with an internal temperature of 70^{o}F (21.11^{o}C) that would represent the average and maximum heating loads. This process was then repeated to calculate the average and maximum cooling loads in the summer, with an average temperature of 78^{o}F (25.5^{o}C) and a worst case-scenario of 90^{o}F (32.22^{o}C). Initial calculations assumed a CMU R-Value for evaluation and different compositions containing 12 inch, 8 inch, and 4 inch thickness CMU and the filler material was determined to be ½ inch acrylic and 1 inch polycarbonate. Originally using given R-Values for module components, and later using hand calculated R-Values, the heating and cooling capabilities of the structure without any systems added were found.

4.0 Results and Discussion

4.1 Architectural Design

4.1.1 Concepts

The first concept for this pavilion was the coronavirus. This virus has overtaken the world and has forced humans to become socially distant. The idea was to follow the structure of the virus itself. A circular center area that could be used as general space, and smaller spaces coming out of that area to simulate the spikes that come out of the virus. Each space would have tables for users to be able to do work in, but allow enough space to have them socially distanced from each other. The visualization of this concept can be seen in Figure 8

below. This concept focused on the use of the structure, but not so much on the complications in making the structure functional and constructing it in a feasible amount of time.

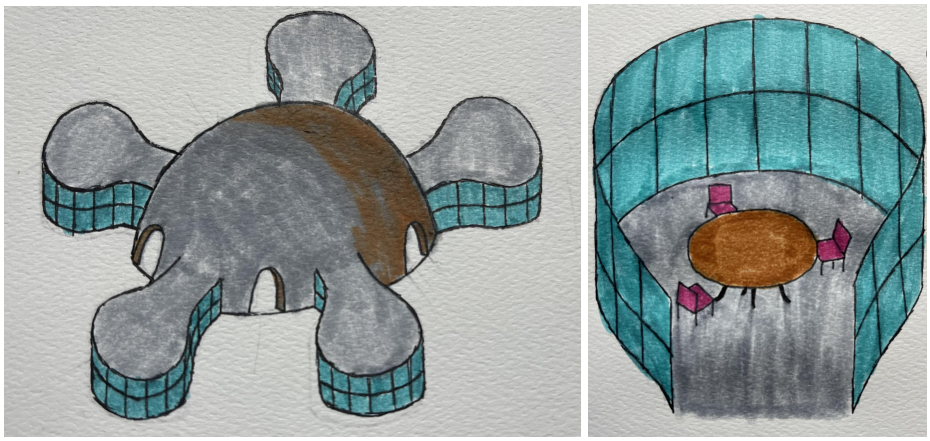

Figure 8: Coronavirus Concept Sketch

The second concept was to simulate the structure of gears working together. WPI is a technical school that is constantly innovating and reworking itself to adjust to the changing present, and the gears would bring an element to the technical side of the university. In looking at the floorplan, which can be seen in Figure 9 below, circular overlays would have been used to create rounded enveloping spaces for the users at varying levels while providing texture to the structure. The gear shaped outer circle areas would have been study spaces similar to the first concept, and much like the first concept, the center area would have been a general use space.

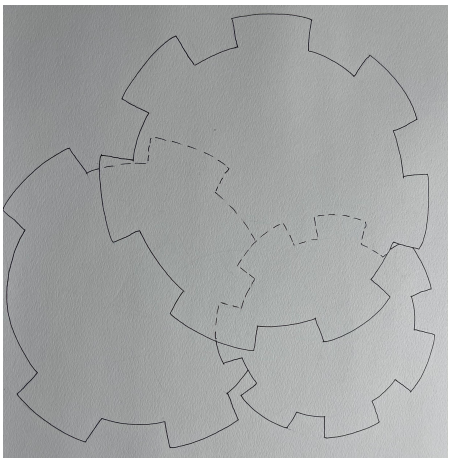

Figure 9: Gears Concept Sketch

The third concept, the one that inspired the current progress, was the one inspired through modular origami. This design is much more geometric than the others and consists of

an alternating repeating hexagon module that would create an arch. This concept allowed for the pavilion to be naturally lit throughout the daytime hours, and the cavities created by the joining of the modules together would be covered with glass, which can be seen in Figure 10 below, to allow for the structure to be used regardless of the climate. This concept design follows the path of an arch to create a tunnel-like structure that users can walk through and enjoy some time in throughout the day.

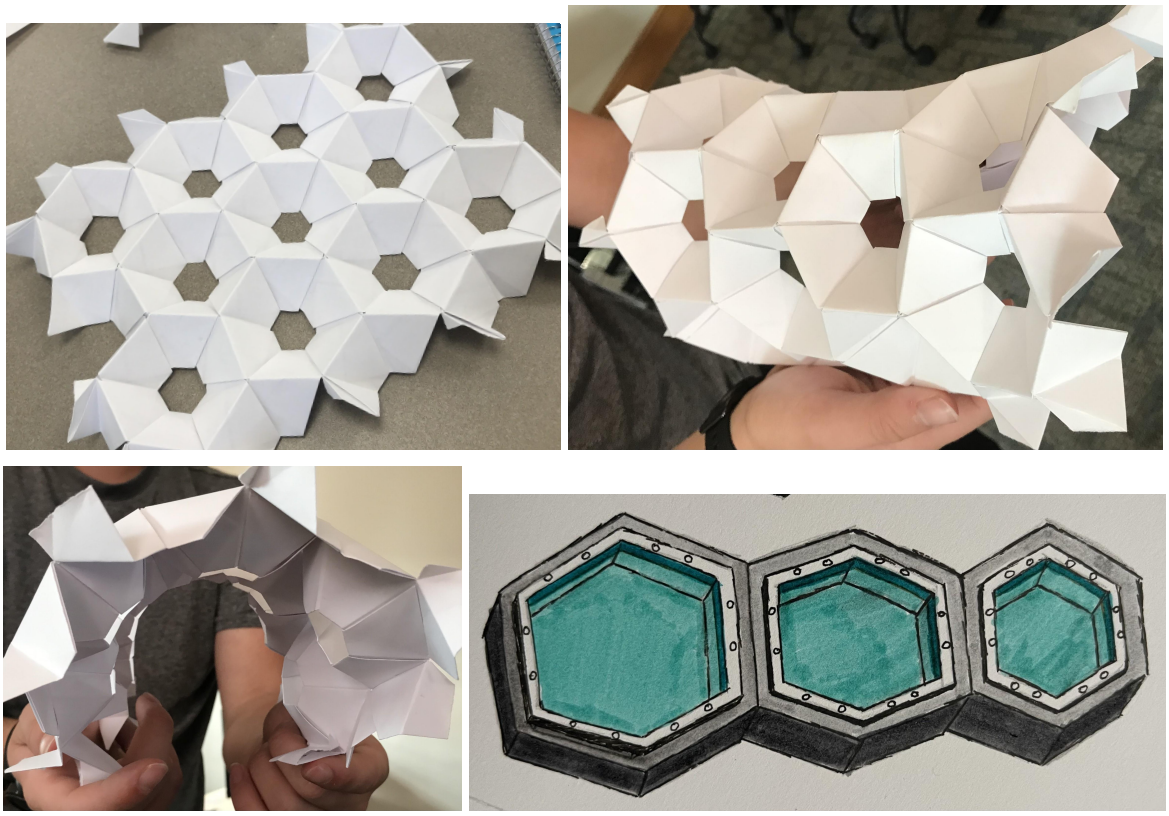

Figure 10: Modular Origami Concept

4.1.2 Final Design Concept

The final iteration of the concept resulted in an arch pathway that users would be able to walk through during the day while also being able to use it as an outdoor study space. The design remained inspired by modular origami and used the module pieces from the diamond designed hemisphere arch from the first iterations. Within the spaces the structure has window-esque components where at the seating level the users can open to create more airflow. At other locations above and below seating level they would be sealed. Tables and seating will be placed on the interior of the structure in varying locations and singular chairs will be present on the exterior and interior, much like the Adirondack chairs that were placed throughout campus during the pandemic. In Figure 11, a portion of the structure can be seen with the varying colors in acrylic sheets that are incorporated into the design. The idea was to

create a variation of colors that resembled the art installation by Stephen Knapp on Gordon Library to tie it in with WPI styling. During the day the different colors would come into the user, but at night, it would glow like the installation in its own way.

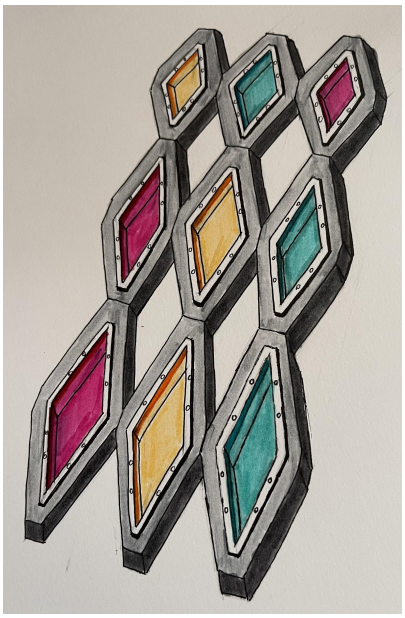

Figure 11: Window Feature Concept

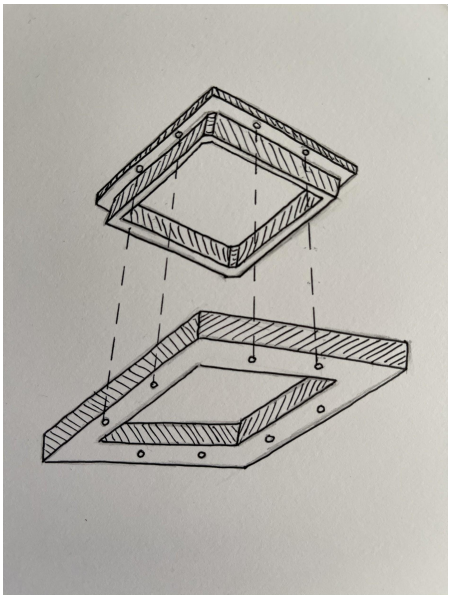

Figure 12: Joining of 3D Printed Window Piece to Module

To allow for the joining of the acrylic to the concrete, a window pane insert was designed that would be 3D printed with plastic and used as the connector. This design can be seen in Figure 12, and it is an inch and a half on the surface parallel to the concrete face as well as the surface perpendicular to it. The acrylic will then be bound to the plastic using epoxy and concrete screws will be used to keep all components in place once assembled.

4.2 Structural Design

Through the completion of the project, three different scenarios were considered and analyzed. The first scenario consisted of two modules, a hexagon and triangle, that once positioned, assembled a hemispheric arch. The second scenario changed the hexagon module to a diamond module and removed the need for two different units. In the third scenario the arch was no longer a semicircle, but was instead an inverted catenary.

4.2.1 Hexagon Structure

The preliminary design consists of modules that were inspired by origami nanotubes, represented in Figure 10 above. Through the production methods of additive manufacturing, the same module could be printed several times and later assembled.

Each module was developed in Solidworks through concentric hexagons, where a smaller hexagon in the back was offset one foot from the larger one in the front. This can be seen in Figure 13 below. The front-facing hexagon diameter was two feet (0.6096 m), with each side at one foot (0.3048 m) long. The inner hexagon diameter was 1.79 feet (0.5456 m), with each side at 0.895 feet (0.2728 m) long. The thickness offset in the x-direction of the module was 1.2 inches (3.048 cm). Provided from the modeling software, an estimate of 33.46 pounds was given for each module.

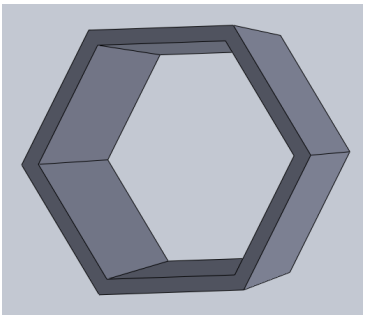

Figure 13: Hexagon Module

With the module developed, a fundamental finite element analysis was conducted using the Solidworks simulation feature (Figure 14). To simulate the module's behavior in the structure as a whole, the bottom was fixed in all directions and the two outside corners were locked in the horizontal direction to simulate the effect of having other modules from other rows. An external distributed load of 1.12 lbf (5 N) was applied across the top face to view a general deformation pattern. Running this simulation pointed to the areas of the module with the highest concentrated stress value. Figure 14 displays the exaggerated deformation of the module with the established boundary conditions. It can be seen that there was bending occurring along the top and side faces of the hexagon, which would fail a concrete structure.

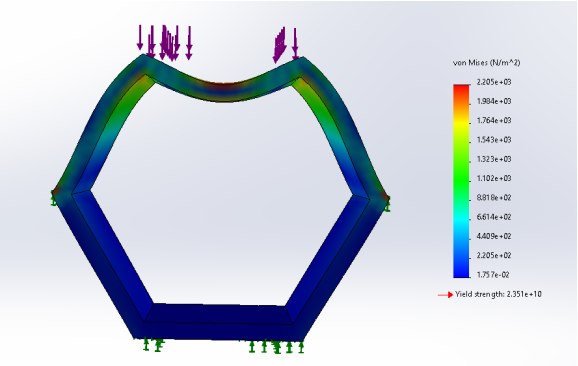

Figure 14: Finite Element Analysis of Hexagon Module

This first scenario consisted of seventeen hexagonal modules assembled into a hemispherical arch, as shown in Figure 15. The next row of modules would need to be

shifted half a module to fit within the gap created by the modules being assembled together. However, the individual rows of modules overlapped with each other and did not align with the gap left by the other row. As the original assembly design was not functioning as intended, a second module was developed (Figure 17). The design was intended to fit into the space created from the connection of two rows of hexagon modules (Figure 16). This module proved to be beneficial as it allowed for the design to be assembled as intended and aided in preventing the hexagon modules from being compressed and bowing outwards.

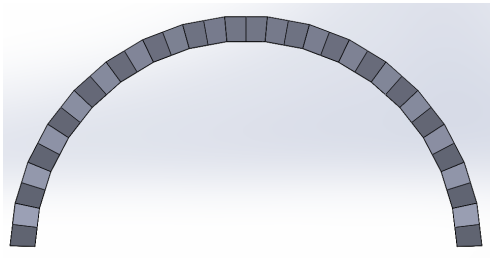

Figure 15: Assembled Hexagon Archway

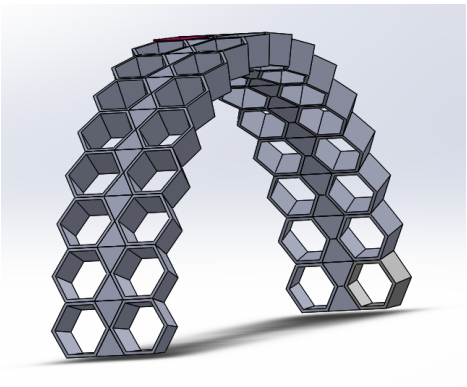

Figure 16: Second Hexagon Design Iteration

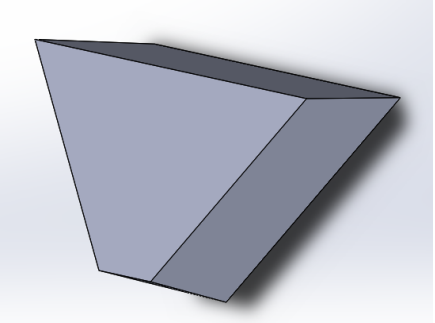

Figure 17: Triangle Filler Module

4.2.1.1 Structural Analysis of Hexagon Structure

An analysis of the structure designed in Solidworks was done in Abaqus, a finite element software, where the assumed material properties were applied. It was found that when using Abaqus, it was essential for material properties to remain in the same unit convention. In this case, the units were converted to english units. The material properties applied to the assembly were:

Mass Density = 0.810185 lb/in3 (1,400 pcf)

Young's Modulus = 4,000,000 psi

Poisson's ratio = 0.2

An essential facet of finite element analysis lies in understanding and applying a mesh size for the desired analysis - the lower the mesh size, the more precise the results. As the software was limited to 250,000 nodes and the arch assembly was a large structure, the default mesh size was increased. The meshed arch can be seen below in Figure 19.

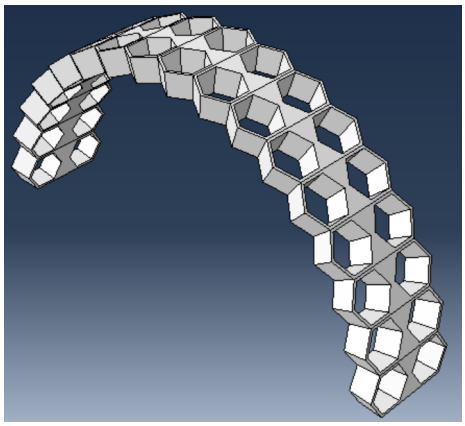

Figure 18: Hexagon Structure in Abaqus

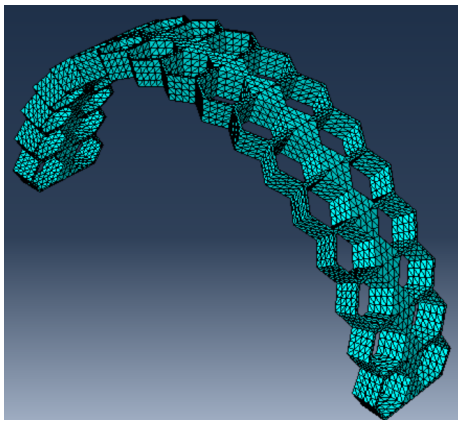

Figure 19: Hexagon Structure after Mesh

Once the arch assembly was meshed, boundary conditions were applied to the structure in order to be loaded. The bottom faces in both ends of the arch were fixed, while the corners on edge were fixed only in the horizontal direction to mimic the behavior if other rows were placed. These boundary conditions can be seen in orange in Figure 20 below. A gravity load was applied to simulate the structure under its own weight. The gravity force applied was 386.09 in/sec^2 (9.8 m/sec^2), represented as a yellow line in Figure 20.

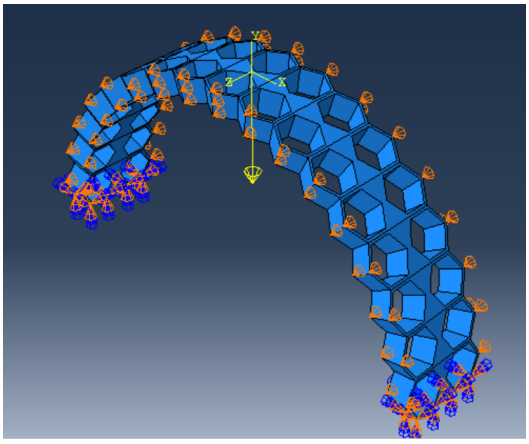

Figure 20: Boundary Conditions and Gravity Force on Hexagon Structure

A simulation was run where Figures 21 and 22 show the vertical and horizontal deflection of the assembly. The assembly is shown to deform downward 11.83 inches (30.0482 cm). As concrete is a brittle material, at these deformation levels the assembly would fracture and catastrophically fail. Figure 22 displays the horizontal displacement of the assembly. Because each of the modules was fixed along their edge from moving outward, minimal deflection is seen in this direction. There was bending occurring in the sides of the hexagon modules, which is indicated in blue and orange in Figure 22. The bending of concrete also creates fractures in the structure, leading to failure.

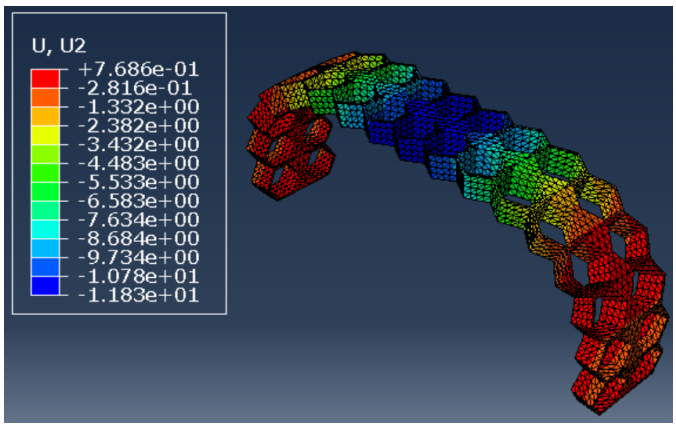

Figure 21: Vertical Deflection in Hexagon Structure(Inches)

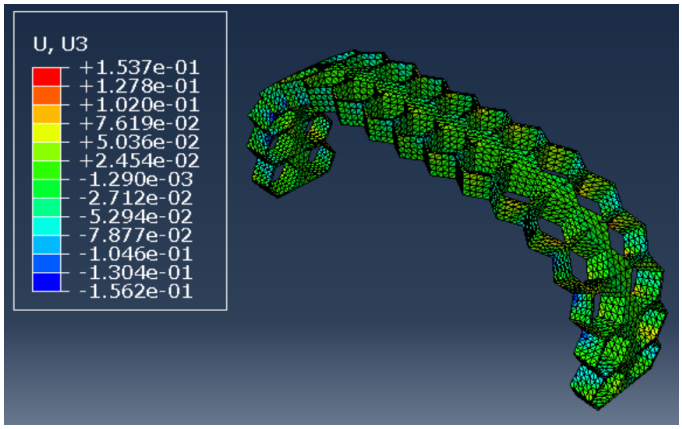

Figure 22: Horizontal Deflection in Hexagon Structure(Inches)

4.2.2 Diamond Structure

The second scenario consisted of diamond-shaped modules. Each diamond module was two feet (0.6096 m) tall, one foot (0.3048 m) wide, and one foot (0.3048 m) in depth. The module's walls were thicker to prevent fractures and the interior corners were rounded, as shown in Figure 23. This module was analyzed with the bottom face fully fixed and the two opposing edges locked in the horizontal direction. It was loaded with a distributed load

of 1.12 lbf (5 N) across the top face, as shown in Figure 24. Much less bending occurred in the diamond module than the hexagon module due to the modifications.

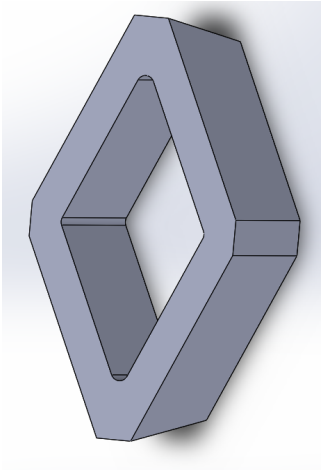

Figure 23: Diamond Module

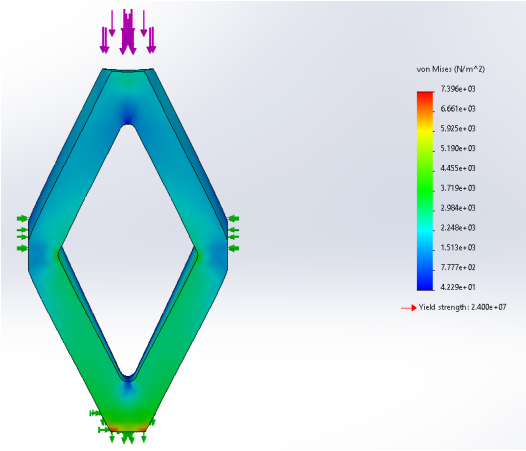

Figure 24: Von Mises Stress of Diamond Module

The top and bottom faces of the diamond formed a six degree angle with the horizontal axis to create a hemispheric arch once assembled. The arch path consisted of 15 modules with a radius of 9.5 feet (2.8956 m) to the outer face of the modules.

4.2.2.1 Structural Analysis of Diamond Structure

This assembly was imported into Abaqus, and the same material properties were applied as the hexagon. An elastic analysis was conducted to ensure that the structure would stand under a gravity load. A concrete damage analysis was also conducted to observe points within the structure that would undergo plastic strain. Concrete cannot be put into plastic strain because it will fracture, thus, this analysis was conducted to find the fragile points in the design to optimize the module further. In this analysis, the material properties in Table 2

for yield stresses in compression and tension and plastic strain values for crushing and cracking (Amadio, Claudio & Akkad, Nader & Fasan, Marco, 2015) were used as well as in the elastic analysis.

Material's parameters				Compression behaviour				Tension behaviour			
Elasticity		*Plasticity*		*Yield Stress (MPa)*	*Inelastic Strain*	*Damage Parameter*	*Inelastic Strain*	*Yield Stress (MPa)*	*Cracking Strain*	*Damage Parameter*	*Inelastic Strain*
Class	20/25	Dilation Angle	38°	11.2	0	0	0	2.9	0	0	0
E[GPa]	30	Eccentricity	0.1	18	0.0007	0	7.5E-5	1.6	0.00015	0	3.3E-5
v	0.20	fb_0/fc_0	1.12	21	0.001	0	9.9E-5	0.75	0.00035	0.4064	16.0E-5
		K	0.666	26	0.002	0	15.4E-5	0.25	0.0006	0.6964	28.0E-5
		Viscosity	0.002	20.5	0.0034	0	76.2E-5				
				13	0.005	0.1954	255.8E-5				
						0.5964	567.5E-5				
						0.8949	1173.3E-5				

Figure 25: Damaged Concrete Plasticity Table (Amadio, Claudio & Akkad, Nader & Fasan, Marco, 2015)

The diamond arch was fixed on its bottom faces and fixed in the horizontal direction on all edge faces, as well as the application of a uniform gravity load (Figure 26). Under the gravity load, the assembly deforms downwards one inch, a vast improvement from the hexagonal assembly, but still in excess of allowable deformation, which results in fracture.

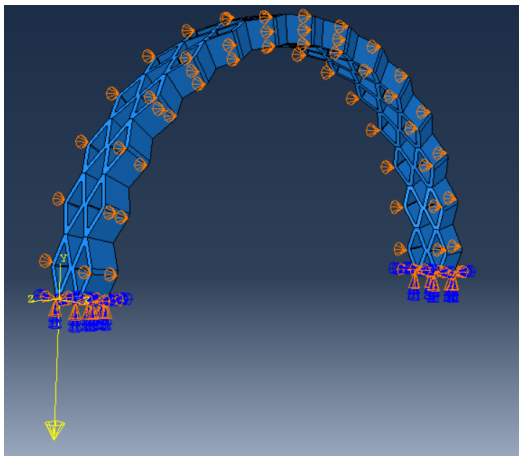

Figure 26: Boundary Conditions and Applied Load of the Diamond Structure

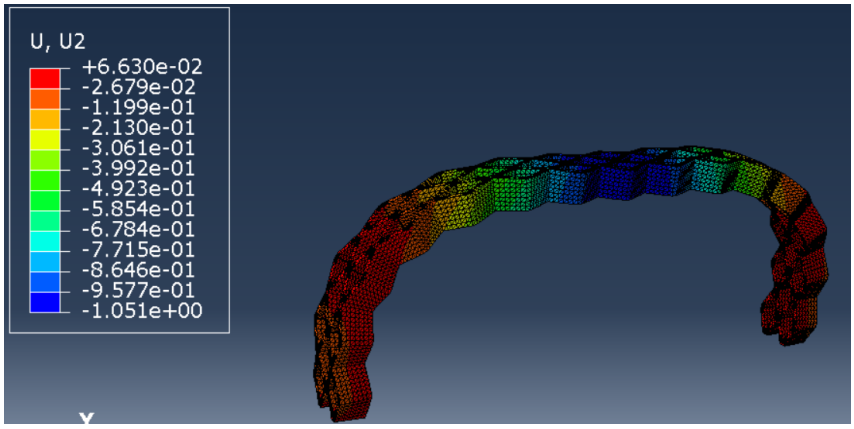

Figure 27: Vertical Deformation of the Diamond Structure(Inches)

With the concrete damaged plasticity analysis, the structure would fail because of key points undergoing plastic strain. For the analysis to succeed, the structure needed to be loaded past the point of failure. As the diamond scenario failed under gravity, the load was not modified. In Figure 28, the green and red areas represent the plastic strain, with the most plastic strain occurring at the base and the joints between the rows. With this information, the diamond modules were optimized by increasing edge thickness.

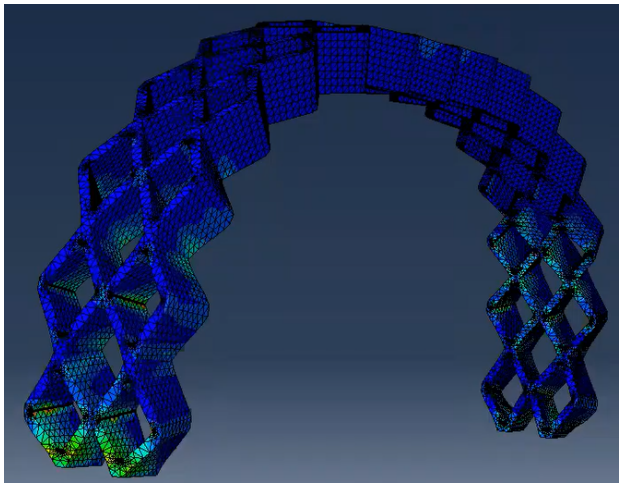

Figure 28: Plastic Strain of the Diamond Structure

4.2.3 Catenary Structure

A catenary curve is created by hanging a cord, or chain, of uniform weight from two endpoints (Figure 29). If this curve were to be inverted, it would create a natural load path so that a structure could be entirely in compression. The strength of concrete lies in its compressive capabilities, and an inverted catenary would be the ideal shape for the assembly.

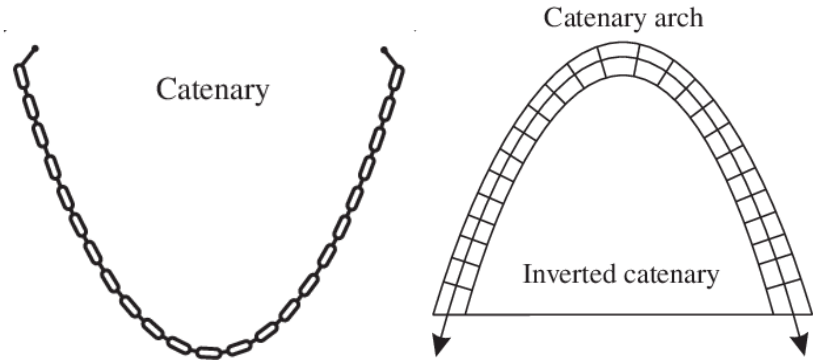

Figure 29: Catenary Curve and Inverted Catenary

In the previous scenarios, the assemblies consisted of the same module encompassing the arch. However, in a catenary pattern, the modules must all be different to account for the narrowing of the arch as it reaches the top. The side lengths were determined using a nine foot (2.74 m) base width. Figure 30 below displays the length that each unique module would have, varying from 2.05 feet (0.62 m) to 0.897 feet (0.27 m). The values on the left side of the image represent the height of the curve passing through the vertical separation lines, while the values on the right represent the member lengths. The values located on the bottom represent the horizontal distance between the vertical lines.

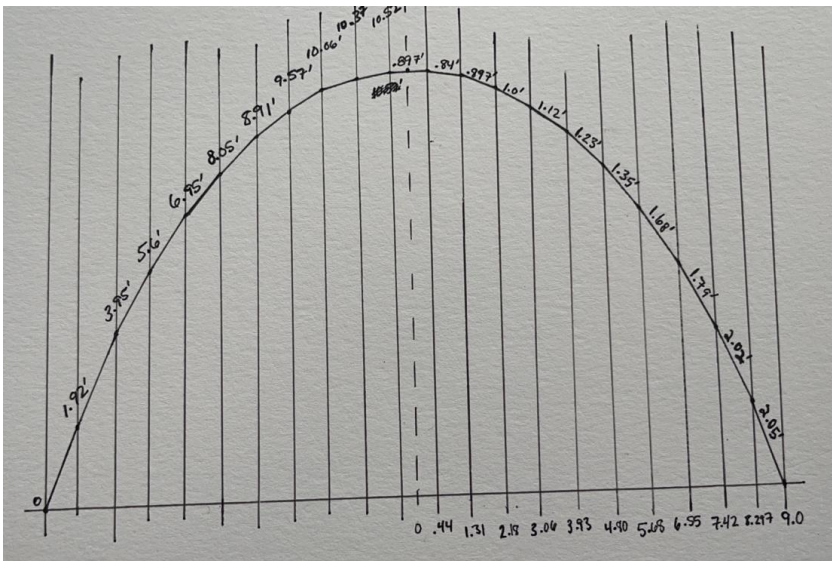

Figure 30: Catenary Dimension Analysis

Using the values given in Figure 30 and the angles determined through trigonometry, twenty-one different modules were modeled in Solidworks. The values were treated as coordinates, and a catenary curve was drawn. To give the assembly a uniform thickness, the curve was offset three inches as well as 12 inches in order to compare analysis results. Figures 31 and 32 below represent the construction of the catenary in a singular row and then

a sequence of them. While it would be tedious to develop twenty-one unique modules using traditional methods, it is easier accomplished through 3D printing.

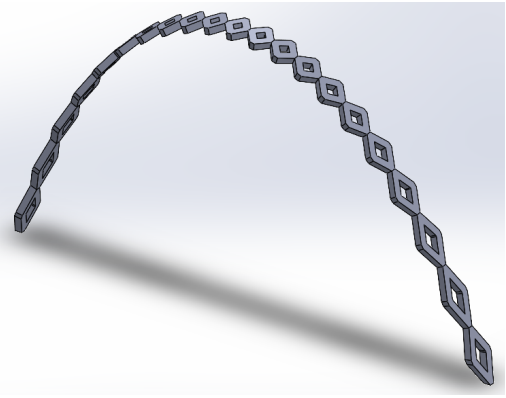

Figure 31: Catenary Arch Assembly

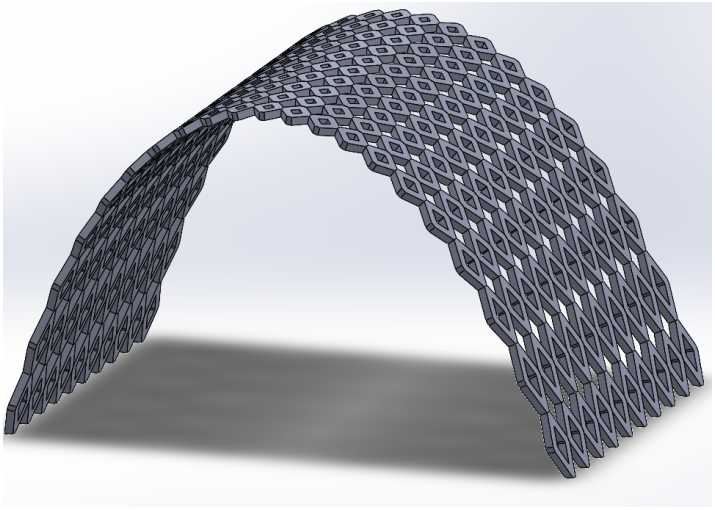

Figure 32: 10 Rows of Three Inch Thick Catenary Arch

4.2.3.1 Structural Analysis of Catenary Structure

The different thickness assemblies were uploaded into Abaqus for analysis, and the same density, elastic modulus, and Poisson's ratio were applied as the previous diamond and hexagon assemblies. Each assembly's strain was to be found and compared to the other thicknesses in addition to the vertical deflections. Strain was used as the measurement as it represents a more defined failure point than deflection. The maximum permissible compressive strain of concrete is given by 0.003 to 0.0035 in/in and 0.00015 to 0.00025 in/in for maximum permissible tensile strain (Shen, 2019). Figures 33 and 34 provide the vertical deflection for the 12 inch catenary as well as the three inch one at deflections of 0.34 inches

and 1 inch, respectively. This made clear that even as the modules' weight was increasing, the less the arch assembly deflected. Initially the thought was that the structure would remain thin so that the modules' weight would not cause as much of a deflection, but the results of analysis presented an opposing effect.

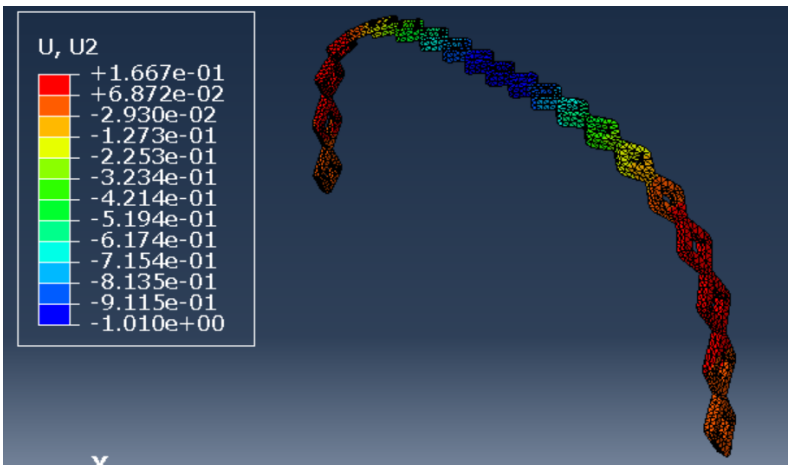

Figure 33: Vertical Deflection of 3 Inch Catenary(Inches)

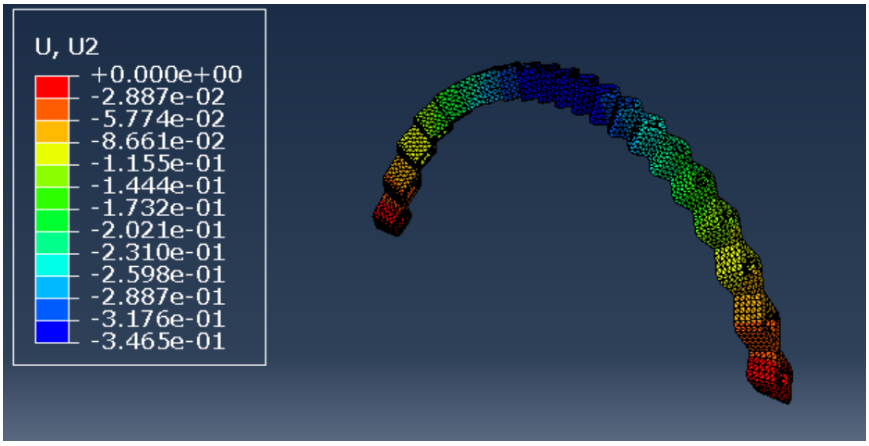

Figure 34: Vertical Deflection of 12 Inch Catenary(Inches)

Tensile and compressive strain were compared for the different arch assemblies along with maximum vertical deflection. Figures 35 and 36 convey the principal tensile strains for the three and 12 inch assemblies. Both assemblies have maximum tensile strains above the acceptable limit for concrete. In Figures 35 and 36, a majority of the values listed on the left surpass the limit for the tensile strain of 0.00025 in/in. Although the bulk of the structure was shaded in dark blue, the only acceptable value for strain, the structure would fail as the limit is surpassed in critical locations such as the corners of the modules and the structure's base.

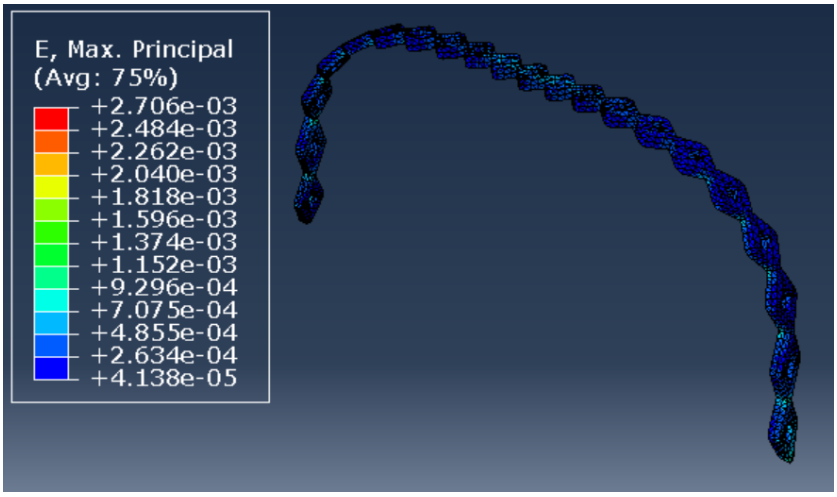

Figure 35: Principal Tensile Strain for 3 Inch Catenary

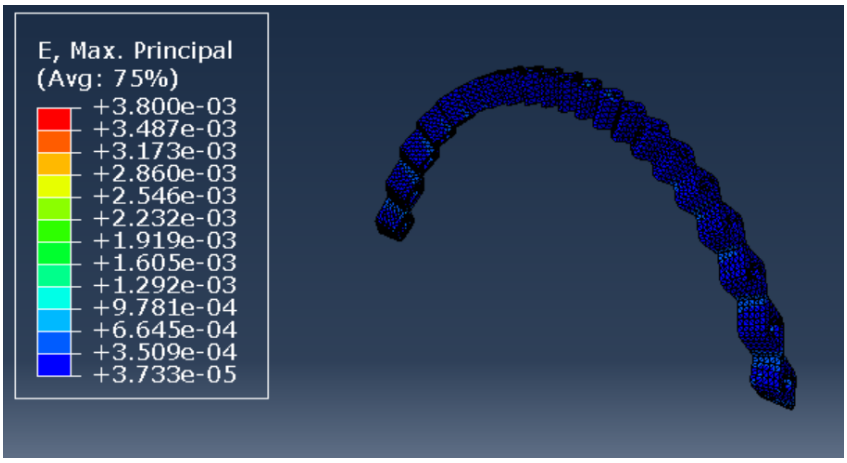

Figure 36: Principal Tensile Strain for 12 Inch Catenary

In Figures 37 and 38, the maximum allowable compressive strain of 0.0035 in/in is also surpassed for a majority of the listed values on the left. For compressive strain, the arch assemblies would stay below the strain limit until the green region. As the compressive strain limit is surpassed, the concrete would fracture in those areas.

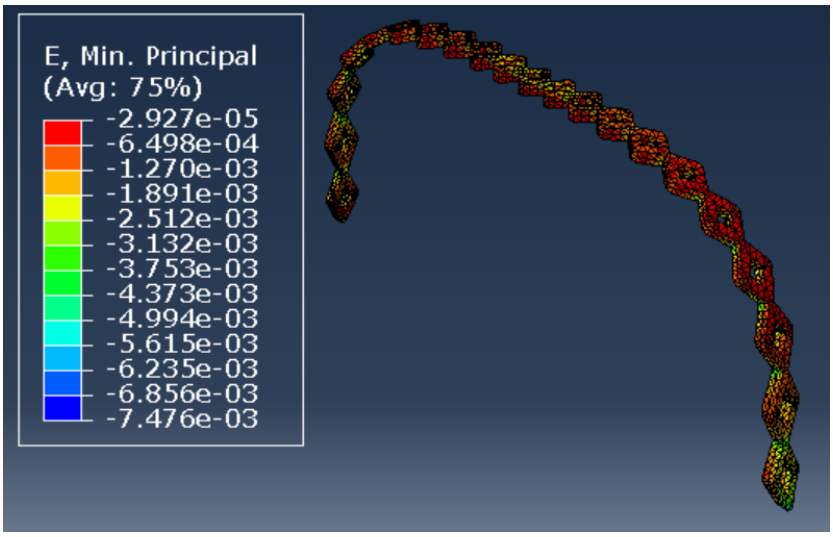

Figure 37: Principal Compressive Strain for 3 Inch Catenary

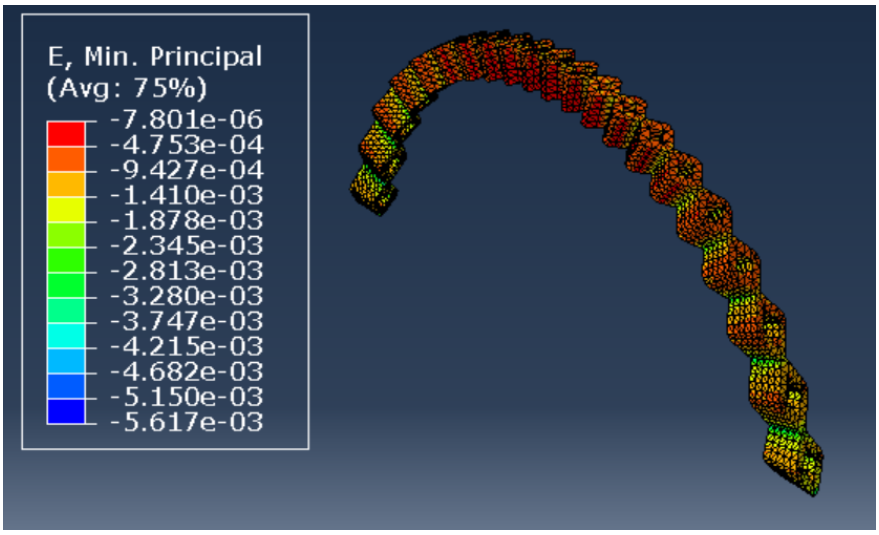

Figure 38: Principal Compressive Strain for 12 Inch Catenary

Upon analyzing the results, the thinner assembly experienced less tensile strain than the thicker assembly, while simultaneously experiencing a greater compressive strain. This was expected due to the increase of the weight of the modules. The thicker modules created greater tension in the assembly because of the support of the heavier upper modules. At the same time, they were able to experience more compressive strain due to the thickness distributing the stresses. The inverse occured for the three inch assembly. The modules were lighter than the 12 inch module, which proved to reduce tension in the assembly, but they were less capable of supporting the compressive load coming from the modules above. As such results were presented, the thinner design was deemed the better alternative as it had a lower value for tensile strain than the thicker design.

4.3 Laboratory Testing

4.3.1 Mix Design

Initial testing of the mix design began as a test to create a base ratio of water to cement to sand before including any chemical additives. From this base, chemical additives, such as superplasticizer and accelerator, were added in small increments, and the quantities of each ingredient for the first six mix designs can be seen in Table 3 below. The results of the buildability and extrudability tests for each mix design can be seen in Table 4. The remaining concrete was used to create 2" diameter by 4" tall cylinders in order to obtain and compare compression tests for each mix design. Photographs of the cured and crushed cylinders developed for each mix can be found in Appendix A.

Table 3: Mix Design Laboratory Trials

	Mix 1	**Mix 2**	**Mix 3**	**Mix 4**	**Mix 5**	**Mix 6**
Sand (kg)	1.400	1.4048	1.4002	1.4002	1.4006	1.4001
Cement (kg)	0.7781	0.7747	0.7706	0.7713	0.7742	0.7761
Water (L)	0.325	0.300	0.285	0.275	0.275	0.300
W:C Ratio	0.418	0.387	0.370	0.357	0.355	0.387
Superplasticizer (mL)	0	5.0	5.0	5.0	2.5	2.5
Accelerator (mL)	0	0	0	0	0	2.5

Table 4: Mix Design Buildability and Extrudability Results

Mix Design	**Results**
1	Base test; flowed well, not enough structure to build
2	Too much liquid, buildability low, extrudability high
3	Too much water, buildability low, extrudability high
4	Less water, buildability medium, extrudability high
5	Ideal quantity of water, buildability high, extrudability high
6	Not enough water, buildbility high, extrudability low Reduce accelerator quantity

Each of the mix designs were tested to determine their compressive strength values. Three samples from each mix were used to provide for a larger sample size and eliminate irregularities. The stresses for each test were provided by the software, while the Young's modulus was calculated. Upon calculation for the modulus, there was a large variation in value between the three samples of each mix design. The results of those tests can be seen in Table 5 and Figure 39 below. Table 5 presents the maximum and minimum stresses for each mix, as well as the maximum and minimum Young's Modulus. Figure 39 displays the average Young's Modulus, along with one standard deviation bars above the values.

Table 5: Initial Mix Design Strength Results

	Mix 1	Mix 2	Mix 3	Mix 4	Mix 5	Mix6
Maximum Stress(psi)	3,902	6,225	7,230	5,250	6,193	1,950
Minimum Stress(psi)	2,828	5,305	5,768	3,050	4,435	1,779
Maximum Young's Modulus(psi)	280,495	474,854	740,555	687,909	586,040	137,558
Minimum Young's Modulus(psi)	135,182	387,012	558,034	286,645	344,865	65,695

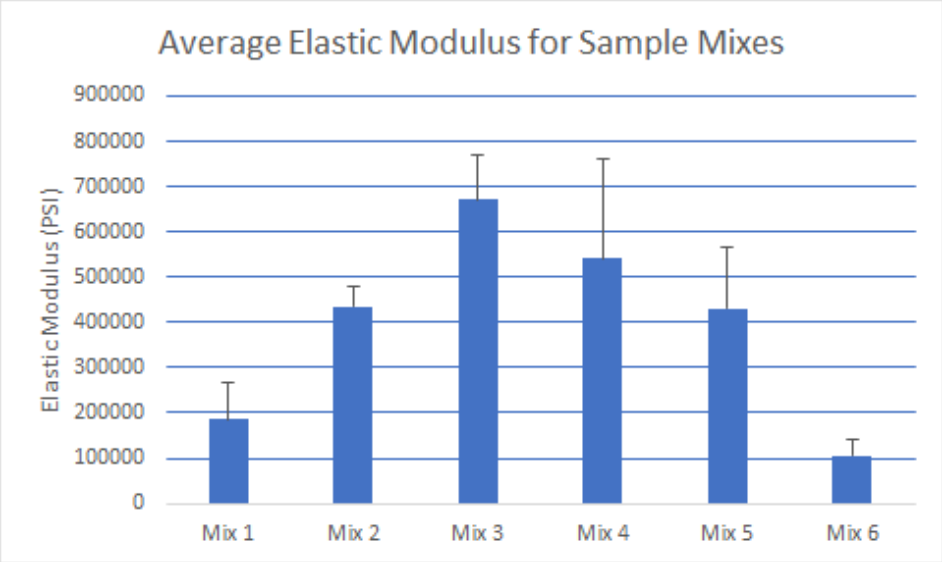

Figure 39: Average Elastic Modulus for Test Mix Designs

All of the mixes either contained too much liquid and were unable to hold their shape, or were too dry and would likely be unable to be extruded from the printer nozzle. This meant that none of the mix designs were suited for the printhead. The manufacturer was able to provide a mix design that would be tested with the printer. The mix contained additives that were absent in the original designs, as well as varying ratios of additives than previously analyzed. It called for the addition of cellulose, micro-silica, fast setting and hardening

cement, an expansive agent, and water reducer. The percentages for each of these materials is provided below in Table 6.

Table 6: Mix Design from Manufacturer

Material	Amount(Percent)
Sand	41.83%
Cement	33.46%
Micro-silica	4.18%
Cellulose	0.01%
Fast Setting and Hardening Cement	3.70%
Water	13.23%
Water Reducer	0.41%
Expansive Agent	3.18%

The mix design provided by the manufacturer was specific about the percent ratio of each material but did not specify the type of material. Micro-silica was assumed to be silica fume, while cellulose was assumed to be small fibers that would increase the buildability of the mix. The specific types of water reducer and expansive agent used were not listed as well. Due to the lack of specificity, some ingredients were excluded from the initial tests with this mix design. A simplified version of the mix is shown in Table 7 below, and Figure 40 depicts the two 2” diameter by 4” tall cylinders that were made from this mix. These cylinders had better buildability and extrudability for 3D printing with this printer. The mix had a relatively small amount of water but was able to flow well and was capable of piling multiple layers without collapsing. Additionally, they set rapidly, an important characteristic in 3D printing, as the bottom layers must harden rapidly in order to support additional layers printed above them.

Table 7: Original Mix Design Used for Printing

Concrete Mixture	Amount (grams)
Cement	1675
Silica Fume	213
Fast Setting/Hardening Cement	187
Sand	2100
Water	677
Water Reducer	20.4

Figure 40: Cylinders Following Manufacturer's Mix Design

Various trials resulted in an additional 75 to 100 grams of water added in 10 gram increments to the mix provided by the manufacturer, as the original mix was unable to flow constantly through the nozzle of the printer. This method was used to avoid over saturating the mix, as once this happened the water was unable to be extracted from the mix. To

determine the extrudability of the mix it was inserted into the printer. If the mix was too dry to be extruded, more water was added once the mix was removed from the printhead. This process was repeated until there was successful extrusion from the printhead, or the mix became oversaturated through the addition of liquid. An ideal mixture consistency was derived from the trials conducted previously.

The research of additional mix designs and print testing resulted in a final mix design related to the one provided by the manufacturer, but included no fast setting and hardening cement. The design mixture for this was found in a report working with 3D printing concrete (Okamura, 2012) and instead, called for the addition of a superplasticizer and accelerator. Table 8 displays the amount of each ingredient included in the final mix design that was used through the end of the project.

Table 8: Final Mix Design

Concrete Mixture	**Amount (grams)**
Cement	1,158
Silica Fume	496
Sand	2,482
Water	603.2
Superplasticizer	8.27
Retarder	8.27
Accelerator	8.27

The mix provided in Table 8 includes the addition of extra water. Following the design precisely resulted in a dry concrete mix, and using trial and error, water was added in increments of about 10 to 20 grams to avoid oversaturation. A mix was finalized and was extruded out of the printer to print a seven layer test code as shown in Figure 41. This was a breakthrough from other mixes as only two layers were able to be applied in previous trials.

Figure 41: Seven Layer Test Print

The mix was replicated in order to optimize the amount of water required for the ideal consistency. A detailed set of instructions were created to allow for this final mix design to be reproducible. The mixing instructions, located in Appendix C, include how long to mix for, how fast to mix, the amount of water added, and the intervals in which they were added. From the instructions, three 2” diameter by 4” height test cylinders were produced. None of the cylinders printed were precisely 2” in diameter or 4” in height (Figure 42) as they were irregular in shape, so the compressive strength test results could not safely be used as the mix's compressive strength. It would not be prudent to assume that the 3D-printed concrete is consistent throughout, as in the exterior, where the layers meet, there would be stress concentrations. On the interior, the concrete is uniform, which would make it much stronger than the exterior. This further reinforced the assumption of generic concrete values for the structural analysis. A method to use exact compression values for 3D printed concrete instead of generic values would be to print a large cylinder and extract a small cylinder from the core that would have uniform shape and properties. Once extracted, the cylinder would then have to cure before testing. Due to time constraints, this process was not utilized.

Figure 42: 2” x 4” Inch Test Cylinders Using Final Mix Design

There were several iterations to advance from the original mix design to the final mix design that was capable of being printed successfully. The concrete necessary for 3D printing has a different ratio of ingredients from typical structural concrete. Through much trial and error, as well as referring to existing resources, a mix design was created that had the potential to work for 3D printing.

4.3.2 Concrete 3D Printer

4.3.2.1 Setup

When the project began the printer had not yet arrived on campus, but it was in transit. When the printer arrived there were discussions on where the printer was to be housed, and the printer sat unpackaged for a full term. After it was determined that the printer would be located in the Structural Laboratory in Kaven Hall, it had to be unpackaged and moved into this area. Professional movers were needed to move the printer into its permanent location. Once the printer was in place, an electrician was called to run power directly to the machine. The first time the printer was turned on was in November of 2020.

4.3.2.2 Sensor Troubleshooting

Two photogate sensors on the y-axis had been broken during the installation process of the printer. The two sensors were what controlled the printhead along the y-axis. The printhead was manually moved in the x and z-axis to attempt extrusion. This trial proved that the concrete was too dry for extrusion, and thus the mix was modified. Once a sufficient mix was developed, it was possible to extrude the concrete manually, however, there were several flaws. First, the printhead did not follow a linear path for the layers of concrete to remain on top of each other, and the mix design was dry. The second reason was that in order to print multiple layers, the second layer had to be perfectly aligned with the base layer, as there was

no control in the y-axis. Small pieces of concrete would fall off of the base layer and roll, which can be seen in Figure 43 below. This prevented the adhesion between layers and the continuity of the layers before the sensor could be repaired. A video call with the manufacturer diagnosed the sensor complication and new sensors were replaced.

Figure 43: Manual Print of Concrete

4.3.2.3 G-Code Files

A concrete 3D printer, like most plastic 3D printers, requires an input of a gcode file. The gcode files for this project were generated using an old version of Cura, version 15.02.1, as newer versions were not suited for the printer. Models created in Solidworks were saved as STL files, imported into Cura, and exported as gcode files for printing. A custom printer was created and values for the dimension of the print space, nozzle diameter, and print speeds were added into Cura. Using a sample gcode provided by the manufacturer, the pattern shown in Figure 44 below was printed. The use of new gcode revealed that the header and footer of the sample gcode file must be used for the printer to operate. Once this was discovered, a gcode for any Solidworks model could be printed.

Figure 44: Sample G-Code Test

4.3.2.4 Operating and Cleaning the Printer

First, the printer was turned on and prepared for the mix by dampening the interior of the printhead with water. Once damp, the mix was poured into the hopper and the mixing screw was turned until a steady stream of mix extruded from the nozzle. Next, the desired gcode was selected and printed. Detailed directions on printer use with images are located in Appendix D. Once the print job was complete, the printhead was cleaned. The print head was taken apart and all parts were thoroughly rinsed off and left to dry. Detailed cleaning instructions are located in Appendix E.

4.4 Mechanical Design

4.4.1 HVAC Analysis

For the purpose of heating analysis, the structure was assumed to be enclosed, and the two ends were assumed to be composed of the material that will be filling the gaps in the concrete modules. The original calculations were conducted for both heat loss and gain, which was then done for the summer and winter temperatures. The calculations were also done for different thicknesses concrete as a basis, set initially at 12, 8, and 4 inches (0.3, 0.2 and 0.1 meters) thick. Additionally, two types of infill material were used for the air spaces in the design, which are to be used as windows, in order to determine heat gain and loss for one material versus the other. To obtain composition R and U-Values, the convection coefficients, h, of air were needed. These are given as 8 W/mK for inside air, and 20 W/mK for outside air. The R-values and U-values seen in Table 9 below are obtained from using the equations:

$$R = x/k \qquad \text{(eq. 1)}$$

where:

x = thickness of the material (m)

k = the thermal conductivity (W/mK)

$$U = 1/R \qquad \text{(eq.2)}$$

where:

R = R-value of component (m^2K/W)

Table 9: R and U-Values for Individual Materials

Material	R-Value (m^2K/W)	U-Value (W/m^2K)
Concrete 12” (0.3m)	0.4798	2.0842
Concrete 8” (0.2m)	0.3782	2.6441
Concrete 4” (0.1m)	0.2766	3.6153
Acrylic ½” (0.01m)	0.2418	4.1349
Polycarbonate 1” (0.025m)	0.3087	3.2396

After the determination of the R-values for each building component individually, the surface area for each piece of the structure had to be calculated in order to determine final heat loss and gain. This process was repeated for both iterations of the pavilion. The areas of each material can be found in Table 10 below and were given by software outputs in which the structures were modeled.

Table 10: Surface Area Values for Components of Hemisphere Arch Designs

Surface	**Area (m^2)**
Diamond Design	
Diamond Shape	0.0637
Air Space within Module	0.051
Air Space between Modules	0.1148
Hexagon Design	
Hexagon Shape	0.0527
Air Space within Module	0.1885
Diamond Shape	0.0804

In addition to the R-values of each material and the surface area it would cover, the inside and outside temperature variations were needed. A standard 70°F (21°C) was assumed for the interior temperature, and the outdoor temperature was determined based on the location of the structure. For analysis purposes, Worcester, MA was used as the location, and an average as well and worst case-scenario temperature was found for both the winter and summer seasons. The values can be seen in Table 11 below:

Table 11: Seasonal Temperature Values for Worcester, MA

	Temperature (°C)
Winter	
Average	5.42
Worst Case Scenario	-21.61
Summer	
Average	25.5
Worst Case Scenario	32.22

After acquiring the information needed, the heat loss and gain were calculated for the modules as individuals, and then the structure as a whole. Due to the nature and size of the shapes, in the original hemispherical design, there are 17 hexagon modules in an arch, and there are 15 diamond modules in an arch in the diamond design. At a length of 36 ft (10.97 m), in the hexagon design there were going to be 306 hex modules and 289 filler diamonds. In the diamond design, there were going to be 540 diamond modules, with 490 filler pieces. In order to best determine the composition to move forward with for each design, calculations were completed for every possible combination of materials, and temperatures. The values for these gains and losses are presented in Tables B.1 and B.2 in Appendix B.

The results aforementioned are all in reference to the original idea that the model was to be hemispheric in nature and consisted of either the hexagon or diamond modules. As the project progressed, the form of the pavilion was changed to allow for a natural flowing arch in the form of a catenary. In a catenary arch, as the structure moves towards the keystone piece, the parts that it consists of change shape. The length of each piece was kept the same, but the height was adjusted to account for the new shape. Because each shape was now

unique, the HVAC calculations were adjusted to account for differences in areas and module count within the new arch. The areas for each part were updated and replaced as seen Table 12 below:

Table 12: Surface Area Values for Catenary Design Components

Part	Concrete Surface Area (m^2)	Air Space Area (m^2)
1	0.0883	0.029
2	0.094	0.0314
3	0.0819	0.0262
4	0.0722	0.0216
5	0.0645	0.0178
6	0.0585	0.0145
7	0.05398	0.0118
8	0.0495	0.0089
9	0.0485	0.00824
10	0.0471	0.00734
11	0.0467	0.00706

A sample calculation for calculating heat gains and losses can be seen below. The example provides calculations for 12” (0.3m) thick concrete with ½” (0.01m) thick acrylic in an average winter temperature difference. Figures 45, 46 and 47 below depict the visualization of a module of the pavilion used to calculate the heat gains and losses and the visualization of the end pieces.

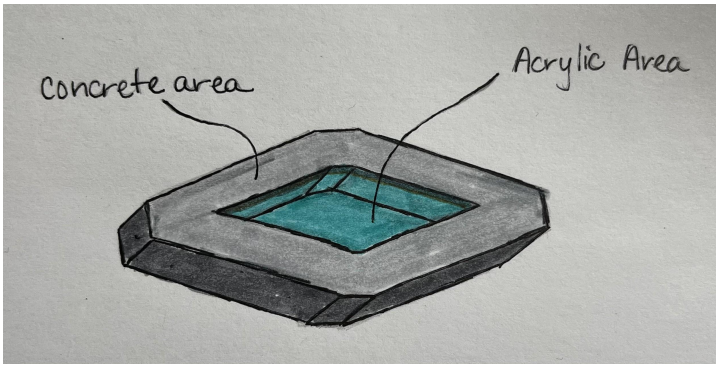

Figure 45: 3-Dimensional View of Module for Analysis

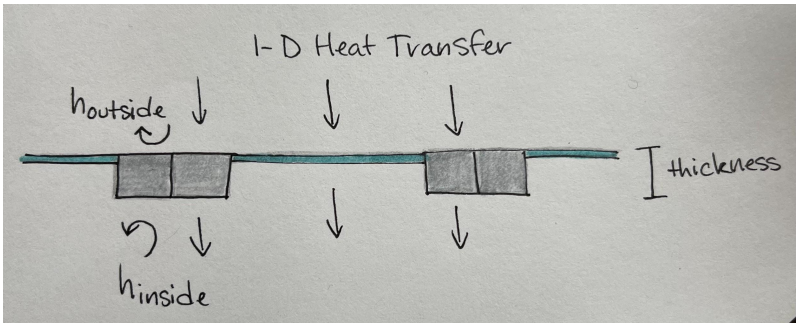

Figure 46: Side View of Module for Analysis

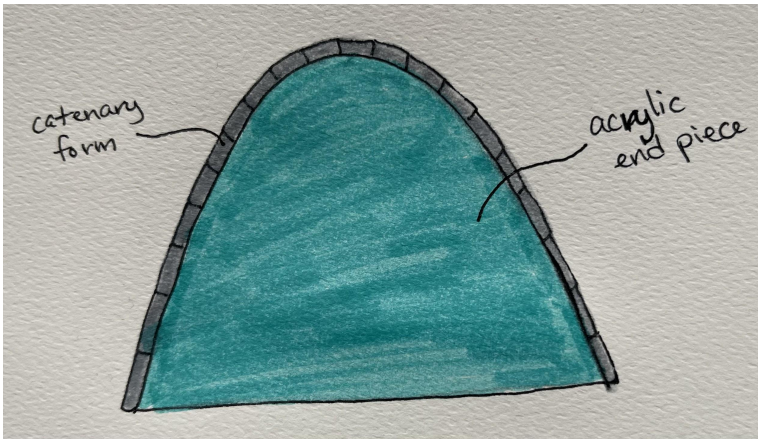

Figure 47: View of Pavilion End Pieces

Sample Calculation:

Concrete: x = 0.3m k = 1 W/mK area = 0.0883m^2

Acrylic: x = 0.01m k = 0.19 W/mK area = 0.029m^2

Inside air: $h = 8\ W/m^2K$ Outside Air: $h = 20\ W/mK$

$T_{ambient} = 21.11^oC = 294.26\ K$ $T_{winter\ average} = 5.42^oC = 278.57\ K$

$$R\text{-}Value = 1/h_{inside} + x/k + 1/h_{outside} \quad \text{(eq.3)}$$

$$U\text{-}Value = 1/R\text{-}Value \quad \text{(eq.4)}$$

$$R\text{-}Value_{concrete} = 1/8 + 0.3/1 + 1/20 = 0.4798\ m^2K/W$$

$$U\text{-}Value_{concrete} = 1/0.4798 = 2.0842\ W/m^2K$$

$$R\text{-}Value_{acrylic} = 1/8 + 0.01/0.19 + 1/20 = 0.2418\ m^2K/W$$

$$U\text{-}Value_{acrylic} = 1/0.2418 = 4.1349\ W/m^2K$$

$$Weighted\ U\text{-}Value = total\ U*Area\ /\ total\ Area \quad \text{(eq.5)}$$

$$Weighted\ U\text{-}Value = (2.0842W/m^2K*0.0883m^2 + 4.1349w/m^2K*0.029m^2)\ /\ (0.0883 + 0.029)$$

$$Weighted\ U\text{-}Value = 2.59\ W/m^2K$$

$$Q = U*A*\Delta T \quad \text{(eq.6)}$$

$$Q = 2.59\ W/m^2K * (0.0883m^2 + 0.029m^2) * (294.26\ K - 278.57\ K)$$

$$Q = 4.767\ W$$

The result of heat loss seen above is for part 1 of the catenary structure and the acrylic contained within its air space. The results of the new catenary design's total heat gain and loss analysis can be seen in Appendix B, Tables B.5, B.6 and B.7. Table B.5 shows the results of each of the 11 unique module pieces heat gain and loss with six different material compositions and in four different temperature variations. Table B.6 and B.7 illustrate the results of heat gain and loss for the structure per row and as a whole in metric and imperial units. Comparing the hemisphere structures to the catenary one, it can be seen that the catenary loses and gains less heat than the former.

5.0 Conclusions and Recommendations

Collectively, the team worked to design and evaluate a pavilion through the techniques provided through additive manufacturing. Overall, the final design achieved the objectives of maximizing the capabilities of the printer in design, and providing an area for users to be able to come together outdoors. The architectural design aspects of the pavilion floor layout allow for users to remain socially distant. The addition of the windows also provides a tie to WPI through similarities to the art installation on Gordon Library as they would vary in color to provide a mosaic lighting effect. The structural analysis established criteria for which the project would succeed and determined the best alternative for construction. Lastly, the mix design developed through research and experimentation provided the best solution for printer use during the timespan of this project. Due to the project's time constraint, the following sections provide recommendations for future collaboration, as they would help successfully execute this project in its completion.

5.1 Further Growth

5.1.1 Architectural & Mechanical Design

A more comprehensive initial concept would have enveloped all aspects of the project and would have been more instrumental in the development of the structure before its analysis. Additionally, the opportunity to further develop how the window pieces would be meshed with the 3D printed concrete, through concrete screws or an adhesion source, would have provided the finishing aspect to the development of the design. In terms of mechanical design, the HVAC analysis of the structure was hypothetical and plumbing systems were not considered in this project as they would not be utilized. However, the development of a lighting scheme is imperative to the use of the structure during times where little natural light is available. Aspects of lighting in terms of daylight were considered when designing the pavilion, which is why windows were installed that allowed for the harshness of the daylight to be reduced for the user inside the structure. However, to use the structure without artificial light would mean that it can only be used in a certain time span of the day. Providing an energy efficient lighting design that pairs with the theme of efficiency in the printing of the structure would provide users access to the pavilion at all hours of the day.

5.1.2 Structural Design

Although throughout the completion of this project generic values for concrete properties were assumed, the development of real values for the mix design would prove crucial in the realistic portrayal of the pavilion. The strength of the 3D printed concrete would be lower than the established strength of typical concrete as it lacks coarse aggregate in the mixture. Secondly, the catenary arch pathway displayed the most promise due to lower deformation and strain levels than in other scenarios. The perfection of the pathway that the

modules would follow would increase the safety of the users once inside and could increase the strength of arch as the pathway would follow a perfectly natural compression curve. Thirdly, developing reinforcement techniques, such as steel or the addition of fibers, for the attachment and construction of the archway would enable the structure to stand on its own and provide a greater level of tensile strength. Lastly, the use of multiple mix designs throughout the structure, for example using high-strength concrete at the bottom and lightweight concrete at the top, would improve both the compressive and tensile strength of the arch assembly. The high-strength concrete used in the bottom modules would raise the structure's compressive strength, while the lightweight modules at the top of the structure would help lower the tensile stress in the structure.

5.1.3 Mix Design and 3D Printing

Improving the accuracy in the development of the mix design and the ratio of ingredients required is necessary as this printer had a screw and gravity feeding system as opposed to a pump system. This means that the consistency of the mix design, while needing to succeed in buildability and extrudability, also needs sufficient weight and flow in order for the screw to properly extrude. In regards to the 3D printer itself, further understanding of the development of a gcode would aid in the creation of much more complex module components and adaptability in design.

References

Amadio, Claudio & Akkad, Nader & Fasan, Marco. (2015). Three-Dimensional Numerical Simulations of Steel Concrete Composite Beam-to-Column Welded and Bolted Joints.

Brooks, J.J. (2015). Concrete and Masonry Movements. 165-170.

https://www.sciencedirect.com/topics/engineering/expansive-cement#:~:text=opposite%20%5B1%5D.-,Expansive%20cements%20are%20used%20generally%20to%20minimize%20cracking%20caused%20by,%2C%20expanding%20agent%2C%20and%20stabilizer.

Chino, Mike. (2011). Packed Pavilion Constructed Completely from Cardboard.

https://inhabitat.com/

Donnelly, Erin & Navarro, Jamie. (2017). Architecture Builds Mexico City Pavilion One Bucket at a Time

https://www.azuremagazine.com/

Gotnet, Time & Wohlers, Terry. (2014). History of Additive Manufacturing.

http://www.wohlersassociates.com/.

H. Okamura, M. Ouchi, et al. “Mix Design and Fresh Properties for High-Performance Printing Concrete.” *Materials and Structures*, Springer Netherlands, 19 Jan. 2012, link.springer.com/article/10.1617/s11527-012-9828-z#Tab1.

Krimi, Imane & Lafhaj, Zoubeir & Ducoulombier, Laure. (2017). Concrete 3D Printing: Key Parameters to evaluate the printability of cement based materials

https://www.researchgate.net/

Kharvari, Farzam. “3D Printing Technology: The First 3D Printed Research Pavilion in Darak Village.” World Architecture Community, 21 Mar. 2020, https://worldarchitecture.org/

Li, Z., Hojati, M., Wu, Z., Piasente, J., Ashrafi, N., Duarte, J. P., . . . Radlinska, A. (2020, July 13). Fresh and Hardened Properties of Extrusion-Based 3D-Printed Cementitious Materials: A Review. Retrieved from

https://www.mdpi.com/2071-1050/12/14/5628/pdf

Ma, GuoWei & Wang, Li & Ju, Yang.(2018) State-of-the-Art 3D Printing Technology of Cementitious Material- An Emerging Technique for Construction https://link.springer.com/

Ma, G., Wang, L. A critical review of preparation design and workability measurement of concrete material for large scale 3D printing. Front. Struct. Civ. Eng. 12, 382–400 (2018). https://doi-org.ezpxy-web-p-u01.wpi.edu/

Malaeb, Zeina, & Hamzeh, Farook & Tourbah, Adel. (2015). 3D Concrete Printing: Machine and Mix Design https://www.researchgate.net/

Modular Origami. (n.d.). Retrieved March 18, 2021, from https://origami.lovetoknow.com/Modular_Origami

Origami. (n.d.). Retrieved March 18, 2021, from https://www.newworldencyclopedia.org/entry/Origami

Peters, A. (2015, September 15). This Freakishly Strong Origami Can Make Pop-Up Bridges and Buildings. Retrieved March 18, 2021, from https://www.fastcompany.com/3051045/this-freakishly-strong-origami-can-make-pop-up-bridges-and-buildings

Shen, Qingchuan, et al. "The Tensile Strength and Damage Characteristic of Two Types of Concrete and Their Interface." *Materials*, vol. 13, no. 1, 2019, p. 16., doi:10.3390/ma13010016.

Sher, Davide. "Ai Build, 3DVinci, BESIX 3D Collaborate on Deciduous 3D Printed Pavilion by MEAN." 3D Printing Media Network, 4 Dec. 2019, www.3dprintingmedia.network/

Stott, R. (2015, March 25). Emerging objects creates "bloom" pavilion from 3d printed cement. Retrieved from https://www.archdaily.com/613171/emerging-objects-creates-bloom-pavilion-from-3-d-printed-cement

Vyas, Khushboo. "Vulcan : World's Largest 3D-Printed Architectural Pavilion." Arch2O.com, 9 Dec. 2016, www.arch2o.com/.

Appendix A - Initial Mix Design Cylinder Results

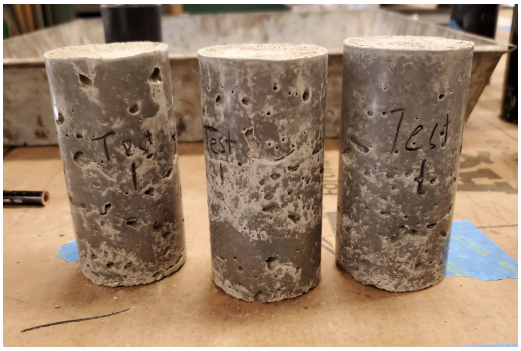

Figure A1: Design 1

Figure A2: Design 2

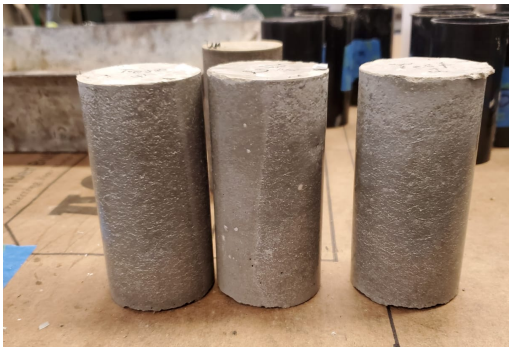

Figure A3: Design 3

Figure A4: Design 4

Figure A5: Design 5

Figure A6: Design 6

Appendix B - Heat Gain/Loss Tables

Table B.1: Heat Losses and Gains for the Total Structure (Metric), Hemispheric Scenario

	Composition		Heat Loss/Gain (W) (per row)	Heat Loss/Gain (W) (filler rows)	Heat Loss/Gain (W) (ends)	Heat Loss/Gain (W) (total)
Diamond	0.3m concrete 0.01m acrylic	winter (avg)	80.877	73.03	1506.185	8479.834
		winter (worst)	220.208	198.83	4100.971	23088.495
		summer (avg)	-22.629	-20.43	-421.425	-2372.624
		summer (worst)	-57.268	-51.71	-1066.521	-6004.522
	0.3m concrete 0.025m poly	winter (avg)	70.130	57.21	1180.038	6887.195
		winter (worst)	190.946	155.78	3212.952	18752.133
		summer (avg)	-19.622	-16.01	-330.170	-1927.010
		summer (worst)	-49.659	-40.51	-835.578	-4876.784
	0.2m concrete 0.01m acrylic	winter (avg)	89.271	73.03	1506.185	8782.015
		winter (worst)	243.062	198.83	4100.971	23911.261
		summer (avg)	-24.978	-20.43	-421.425	-2457.173
		summer (worst)	-63.212	-51.71	-1066.521	-6218.495
	0.2m concrete 0.025m poly	winter (avg)	78.524	57.21	1180.038	7189.377
		winter (worst)	213.801	155.78	3212.952	19574.900
		summer (avg)	-21.971	-16.01	-330.170	-2011.559
		summer (worst)	-55.602	-40.51	-835.578	-5090.757
	0.1m concrete 0.01m acrylic	winter (avg)	103.831	73.03	1506.185	9306.190
		winter (worst)	282.707	198.83	4100.971	25338.460
		summer (avg)	-29.052	-20.43	-421.425	-2603.835
		summer (worst)	-73.522	-51.71	-1066.521	-6589.660
	0.1m concrete 0.025m poly	winter (avg)	93.084	57.21	1180.038	7713.552
		winter (worst)	253.445	155.78	3212.952	21002.098
		summer (avg)	-26.045	-16.01	-330.170	-2158.221
		summer (worst)	-65.912	-40.51	-835.578	-5461.922

	Composition		Heat Loss/Gain (W) (per row)	Heat Loss/Gain (W) (filler rows)	Heat Loss/Gain (W) (ends)	Heat Loss/Gain (W) (total)
Hexagon	0.3m concrete 0.01m acrylic	winter (avg)	237.1954138	60.07	1506.185	8303.000
		winter (worst)	645.8246067	163.54	4100.971	22607.022
		summer (avg)	-66.3663395	-16.81	-421.425	-2323.147
		summer (worst)	-167.9567271	-42.53	-1066.521	-5879.308
	0.3m concrete 0.025m poly	winter (avg)	192.1773296	60.07	1180.038	6840.380
		winter (worst)	523.2514672	163.54	3212.952	18624.667
		summer (avg)	-53.77045742	-16.81	-330.170	-1913.911
		summer (worst)	-136.079677	-42.53	-835.578	-4843.634
	0.2m concrete 0.01m acrylic	winter (avg)	245.0657706	76.20	1506.185	8718.979
		winter (worst)	667.2536469	207.48	4100.971	23739.630
		summer (avg)	-68.56843422	-21.32	-421.425	-2439.536
		summer (worst)	-173.529682	-53.96	-1066.521	-6173.860
	0.2m concrete 0.025m poly	winter (avg)	200.0476864	76.20	1180.038	7256.359
		winter (worst)	544.6805075	207.48	3212.952	19757.275
		summer (avg)	-55.97255215	-21.32	-330.170	-2030.301
		summer (worst)	-141.652632	-53.96	-835.578	-5138.186
	0.1m concrete 0.01m acrylic	winter (avg)	258.7179658	104.19	1506.185	9440.551
		winter (worst)	704.425207	283.69	4100.971	25704.292
		summer (avg)	-72.38826448	-29.15	-421.425	-2641.429
		summer (worst)	-183.196724	-73.78	-1066.521	-6684.801
	0.1m concrete 0.025m poly	winter (avg)	213.6998815	104.19	1180.038	7977.930
		winter (worst)	581.8520675	283.69	3212.952	21721.937
		summer (avg)	-59.79238241	-29.15	-330.170	-2232.193
		summer (worst)	-151.3196739	-73.78	-835.578	-5649.127

Table B.2 Heat Losses and Gains for the Total Structure (Imperial), Hemispheric Scenario

	Composition		Heat Loss/Gain (Btu) (per row)	Heat Loss/Gain (Btu) (filler rows)	Heat Loss/Gain (Btu) (ends)	Heat Loss/Gain (Btu) (total)
Diamond	0.3m concrete 0.01m acrylic	winter (avg)	275.963	249.17	5139.315	28934.379
		winter (worst)	751.380	678.44	13993.088	78781.179
		summer (avg)	-77.213	-69.72	-1437.960	-8095.725
		summer (worst)	-195.408	-176.44	-3639.120	-20488.270
	0.3m concrete 0.025m poly	winter (avg)	239.293	195.22	4026.454	23500.074
		winter (worst)	651.535	531.53	10963.042	63984.905
		summer (avg)	-66.953	-54.62	-1126.586	-6575.228
		summer (worst)	-169.442	-138.23	-2851.109	-16640.269
	0.2m concrete 0.01m acrylic	winter (avg)	304.604	249.17	5139.315	29965.466
		winter (worst)	829.363	678.44	13993.088	81588.572
		summer (avg)	-85.227	-69.72	-1437.960	-8384.219
		summer (worst)	-215.689	-176.44	-3639.120	-21218.376
	0.2m concrete 0.025m poly	winter (avg)	267.934	195.22	4026.454	24531.160
		winter (worst)	729.518	531.53	10963.042	66792.298
		summer (avg)	-74.967	-54.62	-1126.586	-6863.722
		summer (worst)	-189.723	-138.23	-2851.109	-17370.375
	0.1m concrete 0.01m acrylic	winter (avg)	354.287	249.17	5139.315	31754.023
		winter (worst)	964.635	678.44	13993.088	86458.373
		summer (avg)	-99.128	-69.72	-1437.960	-8884.650
		summer (worst)	-250.868	-176.44	-3639.120	-22484.844
	0.1m concrete 0.025m poly	winter (avg)	317.616	195.22	4026.454	26319.718
		winter (worst)	864.791	531.53	10963.042	71662.099
		summer (avg)	-88.868	-54.62	-1126.586	-7364.153
		summer (worst)	-224.902	-138.23	-2851.109	-18636.843

	Composition		Heat Loss/Gain (Btu) (per row)	Heat Loss/Gain (Btu) (filler rows)	Heat Loss/Gain (Btu) (ends)	Heat Loss/Gain (Btu) (total)
Hexagon	0.3m concrete 0.01m acrylic	winter (avg)	809.3439593	204.95	5139.315	28331.000
		winter (worst)	2203.643973	558.03	13993.088	77138.325
		summer (avg)	-226.4512416	-57.34	-1437.960	-7926.902
		summer (worst)	-573.0918667	-145.13	-3639.120	-20061.020
	0.3m concrete 0.025m poly	winter (avg)	655.7359535	204.95	4026.454	23340.334
		winter (worst)	1785.407261	558.03	10963.042	63549.971
		summer (avg)	-183.4723286	-57.34	-1126.586	-6530.533
		summer (worst)	-464.322909	-145.13	-2851.109	-16527.158
	0.2m concrete 0.01m acrylic	winter (avg)	836.1987185	260.01	5139.315	29750.378
		winter (worst)	2276.762859	707.94	13993.088	81002.942
		summer (avg)	-233.9650971	-72.75	-1437.960	-8324.038
		summer (worst)	-592.1075693	-184.11	-3639.120	-21066.074
	0.2m concrete 0.025m poly	winter (avg)	682.5907126	260.01	4026.454	24759.712
		winter (worst)	1858.526147	707.94	10963.042	67414.589
		summer (avg)	-190.9861841	-72.75	-1126.586	-6927.670
		summer (worst)	-483.3386117	-184.11	-2851.109	-17532.212
	0.1m concrete 0.01m acrylic	winter (avg)	882.7819197	355.52	5139.315	32212.482
		winter (worst)	2403.597426	967.98	13993.088	87706.643
		summer (avg)	-246.9988928	-99.47	-1437.960	-9012.925
		summer (worst)	-625.0928698	-251.74	-3639.120	-22809.476
	0.1m concrete 0.025m poly	winter (avg)	729.1739138	355.52	4026.454	27221.815
		winter (worst)	1985.360714	967.98	10963.042	74118.289
		summer (avg)	-204.0199797	-99.47	-1126.586	-7616.556
		summer (worst)	-516.3239122	-251.74	-2851.109	-19275.613

Table B.3: Thickness, Conductivity, and Convection Coefficients Used for Calculation

Concrete	1	W/mK	thermal conductivity
Acrylic	0.19	W/mK	
inside air	8	W/mK	convection coefficient
outside air	20	W/mK	
concrete	0.3048	m	concrete thickness
concrete	0.2032	m	
concrete	0.1016	m	
acrylic	0.0127	m	air space material
polycarbonate	0.0254	m	

Table B.4: Calculated R and U-Values for Individual Material

	inside	concrete	outside	R-Value	U-Value
concrete (0.3m)	0.125	0.3048	0.05	0.4798	2.0842
concrete (0.2m)	0.125	0.2032	0.05	0.3782	2.6441
concrete (0.1m)	0.125	0.1016	0.05	0.2766	3.6153
	inside	material	outside	R-Value	U-Value
acrylic (0.01m)	0.125	0.0668	0.05	0.2418	4.1349
polycarbonate (0.025m)	0.125	0.1337	0.05	0.3087	3.2396

Table B.5: Heat Losses and Gains for Individual Modules (Metric), Catenary Scenario

						composition	season	dT	Q (W)
component	U value	area	UA	Part 1 | 0.3m Concrete | Acrylic	Part 1	0.3m concrete 0.01m acrylic	winter (avg)	15.69	4.769
concrete (0.3m)	2.084	0.088	0.184				winter (worst)	42.72	12.985
acrylic (0.01m)	4.135	0.029	0.120	U Value			summer (avg)	-4.39	-1.334
	Total	0.117	0.304	2.59			summer (worst)	-11.11	-3.377
component	U value	area	UA	Part 1 | 0.3m Concrete | Polycarbonate		0.3m concrete 0.025m poly	winter (avg)	15.69	4.362
concrete (0.3m)	2.084	0.088	0.184				winter (worst)	42.72	11.875
polycarbonate (0.025m)	3.240	0.029	0.094	U Value			summer (avg)	-4.39	-1.220
	Total	0.117	0.278	2.37			summer (worst)	-11.11	-3.088
component	U value	area	UA	Part 1 | 0.2m Concrete | Acrylic		0.2m concrete 0.01m acrylic	winter (avg)	15.69	5.545
concrete (0.2m)	2.644	0.088	0.233				winter (worst)	42.72	15.097
acrylic (0.01m)	4.135	0.029	0.120	U Value			summer (avg)	-4.39	-1.551
	Total	0.117	0.353	3.013			summer (worst)	-11.11	-3.926
component	U value	area	UA	Part 1 | 0.2m Concrete | Polycarbonate		0.2m concrete 0.025m poly	winter (avg)	15.69	5.137
concrete (0.2m)	2.644	0.088	0.233				winter (worst)	42.72	13.987
polycarbonate (0.025m)	3.240	0.029	0.094	U Value			summer (avg)	-4.39	-1.437
	Total	0.117	0.327	2.79			summer (worst)	-11.11	-3.638
component	U value	area	UA	Part 1 | 0.1m Concrete | Acrylic		0.1m concrete 0.01m acrylic	winter (avg)	15.69	6.890
concrete (0.1m)	3.615	0.088	0.319				winter (worst)	42.72	18.760
acrylic (0.01m)	4.135	0.029	0.120	U Value			summer (avg)	-4.39	-1.928
	Total	0.117	0.439	3.74			summer (worst)	-11.11	-4.879
component	U value	area	UA	Part 1 | 0.1m Concrete | Polycarbonate		0.1m concrete 0.025m poly	winter (avg)	15.69	6.483
concrete (0.1m)	3.615	0.088	0.319				winter (worst)	42.72	17.651
polycarbonate (0.025m)	3.240	0.029	0.094	U Value			summer (avg)	-4.39	-1.814
	Total	0.117	0.413	3.52			summer (worst)	-11.11	-4.590

component	U value	area	UA	Part 2 | 0.3m Concrete | Acrylic	Part 2	0.3m concrete 0.01m acrylic	winter (avg)	15.69	5.111
concrete (0.3m)	2.084	0.094	0.196				winter (worst)	42.72	13.916
acrylic (0.01m)	4.135	0.031	0.130	U Value			summer (avg)	-4.39	-1.430
	Total	0.125	0.326	2.60			summer (worst)	-11.11	-3.619
component	U value	area	UA	Part 2 | 0.3m Concrete | Polycarbonate		0.3m concrete 0.025m poly	winter (avg)	15.69	4.670
concrete (0.3m)	2.084	0.094	0.196				winter (worst)	42.72	12.715
polycarbonate (0.025m)	3.240	0.031	0.102	U Value			summer (avg)	-4.39	-1.307
	Total	0.125	0.298	2.37			summer (worst)	-11.11	-3.307
component	U value	area	UA	Part 2 | 0.2m Concrete | Acrylic		0.2m concrete 0.01m acrylic	winter (avg)	15.69	5.937
concrete (0.2m)	2.644	0.094	0.249				winter (worst)	42.72	16.165
acrylic (0.01m)	4.135	0.031	0.130	U Value			summer (avg)	-4.39	-1.661
	Total	0.125	0.378	3.017			summer (worst)	-11.11	-4.204
component	U value	area	UA	Part 2 | 0.2m Concrete | Polycarbonate		0.2m concrete 0.025m poly	winter (avg)	15.69	5.496
concrete (0.2m)	2.644	0.094	0.249				winter (worst)	42.72	14.963
polycarbonate (0.025m)	3.240	0.031	0.102	U Value			summer (avg)	-4.39	-1.538
	Total	0.125	0.350	2.79			summer (worst)	-11.11	-3.891
component	U value	area	UA	Part 2 | 0.1m Concrete | Acrylic		0.1m concrete 0.01m acrylic	winter (avg)	15.69	7.369
concrete (0.1m)	3.615	0.094	0.340				winter (worst)	42.72	20.065
acrylic (0.01m)	4.135	0.031	0.130	U Value			summer (avg)	-4.39	-2.062
	Total	0.125	0.470	3.75			summer (worst)	-11.11	-5.218
component	U value	area	UA	Part 2 | 0.1m Concrete | Polycarbonate		0.1m concrete 0.025m poly	winter (avg)	15.69	6.928
concrete (0.1m)	3.615	0.094	0.340				winter (worst)	42.72	18.864
polycarbonate (0.025m)	3.240	0.031	0.102	U Value			summer (avg)	-4.39	-1.938
	Total	0.125	0.442	3.52			summer (worst)	-11.11	-4.906

component	U value	area	UA	Part 3 | 0.3m Concrete | Acrylic	Part 3	0.3m concrete 0.01m acrylic	winter (avg)	15.69	4.378
concrete (0.3m)	2.084	0.082	0.171				winter (worst)	42.72	11.920
acrylic (0.01m)	4.135	0.026	0.108	U Value			summer (avg)	-4.39	-1.225
	Total	0.108	0.279	2.58			summer (worst)	-11.11	-3.100
component	U value	area	UA	Part 3 | 0.3m Concrete | Polycarbonate		0.3m concrete 0.025m poly	winter (avg)	15.69	4.010
concrete (0.3m)	2.084	0.082	0.171				winter (worst)	42.72	10.918
polycarbonate (0.025m)	3.240	0.026	0.085	U Value			summer (avg)	-4.39	-1.122
	Total	0.108	0.256	2.36			summer (worst)	-11.11	-2.839
component	U value	area	UA	Part 3 | 0.2m Concrete | Acrylic		0.2m concrete 0.01m acrylic	winter (avg)	15.69	5.097
concrete (0.2m)	2.644	0.082	0.217				winter (worst)	42.72	13.879
acrylic (0.01m)	4.135	0.026	0.108	U Value			summer (avg)	-4.39	-1.426
	Total	0.108	0.325	3.005			summer (worst)	-11.11	-3.609
component	U value	area	UA	Part 3 | 0.2m Concrete | Polycarbonate		0.2m concrete 0.025m poly	winter (avg)	15.69	4.729
concrete (0.2m)	2.644	0.082	0.217				winter (worst)	42.72	12.877
polycarbonate (0.025m)	3.240	0.026	0.085	U Value			summer (avg)	-4.39	-1.323
	Total	0.108	0.301	2.79			summer (worst)	-11.11	-3.349
component	U value	area	UA	Part 3 | 0.1m Concrete | Acrylic		0.1m concrete 0.01m acrylic	winter (avg)	15.69	6.346
concrete (0.1m)	3.615	0.082	0.296				winter (worst)	42.72	17.277
acrylic (0.01m)	4.135	0.026	0.108	U Value			summer (avg)	-4.39	-1.775
	Total	0.108	0.404	3.74			summer (worst)	-11.11	-4.493
component	U value	area	UA	Part 3 | 0.1m Concrete | Polycarbonate		0.1m concrete 0.025m poly	winter (avg)	15.69	5.977
concrete (0.1m)	3.615	0.082	0.296				winter (worst)	42.72	16.275
polycarbonate (0.025m)	3.240	0.026	0.085	U Value			summer (avg)	-4.39	-1.672
	Total	0.108	0.381	3.52			summer (worst)	-11.11	-4.233

component	U value	area	UA	Part 4 | 0.3m Concrete | Acrylic	Part 4	0.3m concrete 0.01m acrylic	winter (avg)	15.69	3.762
concrete (0.3m)	2.084	0.072	0.150				winter (worst)	42.72	10.244
acrylic (0.01m)	4.135	0.022	0.089	U Value			summer (avg)	-4.39	-1.053
	Total	0.094	0.240	2.56			summer (worst)	-11.11	-2.664
component	U value	area	UA	Part 4 | 0.3m Concrete | Polycarbonate		0.3m concrete 0.025m poly	winter (avg)	15.69	3.459
concrete (0.3m)	2.084	0.072	0.150				winter (worst)	42.72	9.418
polycarbonate (0.025m)	3.240	0.022	0.070	U Value			summer (avg)	-4.39	-0.968
	Total	0.094	0.220	2.35			summer (worst)	-11.11	-2.449
component	U value	area	UA	Part 4 | 0.2m Concrete | Acrylic		0.2m concrete 0.01m acrylic	winter (avg)	15.69	4.397
concrete (0.2m)	2.644	0.072	0.191				winter (worst)	42.72	11.971
acrylic (0.01m)	4.135	0.022	0.089	U Value			summer (avg)	-4.39	-1.230
	Total	0.094	0.280	2.987			summer (worst)	-11.11	-3.113
component	U value	area	UA	Part 4 | 0.2m Concrete | Polycarbonate		0.2m concrete 0.025m poly	winter (avg)	15.69	4.093
concrete (0.2m)	2.644	0.072	0.191				winter (worst)	42.72	11.145
polycarbonate (0.025m)	3.240	0.022	0.070	U Value			summer (avg)	-4.39	-1.145
	Total	0.094	0.261	2.78			summer (worst)	-11.11	-2.898
component	U value	area	UA	Part 4 | 0.1m Concrete | Acrylic		0.1m concrete 0.01m acrylic	winter (avg)	15.69	5.497
concrete (0.1m)	3.615	0.072	0.261				winter (worst)	42.72	14.967
acrylic (0.01m)	4.135	0.022	0.089	U Value			summer (avg)	-4.39	-1.538
	Total	0.094	0.350	3.73			summer (worst)	-11.11	-3.892
component	U value	area	UA	Part 4 | 0.1m Concrete | Polycarbonate		0.1m concrete 0.025m poly	winter (avg)	15.69	5.193
concrete (0.1m)	3.615	0.072	0.261				winter (worst)	42.72	14.140
polycarbonate (0.025m)	3.240	0.022	0.070	U Value			summer (avg)	-4.39	-1.453
	Total	0.094	0.331	3.53			summer (worst)	-11.11	-3.677

component	U value	area	UA	Part 5 | 0.3m Concrete | Acrylic	Part 5	0.3m concrete 0.01m acrylic	winter (avg)	15.69	3.264
concrete (0.3m)	2.084	0.065	0.134				winter (worst)	42.72	8.887
acrylic (0.01m)	4.135	0.018	0.074	U Value			summer (avg)	-4.39	-0.913
	Total	0.082	0.208	2.53			summer (worst)	-11.11	-2.311
component	U value	area	UA	Part 5 | 0.3m Concrete | Polycarbonate		0.3m concrete 0.025m poly	winter (avg)	15.69	3.014
concrete (0.3m)	2.084	0.065	0.134				winter (worst)	42.72	8.206
polycarbonate (0.025m)	3.240	0.018	0.058	U Value			summer (avg)	-4.39	-0.843
	Total	0.082	0.192	2.33			summer (worst)	-11.11	-2.134
component	U value	area	UA	Part 5 | 0.2m Concrete | Acrylic		0.2m concrete 0.01m acrylic	winter (avg)	15.69	3.831
concrete (0.2m)	2.644	0.065	0.171				winter (worst)	42.72	10.430
acrylic (0.01m)	4.135	0.018	0.074	U Value			summer (avg)	-4.39	-1.072
	Total	0.082	0.244	2.967			summer (worst)	-11.11	-2.712
component	U value	area	UA	Part 5 | 0.2m Concrete | Polycarbonate		0.2m concrete 0.025m poly	winter (avg)	15.69	3.581
concrete (0.2m)	2.644	0.065	0.171				winter (worst)	42.72	9.749
polycarbonate (0.025m)	3.240	0.018	0.058	U Value			summer (avg)	-4.39	-1.002
	Total	0.082	0.228	2.77			summer (worst)	-11.11	-2.535
component	U value	area	UA	Part 5 | 0.1m Concrete | Acrylic		0.1m concrete 0.01m acrylic	winter (avg)	15.69	4.814
concrete (0.1m)	3.615	0.065	0.233				winter (worst)	42.72	13.106
acrylic (0.01m)	4.135	0.018	0.074	U Value			summer (avg)	-4.39	-1.347
	Total	0.082	0.307	3.73			summer (worst)	-11.11	-3.408
component	U value	area	UA	Part 5 | 0.1m Concrete | Polycarbonate		0.1m concrete 0.025m poly	winter (avg)	15.69	4.563
concrete (0.1m)	3.615	0.065	0.233				winter (worst)	42.72	12.425
polycarbonate (0.025m)	3.240	0.018	0.058	U Value			summer (avg)	-4.39	-1.277
	Total	0.082	0.291	3.53			summer (worst)	-11.11	-3.231

component	U value	area	UA	Part 6 | 0.3m Concrete | Acrylic	Part 6	0.3m concrete 0.01m acrylic	winter (avg)	15.69	2.854
concrete (0.3m)	2.084	0.059	0.122				winter (worst)	42.72	7.770
acrylic (0.01m)	4.135	0.015	0.060	U Value			summer (avg)	-4.39	-0.798
	Total	0.073	0.182	2.49			summer (worst)	-11.11	-2.021
component	U value	area	UA	Part 6 | 0.3m Concrete | Polycarbonate		0.3m concrete 0.025m poly	winter (avg)	15.69	2.650
concrete (0.3m)	2.084	0.059	0.122				winter (worst)	42.72	7.215
polycarbonate (0.025m)	3.240	0.015	0.047	U Value			summer (avg)	-4.39	-0.741
	Total	0.073	0.169	2.31			summer (worst)	-11.11	-1.876
component	U value	area	UA	Part 6 | 0.2m Concrete | Acrylic		0.2m concrete 0.01m acrylic	winter (avg)	15.69	3.368
concrete (0.2m)	2.644	0.059	0.155				winter (worst)	42.72	9.169
acrylic (0.01m)	4.135	0.015	0.060	U Value			summer (avg)	-4.39	-0.942
	Total	0.073	0.215	2.940			summer (worst)	-11.11	-2.385
component	U value	area	UA	Part 6 | 0.2m Concrete | Polycarbonate		0.2m concrete 0.025m poly	winter (avg)	15.69	3.164
concrete (0.2m)	2.644	0.059	0.155				winter (worst)	42.72	8.615
polycarbonate (0.025m)	3.240	0.015	0.047	U Value			summer (avg)	-4.39	-0.885
	Total	0.073	0.202	2.76			summer (worst)	-11.11	-2.240
component	U value	area	UA	Part 6 | 0.1m Concrete | Acrylic		0.1m concrete 0.01m acrylic	winter (avg)	15.69	4.259
concrete (0.1m)	3.615	0.059	0.211				winter (worst)	42.72	11.596
acrylic (0.01m)	4.135	0.015	0.060	U Value			summer (avg)	-4.39	-1.192
	Total	0.073	0.271	3.72			summer (worst)	-11.11	-3.016
component	U value	area	UA	Part 6 | 0.1m Concrete | Polycarbonate		0.1m concrete 0.025m poly	winter (avg)	15.69	4.055
concrete (0.1m)	3.615	0.059	0.211				winter (worst)	42.72	11.042
polycarbonate (0.025m)	3.240	0.015	0.047	U Value			summer (avg)	-4.39	-1.135
	Total	0.073	0.258	3.54			summer (worst)	-11.11	-2.872

component	U value	area	UA	Part 7 | 0.3m Concrete | Acrylic	Part 7	0.3m concrete 0.01m acrylic	winter (avg)	15.69	2.531
concrete (0.3m)	2.084	0.054	0.113				winter (worst)	42.72	6.891
acrylic (0.01m)	4.135	0.012	0.049	U Value			summer (avg)	-4.39	-0.708
	Total	0.066	0.161	2.45			summer (worst)	-11.11	-1.792
component	U value	area	UA	Part 7 | 0.3m Concrete | Polycarbonate		0.3m concrete 0.025m poly	winter (avg)	15.69	2.365
concrete (0.3m)	2.084	0.054	0.113				winter (worst)	42.72	6.439
polycarbonate (0.025m)	3.240	0.012	0.038	U Value			summer (avg)	-4.39	-0.662
	Total	0.066	0.151	2.29			summer (worst)	-11.11	-1.675
component	U value	area	UA	Part 7 | 0.2m Concrete | Acrylic		0.2m concrete 0.01m acrylic	winter (avg)	15.69	3.005
concrete (0.2m)	2.644	0.054	0.143				winter (worst)	42.72	8.182
acrylic (0.01m)	4.135	0.012	0.049	U Value			summer (avg)	-4.39	-0.841
	Total	0.066	0.192	2.912			summer (worst)	-11.11	-2.128
component	U value	area	UA	Part 7 | 0.2m Concrete | Polycarbonate		0.2m concrete 0.025m poly	winter (avg)	15.69	2.839
concrete (0.2m)	2.644	0.054	0.143				winter (worst)	42.72	7.730
polycarbonate (0.025m)	3.240	0.012	0.038	U Value			summer (avg)	-4.39	-0.794
	Total	0.066	0.181	2.75			summer (worst)	-11.11	-2.010
component	U value	area	UA	Part 7 | 0.1m Concrete | Acrylic		0.1m concrete 0.01m acrylic	winter (avg)	15.69	3.828
concrete (0.1m)	3.615	0.054	0.195				winter (worst)	42.72	10.421
acrylic (0.01m)	4.135	0.012	0.049	U Value			summer (avg)	-4.39	-1.071
	Total	0.066	0.244	3.71			summer (worst)	-11.11	-2.710
component	U value	area	UA	Part 7 | 0.1m Concrete | Polycarbonate		0.1m concrete 0.025m poly	winter (avg)	15.69	3.662
concrete (0.1m)	3.615	0.054	0.195				winter (worst)	42.72	9.970
polycarbonate (0.025m)	3.240	0.012	0.038	U Value			summer (avg)	-4.39	-1.025
	Total	0.066	0.233	3.55			summer (worst)	-11.11	-2.593

component	U value	area	UA	Part 8 | 0.3m Concrete | Acrylic	Part 8	0.3m concrete 0.01m acrylic	winter (avg)	15.69	2.196
concrete (0.3m)	2.084	0.050	0.103				winter (worst)	42.72	5.979
acrylic (0.01m)	4.135	0.009	0.037	U Value			summer (avg)	-4.39	-0.614
	Total	0.058	0.140	2.40			summer (worst)	-11.11	-1.555
component	U value	area	UA	Part 8 | 0.3m Concrete | Polycarbonate		0.3m concrete 0.025m poly	winter (avg)	15.69	2.071
concrete (0.3m)	2.084	0.050	0.103				winter (worst)	42.72	5.639
polycarbonate (0.025m)	3.240	0.009	0.029	U Value			summer (avg)	-4.39	-0.579
	Total	0.058	0.132	2.26			summer (worst)	-11.11	-1.467
component	U value	area	UA	Part 8 | 0.2m Concrete | Acrylic		0.2m concrete 0.01m acrylic	winter (avg)	15.69	2.631
concrete (0.2m)	2.644	0.050	0.131				winter (worst)	42.72	7.163
acrylic (0.01m)	4.135	0.009	0.037	U Value			summer (avg)	-4.39	-0.736
	Total	0.058	0.168	2.871			summer (worst)	-11.11	-1.863
component	U value	area	UA	Part 8 | 0.2m Concrete | Polycarbonate		0.2m concrete 0.025m poly	winter (avg)	15.69	2.506
concrete (0.2m)	2.644	0.050	0.131				winter (worst)	42.72	6.823
polycarbonate (0.025m)	3.240	0.009	0.029	U Value			summer (avg)	-4.39	-0.701
	Total	0.058	0.160	2.73			summer (worst)	-11.11	-1.774
component	U value	area	UA	Part 8 | 0.1m Concrete | Acrylic		0.1m concrete 0.01m acrylic	winter (avg)	15.69	3.385
concrete (0.1m)	3.615	0.050	0.179				winter (worst)	42.72	9.217
acrylic (0.01m)	4.135	0.009	0.037	U Value			summer (avg)	-4.39	-0.947
	Total	0.058	0.216	3.69			summer (worst)	-11.11	-2.397
component	U value	area	UA	Part 8 | 0.1m Concrete | Polycarbonate		0.1m concrete 0.025m poly	winter (avg)	15.69	3.260
concrete (0.1m)	3.615	0.050	0.179				winter (worst)	42.72	8.877
polycarbonate (0.025m)	3.240	0.009	0.029	U Value			summer (avg)	-4.39	-0.912
	Total	0.058	0.208	3.56			summer (worst)	-11.11	-2.309

component	U value	area	UA	Part 9 | 0.3m Concrete | Acrylic	Part 9	0.3m concrete 0.01m acrylic	winter (avg)	15.69	2.121
concrete (0.3m)	2.084	0.049	0.101				winter (worst)	42.72	5.774
acrylic (0.01m)	4.135	0.008	0.034	U Value			summer (avg)	-4.39	-0.593
	Total	0.057	0.135	2.38			summer (worst)	-11.11	-1.502
component	U value	area	UA	Part 9 | 0.3m Concrete | Polycarbonate		0.3m concrete 0.025m poly	winter (avg)	15.69	2.005
concrete (0.3m)	2.084	0.049	0.101				winter (worst)	42.72	5.459
polycarbonate (0.025m)	3.240	0.008	0.027	U Value			summer (avg)	-4.39	-0.561
	Total	0.057	0.128	2.25			summer (worst)	-11.11	-1.420
component	U value	area	UA	Part 9 | 0.2m Concrete | Acrylic		0.2m concrete 0.01m acrylic	winter (avg)	15.69	2.547
concrete (0.2m)	2.644	0.049	0.128				winter (worst)	42.72	6.934
acrylic (0.01m)	4.135	0.008	0.034	U Value			summer (avg)	-4.39	-0.713
	Total	0.057	0.162	2.861			summer (worst)	-11.11	-1.803
component	U value	area	UA	Part 9 | 0.2m Concrete | Polycarbonate		0.2m concrete 0.025m poly	winter (avg)	15.69	2.431
concrete (0.2m)	2.644	0.049	0.128				winter (worst)	42.72	6.619
polycarbonate (0.025m)	3.240	0.008	0.027	U Value			summer (avg)	-4.39	-0.680
	Total	0.057	0.155	2.73			summer (worst)	-11.11	-1.721
component	U value	area	UA	Part 9 | 0.1m Concrete | Acrylic		0.1m concrete 0.01m acrylic	winter (avg)	15.69	3.286
concrete (0.1m)	3.615	0.049	0.175				winter (worst)	42.72	8.946
acrylic (0.01m)	4.135	0.008	0.034	U Value			summer (avg)	-4.39	-0.919
	Total	0.057	0.209	3.69			summer (worst)	-11.11	-2.327
component	U value	area	UA	Part 9 | 0.1m Concrete | Polycarbonate		0.1m concrete 0.025m poly	winter (avg)	15.69	3.170
concrete (0.1m)	3.615	0.049	0.175				winter (worst)	42.72	8.631
polycarbonate (0.025m)	3.240	0.008	0.027	U Value			summer (avg)	-4.39	-0.887
	Total	0.057	0.202	3.56			summer (worst)	-11.11	-2.245

component	U value	area	UA	Part 10 | 0.3m Concrete | Acrylic	Part 10	0.3m concrete 0.01m acrylic	winter (avg)	15.69	2.016
concrete (0.3m)	2.084	0.047	0.098				winter (worst)	42.72	5.490
acrylic (0.01m)	4.135	0.007	0.030	U Value			summer (avg)	-4.39	-0.564
	Total	0.054	0.129	2.36			summer (worst)	-11.11	-1.428
component	U value	area	UA	Part 10 | 0.3m Concrete | Polycarbonate		0.3m concrete 0.025m poly	winter (avg)	15.69	1.913
concrete (0.3m)	2.084	0.047	0.098				winter (worst)	42.72	5.209
polycarbonate (0.025m)	3.240	0.007	0.024	U Value			summer (avg)	-4.39	-0.535
	Total	0.054	0.122	2.24			summer (worst)	-11.11	-1.355
component	U value	area	UA	Part 10 | 0.2m Concrete | Acrylic		0.2m concrete 0.01m acrylic	winter (avg)	15.69	2.430
concrete (0.2m)	2.644	0.047	0.125				winter (worst)	42.72	6.617
acrylic (0.01m)	4.135	0.007	0.030	U Value			summer (avg)	-4.39	-0.680
	Total	0.054	0.155	2.845			summer (worst)	-11.11	-1.721
component	U value	area	UA	Part 10 | 0.2m Concrete | Polycarbonate		0.2m concrete 0.025m poly	winter (avg)	15.69	2.327
concrete (0.2m)	2.644	0.047	0.125				winter (worst)	42.72	6.336
polycarbonate (0.025m)	3.240	0.007	0.024	U Value			summer (avg)	-4.39	-0.651
	Total	0.054	0.148	2.72			summer (worst)	-11.11	-1.648
component	U value	area	UA	Part 10 | 0.1m Concrete | Acrylic		0.1m concrete 0.01m acrylic	winter (avg)	15.69	3.148
concrete (0.1m)	3.615	0.047	0.170				winter (worst)	42.72	8.571
acrylic (0.01m)	4.135	0.007	0.030	U Value			summer (avg)	-4.39	-0.881
	Total	0.054	0.201	3.69			summer (worst)	-11.11	-2.229
component	U value	area	UA	Part 10 | 0.1m Concrete | Polycarbonate		0.1m concrete 0.025m poly	winter (avg)	15.69	3.045
concrete (0.1m)	3.615	0.047	0.170				winter (worst)	42.72	8.290
polycarbonate (0.025m)	3.240	0.007	0.024	U Value			summer (avg)	-4.39	-0.852
	Total	0.054	0.194	3.56			summer (worst)	-11.11	-2.156

component	U value	area	UA	Part 11 | 0.3m Concrete | Acrylic	Part 11	0.3m concrete 0.01m acrylic	winter (avg)	15.69	1.985
concrete (0.3m)	2.084	0.047	0.097				winter (worst)	42.72	5.405
acrylic (0.01m)	4.135	0.007	0.029	U Value			summer (avg)	-4.39	-0.555
	Total	0.054	0.127	2.35			summer (worst)	-11.11	-1.406
component	U value	area	UA	Part 11 | 0.3m Concrete | Polycarbonate		0.3m concrete 0.025m poly	winter (avg)	15.69	1.886
concrete (0.3m)	2.084	0.047	0.097				winter (worst)	42.72	5.135
polycarbonate (0.025m)	3.240	0.007	0.023	U Value			summer (avg)	-4.39	-0.528
	Total	0.054	0.120	2.24			summer (worst)	-11.11	-1.335
component	U value	area	UA	Part 11 | 0.2m Concrete | Acrylic		0.2m concrete 0.01m acrylic	winter (avg)	15.69	2.395
concrete (0.2m)	2.644	0.047	0.123				winter (worst)	42.72	6.522
acrylic (0.01m)	4.135	0.007	0.029	U Value			summer (avg)	-4.39	-0.670
	Total	0.054	0.153	2.840			summer (worst)	-11.11	-1.696
component	U value	area	UA	Part 11 | 0.2m Concrete | Polycarbonate		0.2m concrete 0.025m poly	winter (avg)	15.69	2.296
concrete (0.2m)	2.644	0.047	0.123				winter (worst)	42.72	6.252
polycarbonate (0.025m)	3.240	0.007	0.023	U Value			summer (avg)	-4.39	-0.642
	Total	0.054	0.146	2.72			summer (worst)	-11.11	-1.626
component	U value	area	UA	Part 11 | 0.1m Concrete | Acrylic		0.1m concrete 0.01m acrylic	winter (avg)	15.69	3.107
concrete (0.1m)	3.615	0.047	0.169				winter (worst)	42.72	8.460
acrylic (0.01m)	4.135	0.007	0.029	U Value			summer (avg)	-4.39	-0.869
	Total	0.054	0.198	3.68			summer (worst)	-11.11	-2.200
component	U value	area	UA	Part 11 | 0.1m Concrete | Polycarbonate		0.1m concrete 0.025m poly	winter (avg)	15.69	3.008
concrete (0.1m)	3.615	0.047	0.169				winter (worst)	42.72	8.190
polycarbonate (0.025m)	3.240	0.007	0.023	U Value			summer (avg)	-4.39	-0.842
	Total	0.054	0.192	3.57			summer (worst)	-11.11	-2.130

Table B.6: Heat Losses and Gains for Single Rows and Total Structure (Metric) Catenary Scenario

Composition		Heat Loss/Gain (W) (per row)	Heat Loss/Gain (W) (total)
0.3m concrete 0.01m acrylic	winter (avg)	67.989	2447.61
	winter (worst)	185.118	6664.24
	summer (avg)	-19.023	-684.83
	summer (worst)	-48.143	-1733.14
0.3m concrete 0.025m poly	winter (avg)	62.923	2265.23
	winter (worst)	171.324	6167.66
	summer (avg)	-17.606	-633.80
	summer (worst)	-44.555	-1604.00
0.2m concrete 0.01m acrylic	winter (avg)	79.969	2878.87
	winter (worst)	217.735	7838.47
	summer (avg)	-22.375	-805.50
	summer (worst)	-56.625	-2038.51
0.2m concrete 0.025m poly	winter (avg)	74.903	2696.49
	winter (worst)	203.941	7341.89
	summer (avg)	-20.957	-754.47
	summer (worst)	-53.038	-1909.37
0.1m concrete 0.01m acrylic	winter (avg)	100.749	3626.96
	winter (worst)	274.314	9875.32
	summer (avg)	-28.189	-1014.81
	summer (worst)	-71.340	-2568.23
0.1m concrete 0.025m poly	winter (avg)	95.683	3444.58
	winter (worst)	260.521	9378.74
	summer (avg)	-26.772	-963.78
	summer (worst)	-67.752	-2439.09

Table B.7: Heat Losses and Gains for Single Rows and Total Structure (Imperial) Catenary Scenario

Composition		Heat Loss/Gain (Btu/hr) (per row)	Heat Loss/Gain (Btu/hr) (total)
0.3m concrete 0.01m acrylic	winter (avg)	231.989	8351.589
	winter (worst)	631.648	22739.317
	summer (avg)	-64.909	-2336.742
	summer (worst)	-164.270	-5913.713
0.3m concrete 0.025m poly	winter (avg)	214.702	7729.280
	winter (worst)	584.581	21044.924
	summer (avg)	-60.073	-2162.622
	summer (worst)	-152.029	-5473.060
0.2m concrete 0.01m acrylic	winter (avg)	272.865	9823.123
	winter (worst)	742.943	26745.941
	summer (avg)	-76.346	-2748.471
	summer (worst)	-193.214	-6955.698
0.2m concrete 0.025m poly	winter (avg)	255.578	9200.814
	winter (worst)	695.876	25051.548
	summer (avg)	-71.510	-2574.352
	summer (worst)	-180.973	-6515.044
0.1m concrete 0.01m acrylic	winter (avg)	343.769	12375.697
	winter (worst)	935.999	33695.972
	summer (avg)	-96.185	-3462.671
	summer (worst)	-243.421	-8763.161
0.1m concrete 0.025m poly	winter (avg)	326.483	11753.389
	winter (worst)	888.933	32001.578
	summer (avg)	-91.349	-3288.552
	summer (worst)	-231.181	-8322.508

Appendix C - Directions for Mix Design

1. Pour all solids(sand, portland cement, silica fume, and retarder) into the mixer. Mix on lowest speed for one minute and thirty seconds
2. Begin adding water. First amount poured in was 464 grams. Mix on lowest speed for one minute
3. Mix with spoon, making sure to scrape the bottom of the bowl to fully mix in all of the ingredients
4. Add 125 grams of water to the mixer. Mix on lowest speed for one minute
5. Add 100 grams of water to the mixer. Mix on lowest speed for one minute
6. Add 50 grams of water to the mixer. Mix on Speed 1 for one minute
7. Add 22 grams of water to the mixer. Mix on Speed 1 for one minute
8. Add 21 grams of water to the mixer. Mix on Speed 1 for one minute
9. Add final 10 grams of water to the mixer. Mix on Speed 2 for one minute
10. Following the completion of the concrete, mix again with spoon
11. Immediately after mixing the concrete with the spoon, bring it to the print bed to be poured into the hopper.
12. Spray the hooper with the hose to wet the surface before putting the concrete in
13. Pour the concrete into the hopper

Appendix D - Directions for Printer Use

1. Turn on the printer
    a. Turn on the power by moving the switch to on

    b. Power on the printer by turning the knob to the right

    c. Turn on the display by holding the power button until the screen lights up

2. Place a bucket under the print head
    a. Run water through the print head

3. Pour concrete into the hopper on the print head

4. On the main menu press the ‘Tool’ button

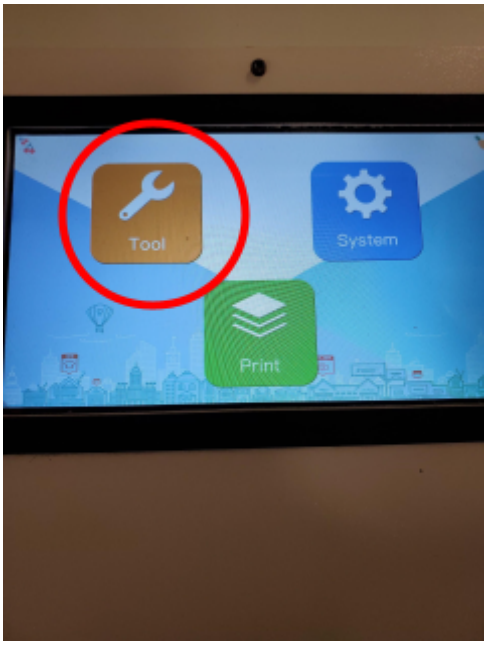

5. In the tool menu press the ‘Manual’ button

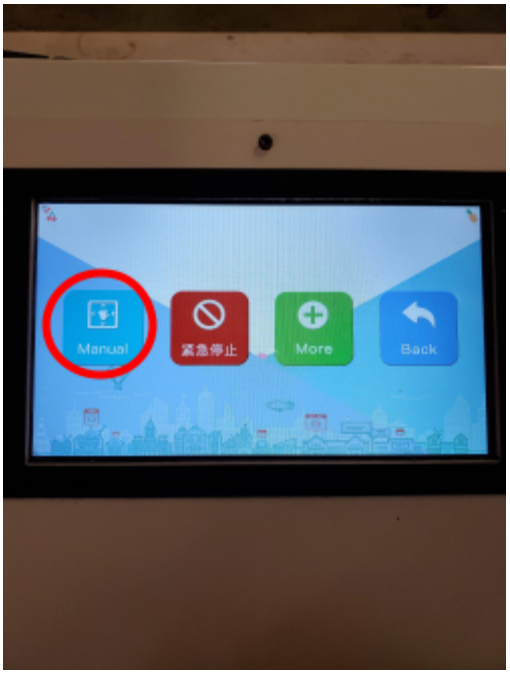

6. Press the E1 button and then the down E arrow to move concrete to the nozzle to ensure a solid flow of concrete when the printing process begins

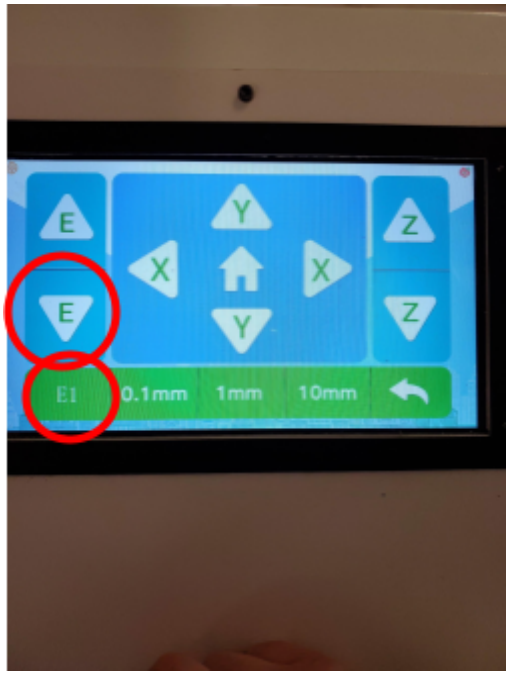

   a. Check to see if concrete is at the tip of the nozzle

7. Inset a flash drive with the gcode file into the right side of the print console
8. Press the back arrow until you reach the main menu and then press the ‘Print’ button

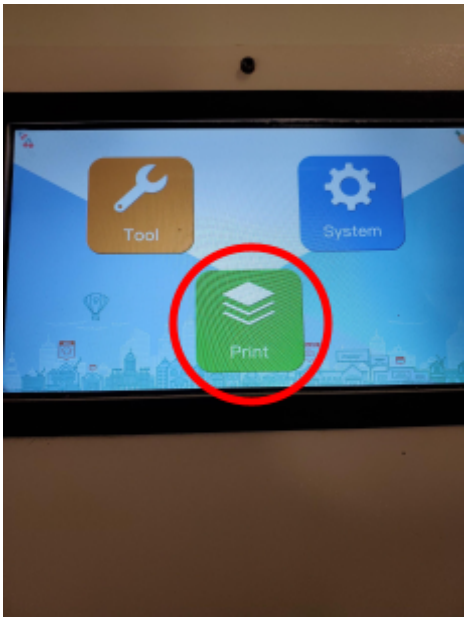

9. In the print menu choose the .gcode file you want to print

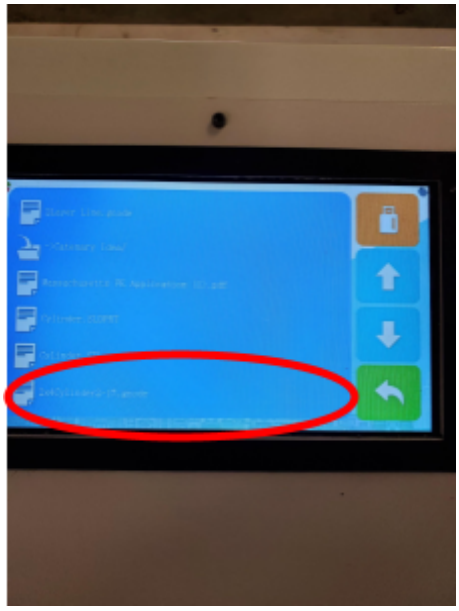

10. Press the ‘Start’ button to begin printing

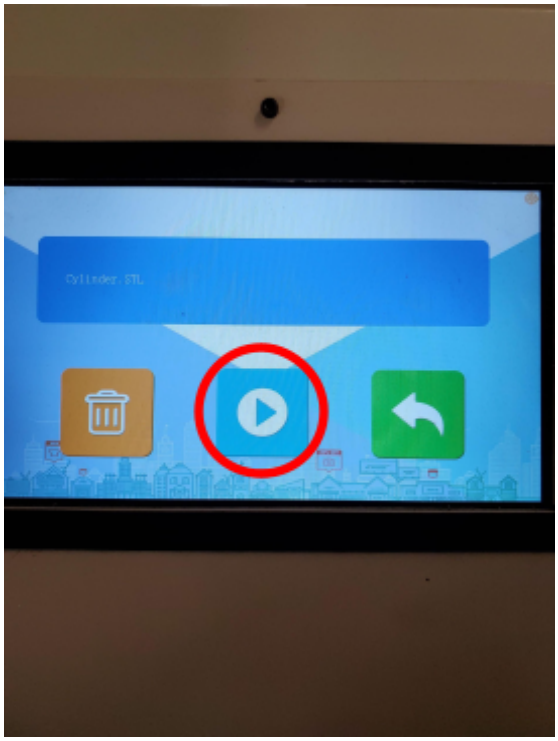

Appendix E - Directions for Cleaning of Printer and List of Parts

List of Parts:

- Printhead

- Mixing screw and lid

- Six Screws

- Nozzle

- White Plastic Ring

- Nozzle Clamp

Directions For Cleaning:

1. Remove the printhead
    a. Unscrew one tightening bolt on each side of print head
2. Remove the mixing screw and lid from the printhead
    a. Unscrew six screw on the lid
3. Remove the nozzle
    a. Unscrew clamp and remove plastic ring
4. Thoroughly wash all parts
5. Wipe down print bed

Appendix F - G-Code for 2X4 Cylinder

```
;Basic settings: Layer height: 10 Walls: 200 Fill: 95
;Print time: 1 minutes
;Filament used: 1.287m 282.0g
;Filament cost: None
;M190 S60 ;Uncomment to add your own bed temperature line
;M109 S0 ;Uncomment to add your own temperature line
G21        ;metric values
G90        ;absolute positioning
M82        ;set extruder to absolute mode
M107       ;start with the fan off
G28 X0 Y0  ;move X/Y to min endstops
G28 Z0     ;move Z to min endstops
G92 E0                  ;zero the extruded length
G1 F200 E3              ;extrude 3mm of feed stock
G92 E0                  ;zero the extruded length again
G1 F3000
;Put printing message on LCD screen
M117 Printing...
;Layer count: 7
;LAYER:0
M106 S255
G0 F9000 X967.050 Y485.688 Z15.000
;TYPE:SKIRT
G1 X968.858 Y482.200 E5.00223
G1 X969.304 Y481.336 E6.24023
G1 X971.571 Y478.125 E11.24486
G1 X972.131 Y477.331 E12.48195
```

G1 X974.817 Y474.456 E17.49150

G1 X975.473 Y473.751 E18.71763

G1 X978.527 Y471.266 E23.73072

G1 X979.282 Y470.652 E24.96978

G1 X982.643 Y468.608 E29.97836

G1 X983.476 Y468.102 E31.21931

G1 X987.078 Y466.538 E36.21919

G1 X987.973 Y466.149 E37.46172

G1 X991.756 Y465.090 E42.46356

G1 X991.756 Y465.091 E42.46483

G1 X992.676 Y464.830 E43.68244

G1 X996.580 Y464.294 E48.69979

G1 X996.580 Y464.293 E48.70107

G1 X997.547 Y464.160 E49.94388

G1 X1002.451 Y464.160 E56.18785

G1 X1006.344 Y464.695 E61.19116

G1 X1007.308 Y464.828 E62.43018

G1 X1011.104 Y465.890 E67.44899

G1 X1012.044 Y466.156 E68.69283

G1 X1015.631 Y467.714 E73.67215

G1 X1016.526 Y468.103 E74.91468

G1 X1019.878 Y470.142 E79.91016

G1 X1019.878 Y470.141 E79.91144

G1 X1020.714 Y470.649 E81.15698

G1 X1023.765 Y473.131 E86.16470

G1 X1024.520 Y473.746 E87.40455

G1 X1027.207 Y476.622 E92.41590

G1 X1027.872 Y477.336 E93.65822

G1 X1030.134 Y480.541 E98.65294

G1 X1030.696 Y481.338 E99.89463

G1 X1032.503 Y484.824 E104.89401

G1 X1032.951 Y485.691 E106.13657

G1 X1034.593 Y490.310 E112.37821

G1 X1035.391 Y494.158 E117.38188

G1 X1035.589 Y495.094 E118.60001

G1 X1035.855 Y499.008 E123.59496

G1 X1035.924 Y499.988 E124.84583

G1 X1035.656 Y503.927 E129.87271

G1 X1035.588 Y504.899 E131.11333

G1 X1034.788 Y508.752 E136.12375

G1 X1034.587 Y509.707 E137.36633

G1 X1032.950 Y514.312 E143.58905

G1 X1031.142 Y517.800 E148.59128

G1 X1030.696 Y518.664 E149.82928

G1 X1028.429 Y521.875 E154.83390

G1 X1027.869 Y522.669 E156.07100

G1 X1025.183 Y525.544 E161.08055

G1 X1024.527 Y526.249 E162.30668

G1 X1021.473 Y528.734 E167.31977

G1 X1020.718 Y529.348 E168.55882

G1 X1017.357 Y531.392 E173.56741

G1 X1016.524 Y531.898 E174.80836

G1 X1012.922 Y533.462 E179.80824

G1 X1012.027 Y533.851 E181.05077

G1 X1008.244 Y534.910 E186.05260

G1 X1008.244 Y534.909 E186.05388

G1 X1007.324 Y535.170 E187.27148

G1 X1003.420 Y535.706 E192.28884

G1 X1003.420 Y535.707 E192.29011

G1 X1002.453 Y535.840 E193.53293

G1 X997.549 Y535.840 E199.77689

G1 X993.656 Y535.305 E204.78020

G1 X992.692 Y535.172 E206.01923

G1 X988.896 Y534.110 E211.03804

G1 X987.956 Y533.844 E212.28188

G1 X984.367 Y532.285 E217.26404

G1 X983.474 Y531.897 E218.50373

G1 X980.122 Y529.858 E223.49921

G1 X980.122 Y529.859 E223.50049

G1 X979.286 Y529.351 E224.74602

G1 X976.235 Y526.869 E229.75374

G1 X975.480 Y526.254 E230.99360

G1 X972.793 Y523.378 E236.00495

G1 X972.128 Y522.664 E237.24727

G1 X969.866 Y519.459 E242.24199

G1 X969.304 Y518.662 E243.48367

G1 X967.497 Y515.176 E248.48306

G1 X967.049 Y514.309 E249.72562

G1 X965.407 Y509.690 E255.96726

G1 X964.609 Y505.842 E260.97093

G1 X964.411 Y504.906 E262.18906

G1 X964.143 Y500.969 E267.21340

G1 X964.076 Y500.012 E268.43487

G1 X964.344 Y496.073 E273.46176

G1 X964.412 Y495.101 E274.70237

G1 X965.212 Y491.248 E279.71279

G1 X965.413 Y490.293 E280.95538

G1 X967.050 Y485.688 E287.17809

G1 F2400 E282.67809

G0 F9000 X983.597 Y492.878

;TYPE:WALL-OUTER

G1 F2400 E287.17809

G1 F6000 X984.723 Y490.707 E290.29197

G1 X986.131 Y488.712 E293.40099

G1 X987.797 Y486.930 E296.50704

G1 X989.688 Y485.390 E299.61215

G1 X991.772 Y484.123 E302.71748

G1 X994.008 Y483.152 E305.82130

G1 X996.367 Y482.491 E308.94055

G1 X998.780 Y482.160 E312.04165

G1 X1001.221 Y482.160 E315.14963

G1 X1003.634 Y482.492 E318.25090

G1 X1005.986 Y483.150 E321.36054

G1 X1008.230 Y484.125 E324.47573

G1 X1010.311 Y485.390 E327.57648

G1 X1012.207 Y486.933 E330.68893

G1 X1013.870 Y488.713 E333.79051

G1 X1015.277 Y490.706 E336.89672

G1 X1016.402 Y492.877 E340.01001

G1 X1017.218 Y495.172 E343.11130

G1 X1017.715 Y497.568 E346.22692

G1 X1017.881 Y500.000 E349.33065

G1 X1017.716 Y502.433 E352.43556

G1 X1017.220 Y504.822 E355.54219

G1 X1016.403 Y507.122 E358.64991

G1 X1015.277 Y509.293 E361.76379

G1 X1013.869 Y511.288 E364.87281

G1 X1012.203 Y513.070 E367.97886

G1 X1010.312 Y514.610 E371.08396

G1 X1008.228 Y515.877 E374.18930

G1 X1005.992 Y516.848 E377.29311

G1 X1003.633 Y517.509 E380.41237

G1 X1001.220 Y517.840 E383.51347

G1 X998.779 Y517.840 E386.62144

G1 X996.366 Y517.508 E389.72272

G1 X994.014 Y516.850 E392.83236

G1 X991.770 Y515.875 E395.94755

G1 X989.689 Y514.610 E399.04829

G1 X987.793 Y513.067 E402.16075

G1 X986.130 Y511.287 E405.26233

G1 X984.723 Y509.294 E408.36854

G1 X983.598 Y507.123 E411.48183

G1 X982.782 Y504.828 E414.58312

G1 X982.285 Y502.432 E417.69874

G1 X982.119 Y499.998 E420.80500

G1 X982.284 Y497.567 E423.90737

G1 X982.780 Y495.178 E427.01401

G1 X983.597 Y492.878 E430.12173

;LAYER:1

G0 F9000 X983.510 Y493.123 Z30.000

;TYPE:WALL-OUTER

G1 F6000 X983.598 Y492.877 E430.45438

G1 X984.601 Y490.940 E433.23167

G1 X984.719 Y490.712 E433.55854

G1 X985.982 Y488.923 E436.34682

G1 X986.128 Y488.717 E436.66830

G1 X987.794 Y486.933 E439.77621

G1 X989.691 Y485.389 E442.89046

G1 X991.556 Y484.255 E445.66956

G1 X991.774 Y484.122 E445.99470

G1 X993.776 Y483.253 E448.77351

G1 X994.009 Y483.152 E449.09684

G1 X996.118 Y482.561 E451.88555

G1 X996.364 Y482.492 E452.21085

G1 X998.529 Y482.195 E454.99323

G1 X998.783 Y482.160 E455.31969

G1 X1001.223 Y482.160 E458.42640

G1 X1003.381 Y482.456 E461.19977

G1 X1003.636 Y482.492 E461.52767

G1 X1005.744 Y483.082 E464.31480

G1 X1005.982 Y483.148 E464.62927

G1 X1007.993 Y484.022 E467.42112

G1 X1008.228 Y484.124 E467.74730

G1 X1010.095 Y485.259 E470.52924

G1 X1010.307 Y485.387 E470.84455

G1 X1012.206 Y486.933 E473.96238

G1 X1013.872 Y488.716 E477.06936

G1 X1015.130 Y490.498 E479.84668

G1 X1015.279 Y490.709 E480.17557

G1 X1016.285 Y492.651 E482.96027

G1 X1016.401 Y492.874 E483.28032

G1 X1017.134 Y494.938 E486.06908

G1 X1017.219 Y495.176 E486.39086

G1 X1017.663 Y497.318 E489.17611

G1 X1017.715 Y497.569 E489.50248

G1 X1017.864 Y499.747 E492.28208

G1 X1017.881 Y500.000 E492.60494

G1 X1017.734 Y502.174 E495.37928

G1 X1017.716 Y502.430 E495.70603

G1 X1017.273 Y504.567 E498.48480

G1 X1017.220 Y504.821 E498.81516

G1 X1016.490 Y506.877 E501.59306

G1 X1016.402 Y507.123 E501.92571

G1 X1015.399 Y509.060 E504.70300

G1 X1015.281 Y509.288 E505.02987

G1 X1014.018 Y511.077 E507.81815

G1 X1013.872 Y511.283 E508.13963

G1 X1012.206 Y513.067 E511.24754

G1 X1010.309 Y514.611 E514.36179

G1 X1008.444 Y515.745 E517.14089

G1 X1008.226 Y515.878 E517.46603

G1 X1006.224 Y516.747 E520.24484

G1 X1005.991 Y516.848 E520.56817

G1 X1003.882 Y517.439 E523.35688

G1 X1003.636 Y517.508 E523.68218

G1 X1001.471 Y517.805 E526.46456

G1 X1001.217 Y517.840 E526.79102

G1 X998.777 Y517.840 E529.89773

G1 X996.619 Y517.544 E532.67110

G1 X996.364 Y517.508 E532.99900

G1 X994.256 Y516.918 E535.78613

G1 X994.018 Y516.852 E536.10060

G1 X992.007 Y515.978 E538.89245

G1 X991.772 Y515.876 E539.21863

G1 X989.905 Y514.741 E542.00057

G1 X989.693 Y514.613 E542.31588

G1 X987.794 Y513.067 E545.43371

G1 X986.128 Y511.284 E548.54069

G1 X984.868 Y509.499 E551.32260

G1 X984.721 Y509.291 E551.64689

G1 X983.715 Y507.349 E554.43160

G1 X983.599 Y507.126 E554.75164

G1 X982.866 Y505.062 E557.54041

G1 X982.781 Y504.824 E557.86219

G1 X982.337 Y502.682 E560.64744

G1 X982.285 Y502.431 E560.97381

G1 X982.136 Y500.253 E563.75341

G1 X982.119 Y500.000 E564.07627

G1 X982.266 Y497.826 E566.85061

G1 X982.284 Y497.570 E567.17736

G1 X982.727 Y495.433 E569.95612

G1 X982.780 Y495.179 E570.28649

G1 X983.510 Y493.123 E573.06438

;LAYER:2

G0 F9000 X983.340 Y493.601 Z45.000

;TYPE:WALL-OUTER

G1 F6000 X983.597 Y492.878 E574.04136

G1 X984.368 Y491.390 E576.17517

G1 X984.718 Y490.713 E577.14553

G1 X985.687 Y489.342 E579.28313

G1 X986.131 Y488.712 E580.26446

G1 X987.271 Y487.492 E582.39043

G1 X987.797 Y486.929 E583.37144

G1 X989.688 Y485.391 E586.47494

G1 X991.117 Y484.522 E588.60441

G1 X991.777 Y484.121 E589.58770

G1 X993.309 Y483.456 E591.71414

G1 X994.008 Y483.152 E592.68466

G1 X995.624 Y482.700 E594.82119

G1 X996.365 Y482.492 E595.80112

G1 X998.021 Y482.265 E597.92932

G1 X998.784 Y482.160 E598.90996

G1 X1001.225 Y482.160 E602.01794

G1 X1002.874 Y482.386 E604.13714

G1 X1003.636 Y482.492 E605.11669

G1 X1005.251 Y482.944 E607.25199

G1 X1005.989 Y483.150 E608.22756

G1 X1007.523 Y483.817 E610.35735

G1 X1008.227 Y484.123 E611.33473

G1 X1009.657 Y484.992 E613.46529

G1 X1010.312 Y485.391 E614.44181

G1 X1012.207 Y486.932 E617.55167

G1 X1013.348 Y488.153 E619.67944

G1 X1013.872 Y488.716 E620.65871

G1 X1014.836 Y490.081 E622.78640

G1 X1015.278 Y490.708 E623.76314

G1 X1016.049 Y492.195 E625.89581

G1 X1016.402 Y492.875 E626.87133

G1 X1016.962 Y494.454 E629.00446

G1 X1017.219 Y495.175 E629.97905

G1 X1017.559 Y496.815 E632.11156

G1 X1017.715 Y497.561 E633.08194

G1 X1017.828 Y499.235 E635.21820

G1 X1017.881 Y500.003 E636.19837

G1 X1017.769 Y501.665 E638.31929

G1 X1017.716 Y502.430 E639.29566

G1 X1017.375 Y504.076 E641.43591

G1 X1017.220 Y504.823 E642.40728

G1 X1016.660 Y506.399 E644.53682

G1 X1016.403 Y507.122 E645.51380

G1 X1015.632 Y508.610 E647.64760

G1 X1015.282 Y509.287 E648.61796

G1 X1014.313 Y510.658 E650.75557

G1 X1013.869 Y511.288 E651.73690

G1 X1012.729 Y512.508 E653.86287

G1 X1012.203 Y513.071 E654.84388

G1 X1010.312 Y514.609 E657.94738

G1 X1008.883 Y515.478 E660.07685

G1 X1008.223 Y515.879 E661.06013

G1 X1006.691 Y516.544 E663.18658

G1 X1005.992 Y516.848 E664.15710

G1 X1004.376 Y517.300 E666.29362

G1 X1003.635 Y517.508 E667.27356

G1 X1001.979 Y517.735 E669.40176

G1 X1001.216 Y517.840 E670.38240

G1 X998.775 Y517.840 E673.49037

G1 X997.126 Y517.614 E675.60957

G1 X996.364 Y517.508 E676.58912

G1 X994.749 Y517.056 E678.72442

G1 X994.011 Y516.850 E679.69999

G1 X992.477 Y516.183 E681.82979

G1 X991.773 Y515.877 E682.80716

G1 X990.343 Y515.008 E684.93772

G1 X989.688 Y514.609 E685.91424

G1 X987.793 Y513.068 E689.02410

G1 X986.652 Y511.847 E691.15187

G1 X986.128 Y511.284 E692.13114

G1 X985.163 Y509.917 E694.26165

G1 X984.722 Y509.292 E695.23558

G1 X983.951 Y507.805 E697.36825

G1 X983.598 Y507.125 E698.34376

G1 X983.038 Y505.546 E700.47690

G1 X982.781 Y504.825 E701.45148

G1 X982.441 Y503.185 E703.58400

G1 X982.285 Y502.439 E704.55438

G1 X982.172 Y500.765 E706.69063

G1 X982.119 Y499.997 E707.67080

G1 X982.231 Y498.335 E709.79173

G1 X982.284 Y497.570 E710.76809

G1 X982.625 Y495.924 E712.90834

G1 X982.780 Y495.177 E713.87971

G1 X983.340 Y493.601 E716.00925

;LAYER:3

G0 F9000 X983.170 Y494.081 Z60.000

;TYPE:WALL-OUTER

G1 F6000 X983.598 Y492.876 E717.63741

G1 X984.131 Y491.847 E719.11290

G1 X984.720 Y490.710 E720.74329

G1 X985.391 Y489.760 E722.22416

G1 X986.127 Y488.718 E723.84846

G1 X986.922 Y487.866 E725.33217

G1 X987.793 Y486.932 E726.95823

G1 X989.686 Y485.392 E730.06531

G1 X991.778 Y484.120 E733.18266

G1 X994.006 Y483.153 E736.27510

G1 X995.131 Y482.838 E737.76259

G1 X996.364 Y482.492 E739.39313

G1 X998.779 Y482.160 E742.49692

G1 X1001.221 Y482.160 E745.60617

G1 X1003.637 Y482.492 E748.71123

G1 X1004.760 Y482.806 E750.19592

G1 X1005.989 Y483.150 E751.82087

G1 X1008.222 Y484.120 E754.92068

G1 X1010.314 Y485.392 E758.03802

G1 X1012.202 Y486.928 E761.13695

G1 X1012.998 Y487.781 E762.62246

G1 X1013.870 Y488.714 E764.24846

G1 X1014.541 Y489.663 E765.72829

G1 X1015.277 Y490.707 E767.35467

G1 X1015.813 Y491.741 E768.83757

G1 X1016.402 Y492.877 E770.46683

G1 X1016.791 Y493.970 E771.94399

G1 X1017.218 Y495.172 E773.56812

G1 X1017.455 Y496.313 E775.05190

G1 X1017.715 Y497.564 E776.67876

G1 X1017.881 Y500.000 E779.78756

G1 X1017.715 Y502.437 E782.89764

G1 X1017.480 Y503.570 E784.37092

G1 X1017.219 Y504.824 E786.00178

G1 X1016.830 Y505.919 E787.48134

G1 X1016.402 Y507.124 E789.10950

G1 X1015.869 Y508.153 E790.58499

G1 X1015.280 Y509.290 E792.21538

G1 X1014.609 Y510.240 E793.69625

G1 X1013.873 Y511.282 E795.32055

G1 X1013.078 Y512.134 E796.80425

G1 X1012.207 Y513.068 E798.43032

G1 X1010.314 Y514.608 E801.53740

G1 X1008.222 Y515.880 E804.65474

G1 X1005.994 Y516.847 E807.74719

G1 X1004.869 Y517.162 E809.23467

G1 X1003.636 Y517.508 E810.86522

G1 X1001.221 Y517.840 E813.96901

G1 X998.779 Y517.840 E817.07826

G1 X996.363 Y517.508 E820.18332

G1 X995.240 Y517.194 E821.66801

G1 X994.011 Y516.850 E823.29296

G1 X991.778 Y515.880 E826.39277

G1 X989.686 Y514.608 E829.51011

G1 X987.798 Y513.072 E832.60904

G1 X987.002 Y512.219 E834.09455

G1 X986.130 Y511.286 E835.72055

G1 X985.458 Y510.335 E837.20319

G1 X984.723 Y509.293 E838.82675

G1 X984.187 Y508.259 E840.30966

G1 X983.598 Y507.123 E841.93891

G1 X983.209 Y506.029 E843.41727

G1 X982.782 Y504.828 E845.04021

G1 X982.545 Y503.687 E846.52398

G1 X982.285 Y502.436 E848.15084

G1 X982.119 Y500.000 E851.25965

G1 X982.285 Y497.563 E854.36972

G1 X982.520 Y496.430 E855.84301

G1 X982.781 Y495.176 E857.47387

G1 X983.170 Y494.081 E858.95343

;LAYER:4

G0 F9000 X982.998 Y494.565 Z75.000

;TYPE:WALL-OUTER

G1 F6000 X983.600 Y492.873 E861.24004

G1 X983.897 Y492.299 E862.06292

G1 X984.721 Y490.709 E864.34307

G1 X985.097 Y490.176 E865.17358

G1 X986.123 Y488.721 E867.44041

G1 X987.798 Y486.929 E870.56358

G1 X989.687 Y485.392 E873.66430

G1 X990.243 Y485.054 E874.49277

G1 X991.773 Y484.123 E876.77314

G1 X992.369 Y483.865 E877.60004

G1 X994.014 Y483.150 E879.88381

G1 X994.637 Y482.976 E880.70739

G1 X996.362 Y482.492 E882.98855

G1 X997.006 Y482.404 E883.81613

G1 X998.780 Y482.160 E886.09612

G1 X1001.224 Y482.160 E889.20792

G1 X1001.863 Y482.248 E890.02920

G1 X1003.640 Y482.493 E892.31315

G1 X1004.268 Y482.668 E893.14321

G1 X1005.988 Y483.150 E895.41755

G1 X1006.583 Y483.408 E896.24328

G1 X1008.231 Y484.125 E898.53157

G1 X1008.782 Y484.460 E899.35261

G1 X1010.312 Y485.390 E901.63231

G1 X1012.202 Y486.929 E904.73563

G1 X1013.872 Y488.716 E907.84981

G1 X1014.245 Y489.245 E908.67395

G1 X1015.278 Y490.707 E910.95320

G1 X1015.578 Y491.286 E911.78349

G1 X1016.401 Y492.875 E914.06193

G1 X1016.619 Y493.488 E914.89031

G1 X1017.220 Y495.179 E917.17530

G1 X1017.351 Y495.811 E917.99709

G1 X1017.715 Y497.562 E920.27419

G1 X1017.759 Y498.212 E921.10369

G1 X1017.881 Y500.000 E923.38554

G1 X1017.837 Y500.649 E924.21377

G1 X1017.715 Y502.440 E926.49943

G1 X1017.584 Y503.070 E927.31872

G1 X1017.219 Y504.825 E929.60108

G1 X1017.002 Y505.435 E930.42543

G1 X1016.400 Y507.127 E932.71205

G1 X1016.103 Y507.701 E933.53492

G1 X1015.279 Y509.291 E935.81508

G1 X1014.903 Y509.824 E936.64558

G1 X1013.877 Y511.279 E938.91242

G1 X1012.202 Y513.071 E942.03559

G1 X1010.313 Y514.608 E945.13631

G1 X1009.757 Y514.946 E945.96478

G1 X1008.227 Y515.877 E948.24514

G1 X1007.631 Y516.135 E949.07204

G1 X1005.986 Y516.850 E951.35581

G1 X1005.363 Y517.024 E952.17940

G1 X1003.638 Y517.508 E954.46055

G1 X1002.994 Y517.596 E955.28814

G1 X1001.220 Y517.840 E957.56813

G1 X998.776 Y517.840 E960.67993

G1 X998.137 Y517.752 E961.50121

G1 X996.360 Y517.507 E963.78516

G1 X995.732 Y517.332 E964.61522

G1 X994.012 Y516.850 E966.88955

G1 X993.417 Y516.592 E967.71529

G1 X991.769 Y515.875 E970.00357

G1 X991.216 Y515.539 E970.82746

G1 X989.688 Y514.610 E973.10432

G1 X987.798 Y513.071 E976.20764

G1 X986.128 Y511.284 E979.32181

G1 X985.755 Y510.755 E980.14595

G1 X984.722 Y509.293 E982.42521

G1 X984.422 Y508.714 E983.25549

G1 X983.599 Y507.125 E985.53393

G1 X983.381 Y506.512 E986.36232

G1 X982.780 Y504.821 E988.64730

G1 X982.649 Y504.189 E989.46910

G1 X982.285 Y502.438 E991.74620

G1 X982.241 Y501.788 E992.57570

G1 X982.119 Y499.999 E994.85882

G1 X982.163 Y499.351 E995.68578

G1 X982.285 Y497.560 E997.97143

G1 X982.416 Y496.930 E998.79073

G1 X982.781 Y495.175 E1001.07308

G1 X982.998 Y494.565 E1001.89744

;LAYER:5

G0 F9000 X982.781 Y495.176 Z90.000

;TYPE:WALL-OUTER

G1 F6000 X983.601 Y492.870 E1005.01363

G1 X984.721 Y490.708 E1008.11382

G1 X986.132 Y488.711 E1011.22713

G1 X987.797 Y486.929 E1014.33231

G1 X989.686 Y485.392 E1017.43303

G1 X991.772 Y484.124 E1020.54120

G1 X994.008 Y483.152 E1023.64552

G1 X996.359 Y482.494 E1026.75394

G1 X998.782 Y482.160 E1029.86817

G1 X1001.225 Y482.160 E1032.97869

G1 X1003.641 Y482.493 E1036.08392

G1 X1005.993 Y483.152 E1039.19391

G1 X1008.224 Y484.122 E1042.29138

G1 X1010.314 Y485.392 E1045.40522

G1 X1012.204 Y486.930 E1048.50774

G1 X1013.872 Y488.716 E1051.61924

G1 X1015.279 Y490.709 E1054.72545

G1 X1016.401 Y492.875 E1057.83133

G1 X1017.218 Y495.173 E1060.93665

G1 X1017.715 Y497.562 E1064.04355

G1 X1017.881 Y500.005 E1067.16124

G1 X1017.714 Y502.444 E1070.27395

G1 X1017.219 Y504.824 E1073.36910

G1 X1016.399 Y507.130 E1076.48530

G1 X1015.279 Y509.292 E1079.58549

G1 X1013.868 Y511.289 E1082.69879

G1 X1012.203 Y513.071 E1085.80397

G1 X1010.314 Y514.608 E1088.90469

G1 X1008.228 Y515.876 E1092.01286

G1 X1005.992 Y516.848 E1095.11719

G1 X1003.641 Y517.506 E1098.22560

G1 X1001.218 Y517.840 E1101.33983

G1 X998.775 Y517.840 E1104.45036

G1 X996.359 Y517.507 E1107.55559

G1 X994.007 Y516.848 E1110.66557

G1 X991.776 Y515.878 E1113.76304

G1 X989.686 Y514.608 E1116.87689

G1 X987.796 Y513.070 E1119.97940

G1 X986.128 Y511.284 E1123.09091

G1 X984.721 Y509.291 E1126.19712

G1 X983.599 Y507.125 E1129.30300

G1 X982.782 Y504.827 E1132.40832

G1 X982.285 Y502.438 E1135.51521

G1 X982.119 Y499.995 E1138.63291

G1 X982.286 Y497.556 E1141.74561

G1 X982.781 Y495.176 E1144.84077

;LAYER:6

G0 F9000 X982.780 Y495.177 Z105.000

;TYPE:WALL-OUTER

G1 F6000 X983.597 Y492.878 E1147.94729

G1 X984.723 Y490.707 E1151.06116

G1 X986.125 Y488.719 E1154.15850

G1 X987.798 Y486.929 E1157.27807

G1 X989.688 Y485.391 E1160.38058

G1 X991.773 Y484.123 E1163.48767

G1 X994.011 Y483.151 E1166.59433

G1 X996.363 Y482.492 E1169.70431

G1 X998.779 Y482.160 E1172.80937

G1 X1001.221 Y482.160 E1175.91862

G1 X1003.637 Y482.492 E1179.02367

G1 X1005.989 Y483.151 E1182.13366

G1 X1008.227 Y484.123 E1185.24032

G1 X1010.312 Y485.391 E1188.34740

G1 X1012.202 Y486.929 E1191.44992

G1 X1013.875 Y488.719 E1194.56949

G1 X1015.277 Y490.707 E1197.66683

G1 X1016.403 Y492.878 E1200.78070

G1 X1017.220 Y495.177 E1203.88722

G1 X1017.715 Y497.559 E1206.98487

G1 X1017.881 Y500.000 E1210.10003

G1 X1017.715 Y502.441 E1213.21518

G1 X1017.220 Y504.823 E1216.31283

G1 X1016.403 Y507.122 E1219.41935

G1 X1015.277 Y509.293 E1222.53323

G1 X1013.875 Y511.281 E1225.63057

G1 X1012.202 Y513.071 E1228.75014

G1 X1010.312 Y514.609 E1231.85265

G1 X1008.227 Y515.877 E1234.95973

G1 X1005.989 Y516.849 E1238.06639

G1 X1003.637 Y517.508 E1241.17638

G1 X1001.221 Y517.840 E1244.28144

G1 X998.779 Y517.840 E1247.39069

G1 X996.363 Y517.508 E1250.49574

G1 X994.011 Y516.849 E1253.60573

G1 X991.773 Y515.877 E1256.71239

G1 X989.688 Y514.609 E1259.81947

G1 X987.798 Y513.071 E1262.92198

G1 X986.125 Y511.281 E1266.04156

G1 X984.723 Y509.293 E1269.13889

G1 X983.597 Y507.122 E1272.25277

G1 X982.780 Y504.823 E1275.35929

G1 X982.285 Y502.441 E1278.45694

G1 X982.119 Y500.000 E1281.57209

G1 X982.285 Y497.559 E1284.68725

G1 X982.780 Y495.177 E1287.78490

M107

G1 F2400 E1283.28490

G0 F9000 X982.780 Y495.177 Z106.599

M104 S0 ;extruder heater off

M140 S0 ;heated bed heater off (if you have it)

G91 ;relative positioning

G1 E-1 F300 ;retract the filament a bit before lifting the nozzle, to release some of the pressure

G1 Z+0.5 E-5 X-20 Y-20 F3000 ;move Z up a bit and retract filament even more

G28 X0 Y0 ;move X/Y to min endstops, so the head is out of the way

M84 ;steppers off

G90 ;absolute positioning

;CURA_PROFILE_STRING:eNrtWktv20YQvhJGf8QcEzRWSUpK4gi8JLVziYsAVtHEF2J
FDsWtSS6xu7QsG/rvnV0+RNly6jRG86IOtjmc2Z355ptHEGVsjTJMkS9THXius2JZFuqUR
xcFKhX4rutI1JJFmosixIItMgxOWKbQUSLjcZjZA7YWdEbC6YwYC8X1OjiaOoW4vs4w
VPwaA3/qlJIXOlQlYhxM3eZRY16iZLqSGOyR+fuE433CSSdcYLxz7HPXUVVZCqmDP0
SBTpkxnQiZhyxOUVF4tbjRCeOKZSFeaVnZd6+FTp0VLzHUYoWywWArCC9FVuUYeF
NHiGuKNuWYxY0aIcJyJJ9iTr81mRMOd4QmyDvC8T7hpC9MMrEKjsb9PNXguiOvL2S5
qAod7CTUBtm88J6Ppv13OS9CerjELPB230QiX/Bi2QS3a8LzHdjckev3NVJRGpmzEFqLv
Mcb17FMcsMVj3UaJqQvJLHJdcTib4yIMLy4MKaeIy5RZqy0zpNd7eOWUM3RNTE7KS8
sLXvPCrV76/mqRc6JhMgsAg2/eW54mbC2BtrMqgtOXMl4gYRKDW8tWrKy+7uFJcNiqd
PmnKQid5rCcwlfI6tvN0F3T2HOrqyk8yghKVEaTalZYYqM6pAneqcwNSE9l1X7WKOy5
WMWNjAGXVmEel1i8I5iUZ2IFcsMeyrW0t6+lV2tiZhKsyLqS693hCWXLDMNoHGR5y
W1hFzErWQhed7HkajLEoKOySUvDGnNk32vShYZ9jWyBVO4w6Ot1KhbOrVSagsoiVp7
DLav7lgxLuts2idVNWqGGMoW4hXRWkpOtAirwpaaaaIEZsjqFHxKZdHlpK9D3osSi3DB
tdqnQBVmGuwlwaG5jtJtOZZZRYgRikT4ZdBWT4QmvvAqOPRuidYk+oUSJfVoGZl8zM
4yHmEMTL+Cm5itN+anRvplqmBzMHvNFI+AykXTreoVvDNIQE1lMsl6I2UDf1GgpHOz
O1g2cEJEInF/VtDR703nBnMPvWt6e33pSdPugKCJa8O6/dXda5P3RKv67mXPKhJK963M
M5166h25cHazd2BsYPZnQa3O2msBLI5hLSoJYlUA6UJPFwxpzHHuUXfcQ4+6c8xb34P
mM6N2LwnsS5ZVqA7ekrftG7agwq40QikIPKIUJePg9KXfKVCCwDbimLJjLm0NTNUdk
KsvOk2TfVhxnYJOEaj3gEgS8uMlfHDho2v8oG4BH377aA6iJgRYxIo6jLJK527jrFE6v6vi
wbk3HblwctPv1ZvGwFzZzmKIDSLeNM8pVh+Ou3C3n9k1SmGNmuBiqPuqueeEFhY4Ht
+yaBRhnOcUGJgGCuRadPH5lwBbMl7Yq3aDIe5WGmzmKRGQE8nZEkEU8O7N76AiiV
gQ6N4LeN/ojEYjhzBqq+64iOHtmyY1Ezjb41UvFlNvVJTSJurUm7j3Gli92BJ2awJPeGIYC
CmFAFw/JSQ8eMBnJpFSRX1nh3YEx/EhQTJ23X8xtotAzbK2NBlQkyP/KP+mABKLn9G
o98Znhk90K1JHByVyNCm0nJGEMRWN5devNELJhyl8OPSJsubHfradQ1U2VzJCvPWo8
wYvsaAKMcdu6f/JoO4rjWfkrXXUzGfgCgQRpPF9xdZUq5P7D1UaS+oKqi7Eo/t92N8HZt
SDBMVkxgPRbblxbI37Q4t/hBY/+fIWX0+KubfvJP8/HeV+3bnzrU+T+T3dbXa2MuuTucV
Y+tQS2g77JRPIc/dPIM991BFk7zq82f8Pus3B3H1Q0AmXSn9PYT/S5PXvGb1z9zOnr7Hx

hok9TOzHn9jjYWIPE/vnnNj+zzixhzVlWFNurSnjr7mmGBt/WG2G1ebxV5vJsNp8U6uN/3i
rzbAl/W9b0vhBs3NCTv9AC8PDVsPxjxX0sBoOq+Gt1XDyva2GxmY8rJPDOvm462TzlZP
+txg64fa/WOtvy+woWUlPQyLN2AhHkboMHEpC3WaOG152C2vdfBaoV1SZNuioktJC3F
LYJMAmmiSd9BmsUjLoKt0uE3mVaV5mXbuQanQwm6cEqrnNgEvrjWW5ZZE5dP6keOo
QJvpb8o8lpgBb9/4Bh0Gxlg==

Appendix G - Graphs from Compression Tests

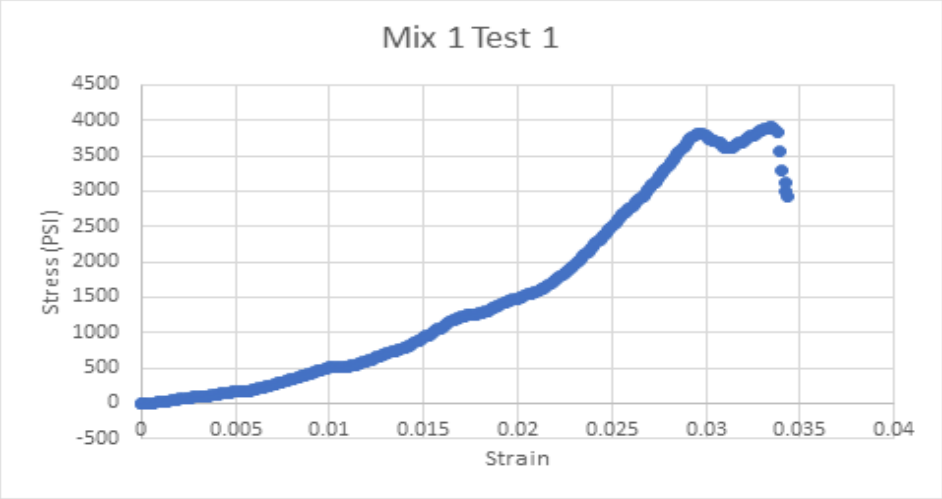

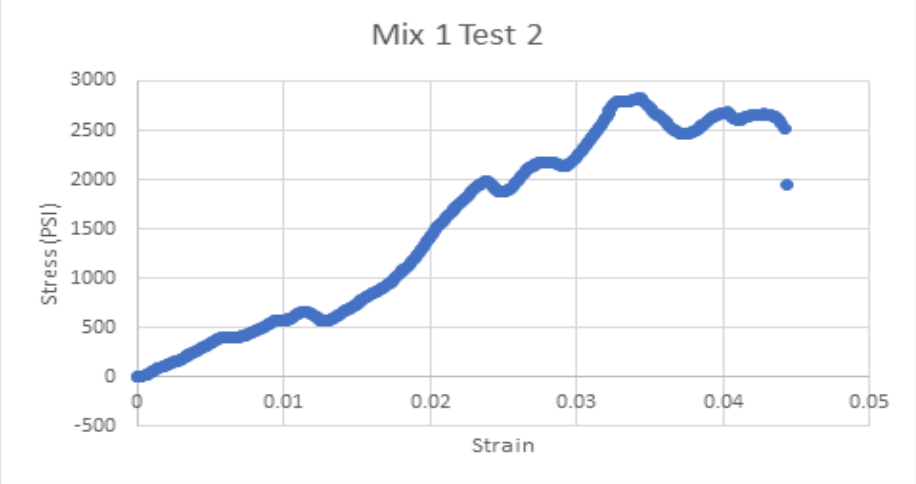

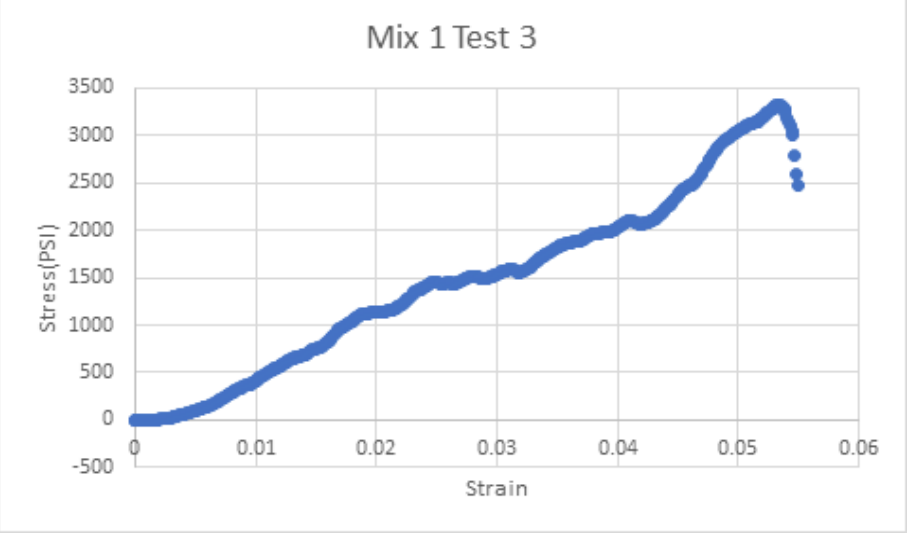

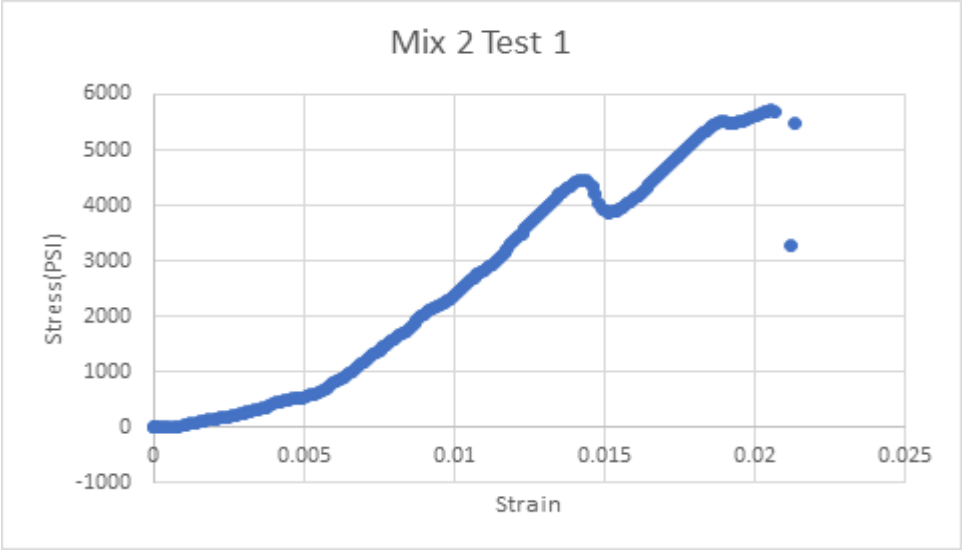
Mix 2 Test 1
6000
5000
4000
3000
2000
1000
0
-1000
Stress(PSI)
0
0.005
0.01
0.015
0.02
0.025
Strain

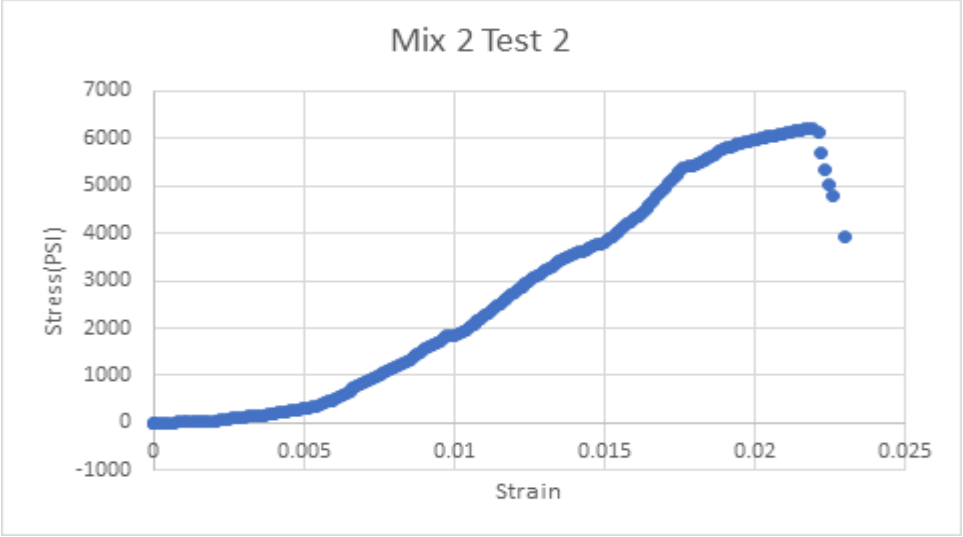
Mix 2 Test 2
7000
6000
5000
4000
3000
2000
1000
0
-1000
Stress(PSI)
0
0.005
0.01
0.015
0.02
0.025
Strain

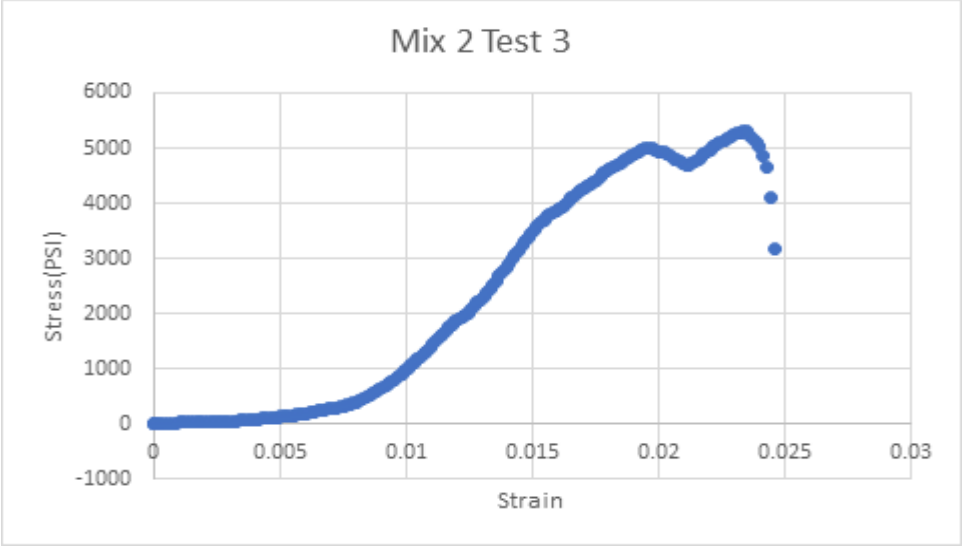
Mix 2 Test 3
6000
5000
4000
3000
2000
1000
0
-1000
Stress(PSI)
0
0.005
0.01
0.015
0.02
0.025
0.03
Strain

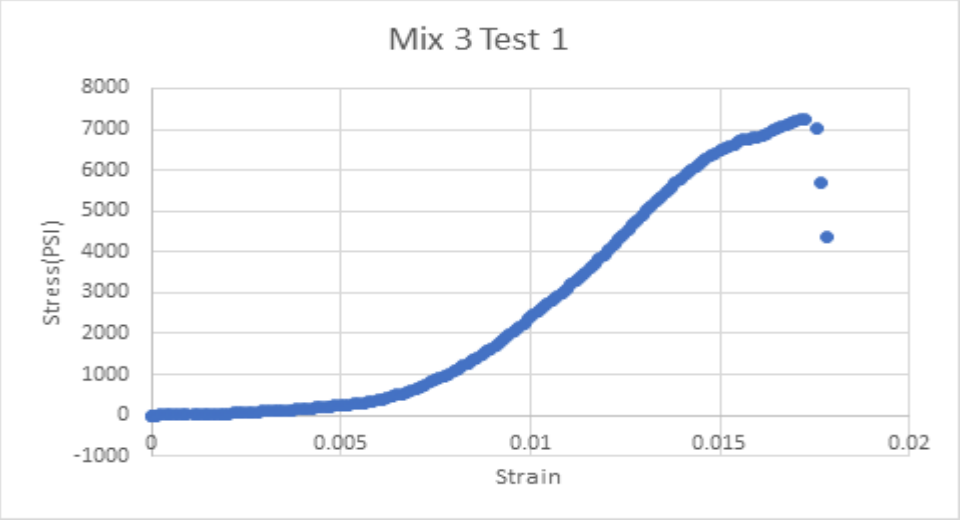
Mix 3 Test 1
Stress(PSI)
8000
7000
6000
5000
4000
3000
2000
1000
0
-1000
0
0.005
0.01
0.015
0.02
Strain

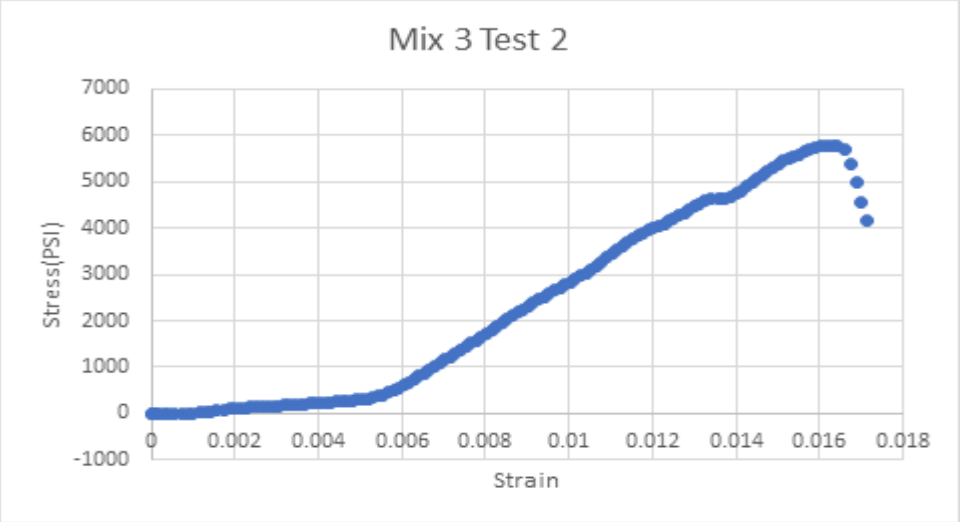
Mix 3 Test 2
Stress(PSI)
7000
6000
5000
4000
3000
2000
1000
0
-1000
0
0.002
0.004
0.006
0.008
0.01
0.012
0.014
0.016
0.018
Strain

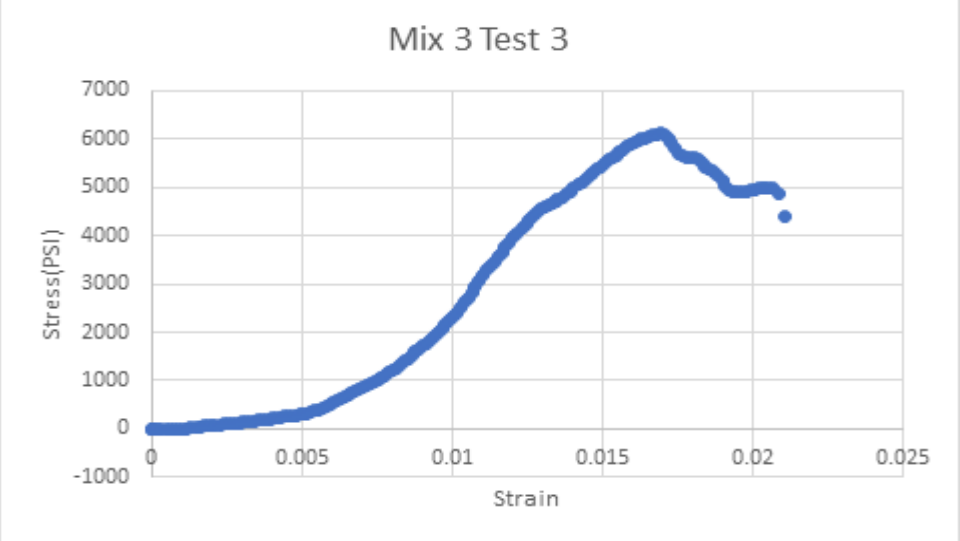
Mix 3 Test 3
Stress(PSI)
7000
6000
5000
4000
3000
2000
1000
0
-1000
0
0.005
0.01
0.015
0.02
0.025
Strain

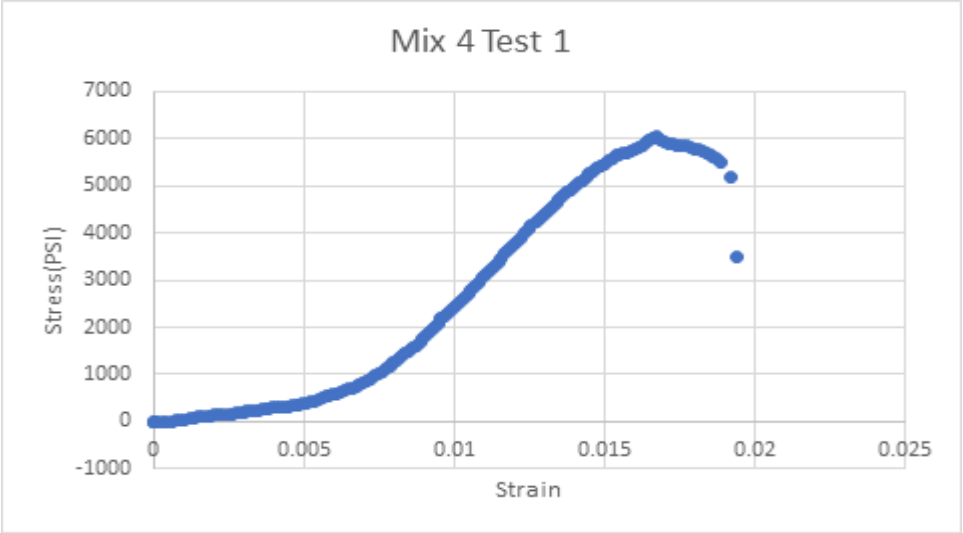
Mix 4 Test 1
7000
6000
5000
4000
3000
2000
1000
0
-1000
Stress(PSI)
0
0.005
0.01
0.015
0.02
0.025
Strain

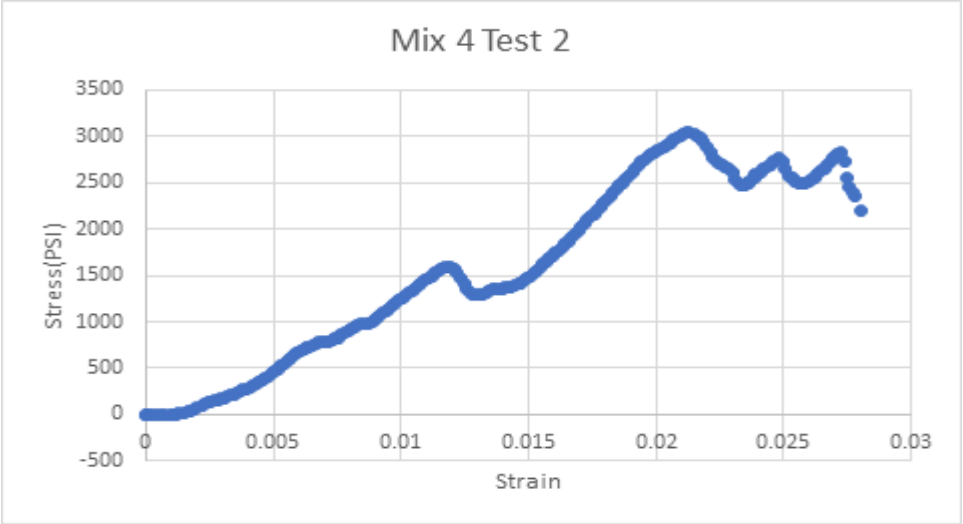
Mix 4 Test 2
3500
3000
2500
2000
1500
1000
500
0
-500
Stress(PSI)
0
0.005
0.01
0.015
0.02
0.025
0.03
Strain

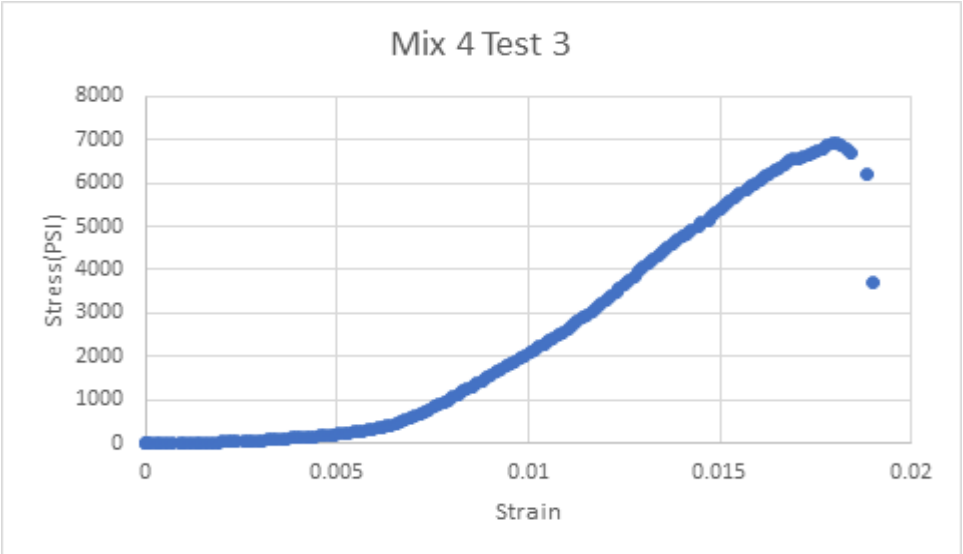
Mix 4 Test 3
8000
7000
6000
5000
4000
3000
2000
1000
0
Stress(PSI)
0
0.005
0.01
0.015
0.02
Strain

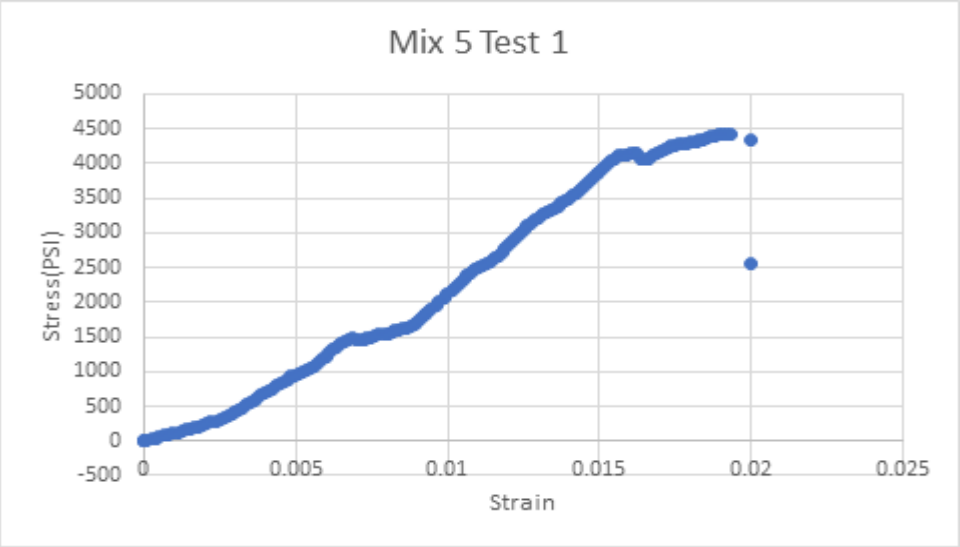
Mix 5 Test 1
Stress(PSI)
5000
4500
4000
3500
3000
2500
2000
1500
1000
500
0
-500
0
0.005
0.01
0.015
0.02
0.025
Strain

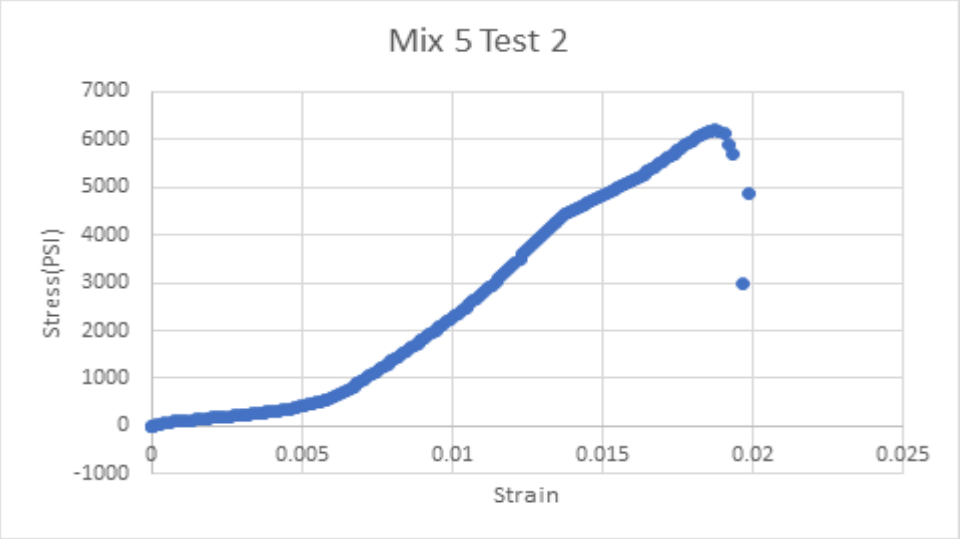
Mix 5 Test 2
Stress(PSI)
7000
6000
5000
4000
3000
2000
1000
0
-1000
0
0.005
0.01
0.015
0.02
0.025
Strain

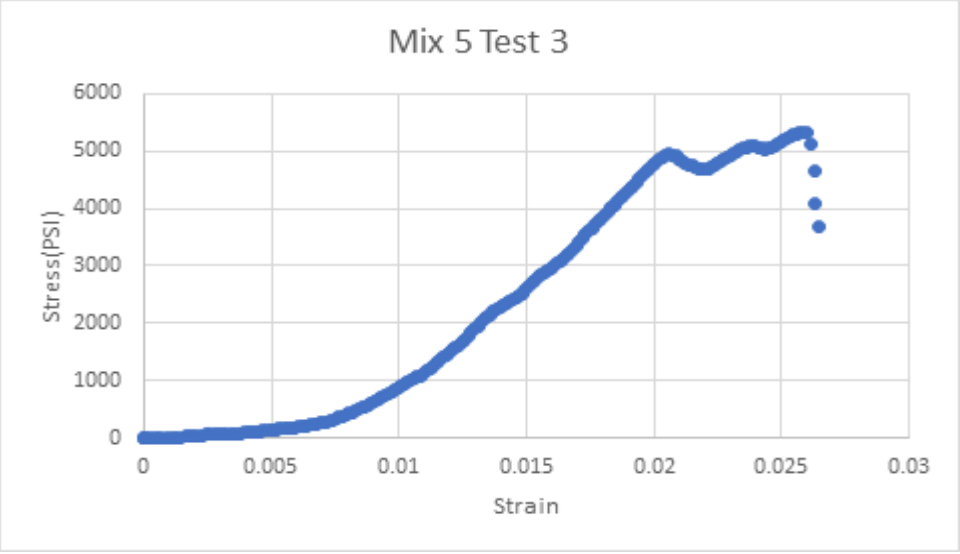
Mix 5 Test 3
Stress(PSI)
6000
5000
4000
3000
2000
1000
0
0
0.005
0.01
0.015
0.02
0.025
0.03
Strain

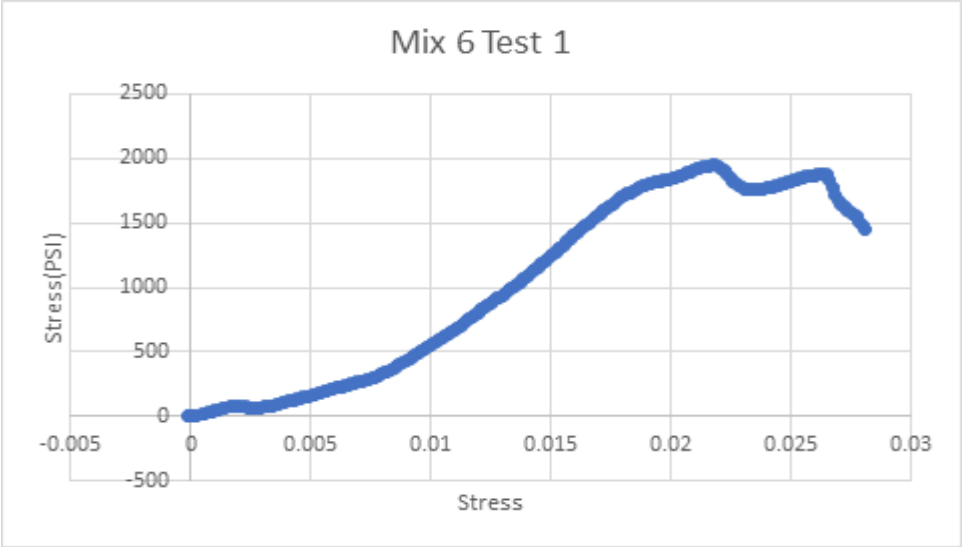
Mix 6 Test 1
2500
2000
1500
1000
500
0
-500
Stress(PSI)
-0.005
0
0.005
0.01
0.015
0.02
0.025
0.03
Stress

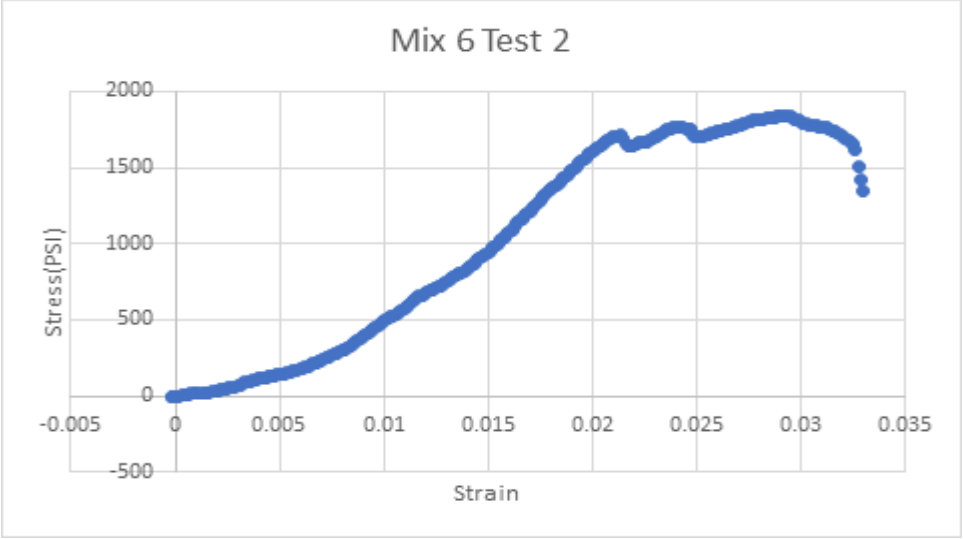
Mix 6 Test 2
2000
1500
1000
500
0
-500
Stress(PSI)
-0.005
0
0.005
0.01
0.015
0.02
0.025
0.03
0.035
Strain

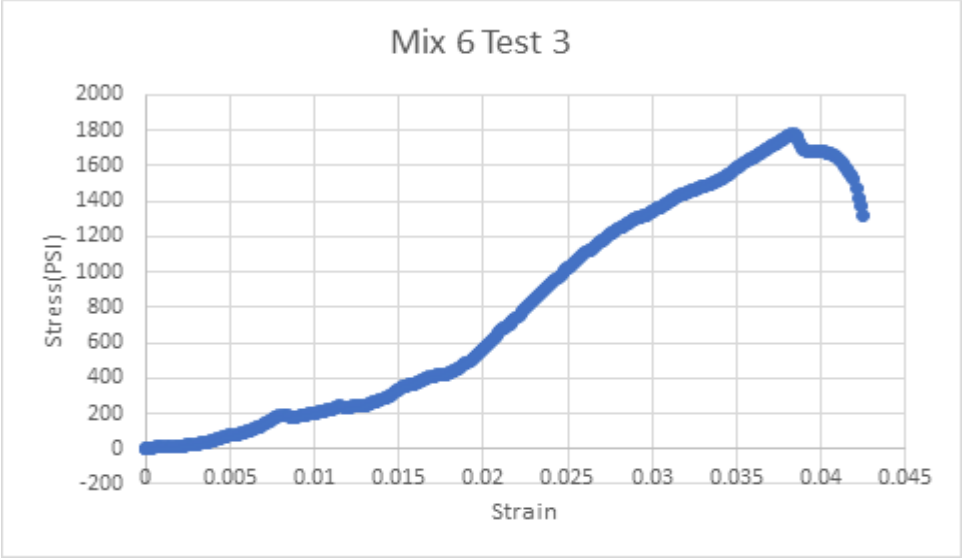
Mix 6 Test 3
2000
1800
1600
1400
1200
1000
800
600
400
200
0
-200
Stress(PSI)
0
0.005
0.01
0.015
0.02
0.025
0.03
0.035
0.04
0.045
Strain

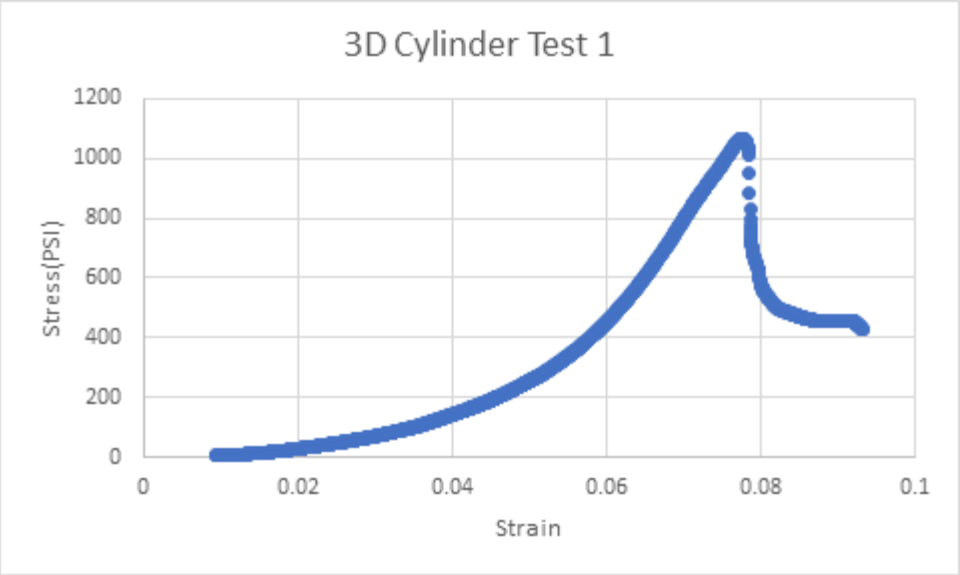
3D Cylinder Test 1
Stress(PSI)
1200
1000
800
600
400
200
0
0
0.02
0.04
0.06
0.08
0.1
Strain

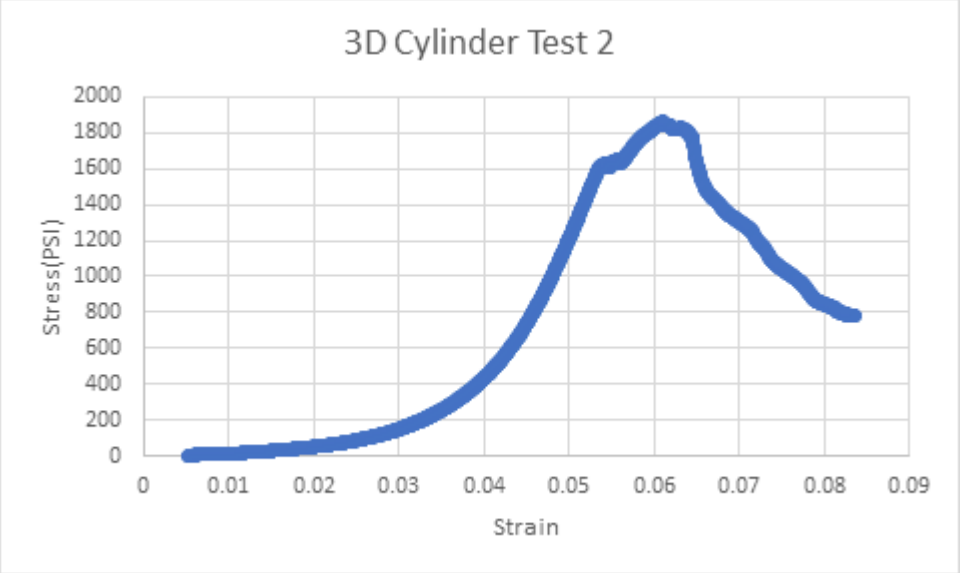
3D Cylinder Test 2
Stress(PSI)
2000
1800
1600
1400
1200
1000
800
600
400
200
0
0
0.01
0.02
0.03
0.04
0.05
0.06
0.07
0.08
0.09
Strain